



DRAINAGE SYSTEMS ANALYSIS

Flooding Topic Area | Extreme Storms Analysis

October 9, 2020



**Seattle
Public
Utilities**

PHOTO CREDITS from top left:

Salmon in Longfellow Creek, Seattle. Holli Margell, 2009. <http://nativelightphoto.com/>

Thornton Creek Confluence Restoration, Seattle. Natural Systems Design, 2014. <http://naturaldes.com>

Flooding in South Park, Seattle. Sheila Harrison, Seattle Public Utilities, 2009.

Lake Union, Seattle. Seattle Public Utilities Photo Archive, date unknown.

Flooding Topic Area

Technical Memorandum

Project: Drainage Systems Analysis


Topic Area: Flooding

Deliverable: Extreme Storms Analysis

Contract: 17-105-S

Date: October 9, 2020

Prepared by: Brown and Caldwell

Approved by: 
Leslie Webster (Oct 21, 2020 16:18 PDT) 10/21/2020
Leslie Webster, Planning Program Manager, SPU

Contributors:

SPU

Holly Scarlett, Project Manager

Colleen O'Brien, Technical Lead

James-Rufo Hill, Climate Science Advisor

Consultants

Mike Milne, Brown and Caldwell

Valerie Fuchs, Brown and Caldwell

Nathan Foged, Brown and Caldwell

Kevin Cook, Murraysmith

Anna Marburg, Murraysmith

This page intentionally left blank.

Table of Contents

1. Introduction	1
2. Extreme Precipitation	2
2.1 Observed Storm Event from December 2007, 100-year.....	2
2.2 Synthetic Storm Event, 1,000-year	3
2.3 Event Frequency and Climate Change.....	4
3. Flooding Analysis	6
3.1 Digital Elevation Model	7
3.2 Excess Precipitation	10
3.3 Collection System Inflows.....	12
3.4 Urban Flooding Simulations	14
3.4.1 Model Grid.....	15
3.4.2 Boundary Conditions.....	15
3.4.3 Manning’s Roughness	17
3.5 Running the Application	18
4. Inundation Mapping	20
5. Risk Scoring.....	23
5.1 Consequence Score	23
5.2 Frequency Score.....	25
5.3 Equity score	25
5.4 Example risk score calculations	26
6. Results Summary	28
7. Limitations	30
References.....	33

Figures

Figure 2-1. 28th Ave NE in December 2007	2
Figure 2-2. Hyetograph from observed rainfall on December 3, 2007	3
Figure 2-3. 1,000-year synthetic event hyetograph.....	4
Figure 3-1. City scale for Seattle	6
Figure 3-2. Process for modeling urban flooding for extreme storms	7
Figure 3-3. Surface Basins for Flood Modeling.....	8
Figure 3-4. Example area showing modified DEM grids	9
Figure 3-5. Schematic of infiltration losses and excess precipitation calculation	11
Figure 3-6. Surface basin areas and impervious area percentages	11
Figure 3-7. Schematic of infiltration losses and system losses.....	12
Figure 3-8. Examples of different inlets to SPU collection systems.....	13
Figure 3-9. CA neighborhood used by CA2D and WCA2D	14
Figure 3-10. Example of an ASCII grid text file.....	15
Figure 3-11. Schematic example of the computational grid and boundary conditions	16
Figure 3-12. Summary plot from sensitivity testing of the global roughness parameter	17
Figure 3-13. Input files used to run CAFlood	18
Figure 4-1. Example of the process used to define the extent of flood inundation for the 1,000-year event.....	20
Figure 4-2. Inundation areas and depths shown for example area with buildings	21
Figure 4-3. Example of simulated 100-year storm inundation compared with historical waterways.....	22
Figure 5-1. Relationship between inundation depth and depth score	23
Figure 5-2. Example risk score calculations	27
Figure 6-1. Distribution of risk scores within the extreme storms risk area.....	28

Tables

Table 3-1. Water Surface Elevations for Water Bodies at Model Boundaries	16
Table 3-2. Surface Basin File Sizes and Model Run Times.....	19
Table 5-1. Summary of Components of Consequence Score	24
Table 5-2. Frequency Scores for Extreme Storm Risk Mapping.....	25
Table 5-3. Equity Scores for the DSA.....	26
Table 6-1. Extreme Storm Risk Categories and Scores	29
Table A-1. Geologic Units, Soil Textures, and Representative USDA Soil Classes.....	A-4
Table A-2. Hydraulic Properties for Soil Types	A-5

Appendices

Appendix A: Green-Ampt Parameters	A-1
Appendix B: Inlet Efficiency Calculations.....	B-1
Appendix C: Routing System Inflows.....	C-1
Appendix D: CAFlood Setup File.....	D-1
Appendix E: GIS Processes.....	E-1
Appendix F: Maps of Simulated Inundation with Historical Watershed Conditions	F-1
Appendix G: Extreme Storm Risk Maps.....	G-1

Abbreviations

1D	one-dimensional	GPU	graphical processing unit
2D	two-dimensional	Hr	hour
ASCII	American Standard Code for Information Interchange	IDF	intensity-duration-frequency
BC	Brown and Caldwell	ISP	Integrated System Plan
CADDIES	Cellular Automata Dual-Drainage Simulation	LiDAR	Light Detection and Ranging
CA	cellular automata	LOB	line of business
cfs	cubic feet per second	MB	megabytes
City	City of Seattle (organization)	NAD83	North American Datum of 1983
Consultant	Brown and Caldwell	NAVD 88	North American Vertical Datum of 1988
CPU	central processing unit	PC	personal computer
DEM	digital elevation model	ROW	right-of-way
DSA	Drainage System Analysis	SPU	Seattle Public Utilities
DWW	Drainage and Wastewater	SWMM	Storm Water Management Model
EPA	Environmental Protection Agency	TM	technical memorandum
GIS	geographic information system	UTM	Universal Transverse Mercator
		WCA2D	Weighted Cellular Automata 2D

1. Introduction

Seattle Public Utilities (SPU) is completing a Drainage System Analysis (DSA) to provide data collection and technical analyses that support the development of the *Vision Plan* and *Integrated System Plan (ISP)* for the Drainage and Wastewater (DWW) line of business (LOB). The DSA will compile and update existing information related to SPU's drainage system and receiving waters, as well as perform new analyses that focus on flooding, climate change impacts, and water quality issues. The DSA efforts are divided into multiple topic areas, including a flooding topic area.

SPU contracted with Brown and Caldwell (Consultant) to perform technical analyses for the DSA flooding topic area. Key objectives for the flooding topic area include:

- Develop a prioritized inventory of drainage system capacity risk areas.
- Define Performance Thresholds for the drainage system and complete modeling to evaluate the capacity under existing and future conditions.
- Estimate inundation extent and develop risk maps for extreme storm events, sea level rise, and creek flooding.
- Estimate runoff and flow in areas served by ditches and culverts.
- Calculate flow metrics in creek watersheds and prioritize areas for runoff reduction to reduce erosive flows to creeks.

While some of the analyses completed for the flooding topic area are specific to the performance of SPU's drainage system, some, including this analysis, identify risks to the City that are beyond drainage system performance. SPU worked with the Consultant team to map the areas at risk of inundation due to extreme precipitation events (i.e., extreme storms). The analysis covers all areas of the city but is limited to existing conditions in terms of both watershed conditions and climate conditions. Key objectives include:

- Select two storms for the analysis
- Devise an efficient approach to simulating extreme storms and urban flooding at a city scale
- Perform a citywide modeling analysis for existing land cover conditions
- Map inundation areas for selected extreme storm events
- Perform geospatial analyses to develop a map of areas at risk of inundation during an extreme storm.

This technical memorandum (TM) describes technical methods and summarizes the results of the analyses conducted by the Consultant team. Section 2 describes the precipitation time series used to define the extreme storm events. Section 3 describes the technical methods for analyzing urban flooding. Section 4 summarizes the results of the citywide analyses. Section 5 describes the risk area analysis. Section 6 summarizes the risk area mapping results. Section 7 describes the limitations of the analysis.

2. Extreme Precipitation

Prolonged wet weather and extreme storms can overwhelm drainage systems and cause urban flooding. Extreme storms are complex phenomena. The amount of precipitation, spatial distribution, and intensities occurring within a single event can all vary greatly, affecting the extent and severity of the resultant flooding. Severe urban flooding can be caused by intense, short-duration rainfall events, prolonged wet periods fueled by atmospheric rivers¹, or a combination of both.

For the purposes of this analysis, SPU evaluated two extreme storm events and selected an observed 100-year event and a synthetic 1,000-year event. SPU developed rainfall time series (rainfall hyetograph) for the two selected events. The magnitude and severity of a storm event is inversely proportional to the likelihood of the event. The likelihood, or probability, of an event is typically specified as an annual exceedance probability, or alternatively as a return period or average recurrence interval².

2.1 Observed Storm Event from December 2007, 100-year

In December 2007, more than 5.6 inches of rain fell within a 24-hour period. Flooding was observed in several locations throughout the city, including the Thornton Creek basin (Figure 2-1), along Longfellow Creek, and in the Densmore area. The event is notable because it is one of the largest in recent history, as significant rainfall continued steadily for nearly 20 hours. The Consultant developed a 24-hour hyetograph for the December 2007 event based on 5-minute data collected at Rain Gage 12 (Magnolia), as shown in Figure 2-2.



Figure 2-1. 28th Ave NE in December 2007

¹ Atmospheric rivers are narrow regions or filaments of concentrated moisture within the atmosphere that transport water vapor from the tropics into areas outside of the tropics. Most extreme precipitation events that occur along the North American west coast are associated with winter atmospheric river events (Warner et al, 2015). The "Pineapple Express" is a well-known, strong atmospheric river condition that can bring substantial amounts of moisture from the tropics near Hawaii to the western coast of North America.

² Storm events are commonly expressed as having a specific return period or average recurrence interval that corresponds to the average period of time one would expect to observe between occurrences of equal or greater magnitude. Annual exceedance probabilities describe the statistical nature of storm frequency because they can be expressed in terms of chance, with each year being conceptualized independently. The annual exceedance probability for an event is equal to the reciprocal of the return period. Thus, a 100-year event has a 1 percent chance of being exceeded in any given year.

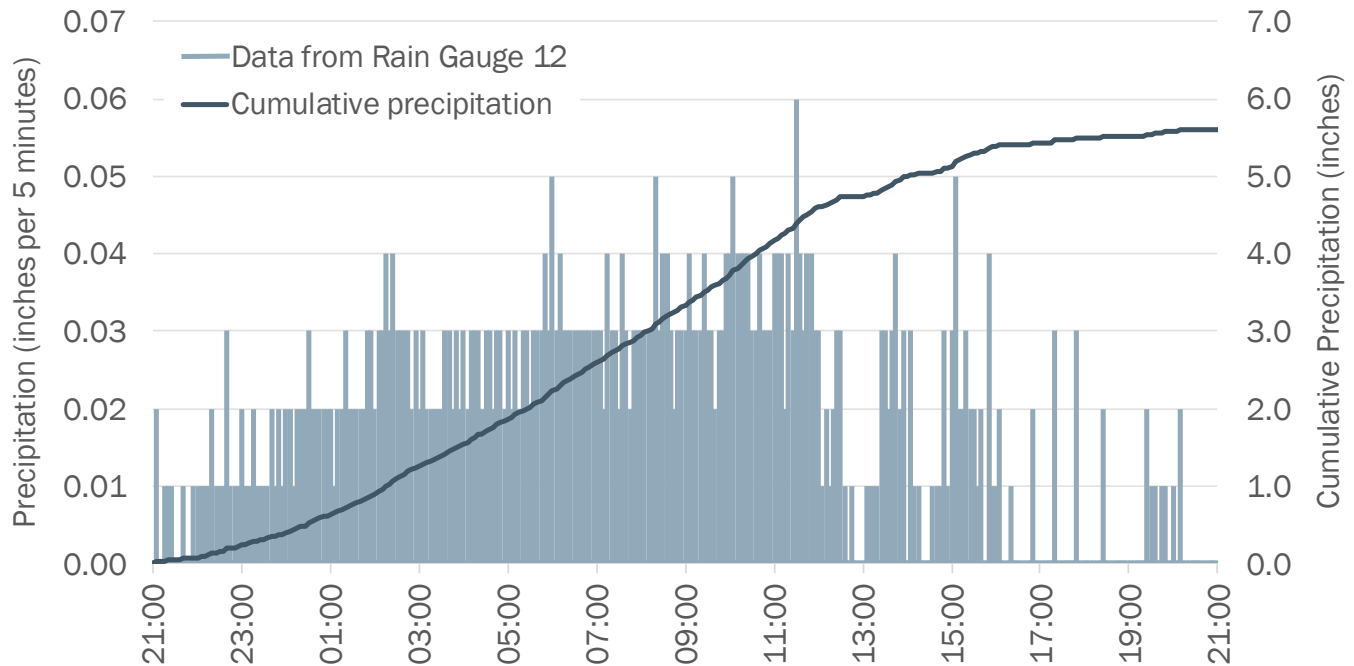


Figure 2-2. Hyetograph from observed rainfall on December 3, 2007

Tetra Tech (2017) developed intensity-duration-frequency (IDF) curves³ for the City covering the Seattle area and based on data collected from SPU's long-term rain gages. These IDF curves indicate that the December 2007 event was approximately equal to a 100-year storm (annual exceedance probability of 1 percent) in terms of the total amount of rainfall accumulated over 24 hours. However, the peak intensity and rainfall over shorter durations were not as extreme. For example, peak rainfall intensities averaged over 5-, 15-, and 30-minute durations were found to be closer to a 2-year event.

SPU selected this as one of the events to evaluate because it is a relatively recent historic event with an average recurrence interval commonly referred to as an extreme event.

2.2 Synthetic Storm Event, 1,000-year

SPU generated a synthetic hyetograph from 1,000-year IDF data using an alternating block methodology as described by Chow et al. (1988), where the peak 5-minute intensity is placed at the center of the hyetograph, and increments associated with longer durations (decreasing intensities) are placed before and after the central peak in an alternating manner. Incremental rainfall values were added until the event duration equaled 24 hours. Figure 2-3 shows a plot of the 1,000-year, 24-hour synthetic hyetograph and the corresponding cumulative precipitation curve.

³ IDF curves characterize the statistical relationship between the magnitude of rainfall occurring over a specified duration (or averaging period) and the expected frequency or exceedance probability. The probability, or likelihood, of an event can be specified in terms of an annual exceedance probability, or alternatively, as a return period or average recurrence interval. The annual exceedance probability is the reciprocal of the return period or average recurrence interval.

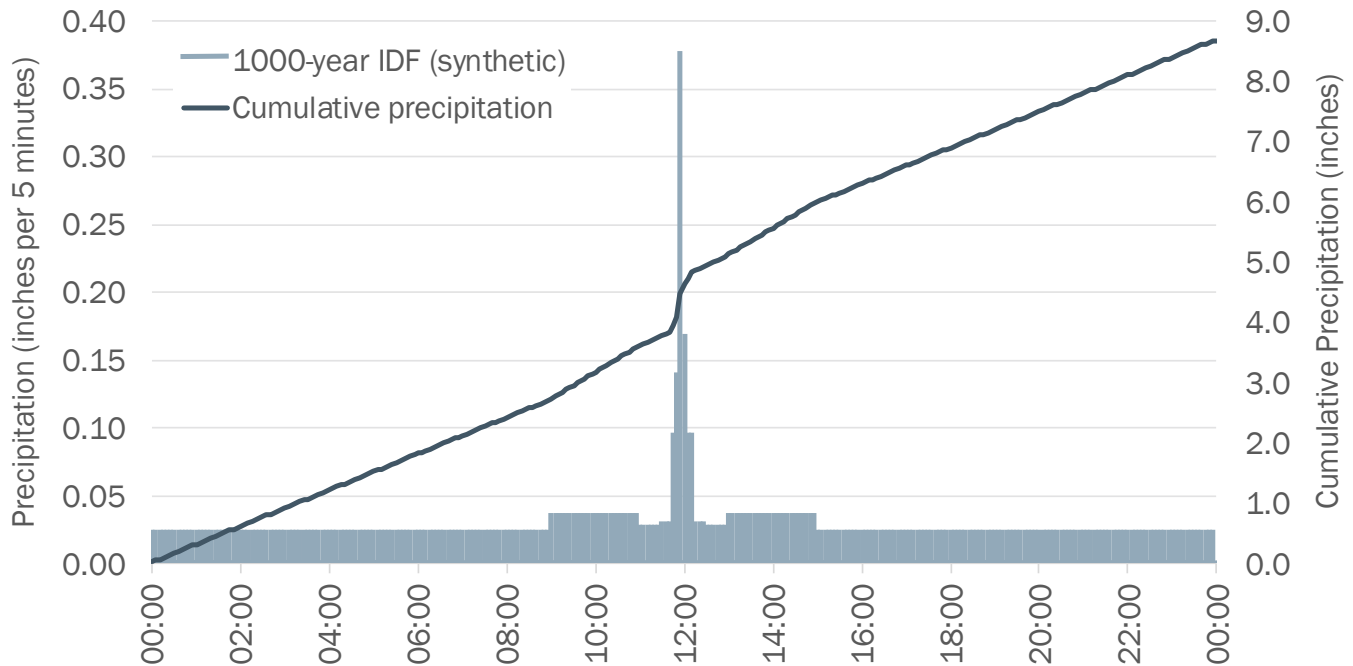


Figure 2-3. 1,000-year synthetic event hyetograph

An IDF-based synthetic storm event reflects a constant average recurrence interval across all durations. In other words, the peak 5-minute intensity has the same average recurrence interval as the total rainfall for the event. The advantage of this type of event is that it provides a consistent interpretation of likelihood, regardless of duration. This is particularly helpful given that the critical rainfall intensity or duration that causes flooding depends on several factors and is not the same for all basins or locations.

2.3 Event Frequency and Climate Change

The City's IDF curves are based on historical data, and while they may be reasonable for evaluating existing conditions, future conditions must be viewed within the context of climate change. Tetra Tech (2017) analyzed SPU's rain gage records and found statistically significant positive trends in extreme precipitation metrics, stating:

These trends in the SPU station extremes, based on the large volume of underlying data, provide strong quantitative support for anticipated changes in precipitation extremes over future decades in the SPU region. The general concept of increasing precipitation extremes is indicated through global climate model analysis, but the changes computed here are based on observed, local data, and provide credible support for consideration of such trends in future planning for infrastructure design by SPU. The rates of change can be used as calculated in this work, by extrapolation into the future, or, as a bookend for increases computed through the results of downscaled global climate model results.

While projected changes in annual and seasonal precipitation in the Seattle area are relatively small when compared with natural year-to-year variability (Mauger, 2015), changes in heavy precipitation events are expected to be much larger, exceeding the range of natural variability shortly after mid-century (Warner et al. 2015). Warner et al. (2015) asserts that winter-mean precipitation along the West Coast could increase

by 11 percent to 18 percent, and precipitation from atmospheric river events could increase by as much as 15 percent to 39 percent. Likewise, the frequency of the heaviest rainfall days (i.e., days above the historical 99th percentile threshold) could increase by as much as 290 percent by the end of this century (Warner et al. 2015). **Observed trends and projected increases in extreme precipitation suggest that the storm events used in this study will become more frequent in the future.**

3. Flooding Analysis

Extreme events produce runoff that is far greater than the design capacity of constructed drainage and combined systems. As a result, runoff may not enter the collection system and overflows might occur in multiple locations. Uncontrolled surface flows may be widespread, multidirectional, and without readily apparent flow paths. Therefore, a 2-dimensional (2D) horizontal flow analysis is required to analyze the surface flooding caused by extreme storms. For this study, the Consultant recommended a modeling approach that:

- Simulates surface flow hydraulics in two horizontal dimensions, especially where the flow paths and primary direction of flow are not apparent
- Recognizes obstructions caused by buildings that could dramatically affect flow depths and directions
- Can be performed rapidly and efficiently at a city scale (Figure 3-1), while still achieving the objectives of the analysis
- Modeling activities need to be deployed across teams to expedite the analysis and facilitate parallel workflow

SPU specified additional considerations for developing the modeling approach:

- Approach must work for all areas of the city regardless of system type (separated or combined sewers)
- Methods should account for infiltration losses and a portion of the runoff being conveyed by the collection systems
- Approach and methods must conform to schedule and budget constraints

Previous Modeling. SPU has developed and calibrated full hydrologic and hydraulic system models for their combined sewer and separated stormwater collections systems. These system models are based on the Stormwater Management Model (SWMM) developed by the U.S. Environmental Protection Agency (EPA)⁴ for simulating stormwater collection systems. SPU

developed the SWMM models for several reasons including evaluating the capacity and performance of the collection systems; however, these models were not intended to simulate surface flow and are not capable of running 2D simulations. Extreme storm simulations using 1D SWMM models can be used to identify system capacity deficiencies at specific locations with the drainage system; however, flooding on the surface



Figure 3-1. City scale for Seattle

The city of Seattle covers approximately 85 square miles; a 4-foot square grid covering the city consists of nearly 230 million grid cells.

⁴ SPU developed a total of 66 drainage basin models covering most of the separated and partially separated stormwater systems in the city. SPU also developed 13 combine sewer system basin models. The drainage system models and combined sewer system models consist of hydrologic basin elements as well as 1-dimensional (1D) hydraulic elements representing SPU collection system infrastructure such as pipes, ditches, maintenance holes, vaults, pump stations, weirs, and outfalls.

may occur at different locations because of the surface topography. Therefore, 1D SWMM modeling for extreme storms was not used to inform or validate inundation mapping for this analysis.

SPU often uses PCSWMM software to develop, modify, and run their SWMM models. PCSWMM functions as a user interface with standard EPA SWMM software, but it also provides ancillary data management and computational modules—including 2D modeling capabilities. SPU performed integrated 1D/2D modeling using its SWMM models and PCSWMM software for the Climate Resiliency Study (Aqualyze 2015), which was focused narrowly on low-lying areas that are vulnerable to sea level rise. The DSA Team recognized that city-scale 2D modeling using similar methods would be enormously challenging and time consuming.

Alternative Modeling Approach. Advanced modeling platforms designed for large-scale 2D flood modeling such as MIKE, SOBEK, TUFLOW, DFLOW, and FLO-2D offer coupled 1D/2D simulations and dynamic wave routing in two dimensions; however, these types of simulations are computationally intensive. Even with modern hardware, these models can require exorbitant time and effort to implement at a city scale. In addition, they are expensive and require licensing agreements that cannot be easily transferred from the Consultant to the City.

To meet the needs of this study, the Consultant devised a novel approach to urban flood modeling that simplifies the problem and emphasizes computational efficiency. The approach focuses on simplified 2D surface flow using a model called Weighted Cellular Automata 2D (WCA2D) developed at the University of Exeter (Guidolin et al. 2016). The overall modeling process used for this study consists of five fundamental steps, as shown on Figure 3-2.

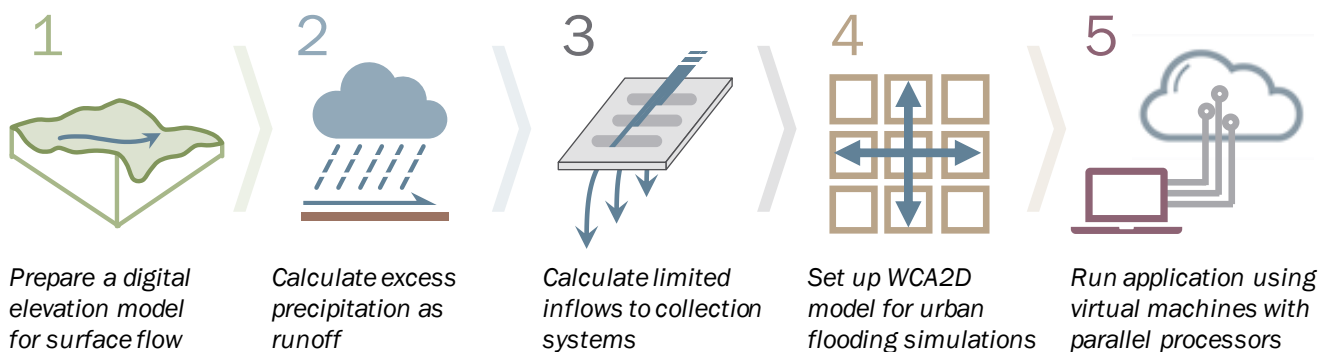


Figure 3-2. Process for modeling urban flooding for extreme storms

The modeling process shown in Figure 3-2 produces geospatial datasets representing peak water surface elevations and flooding depths. The following sections describe the modeling process in more detail. Section 4 describes how the modeling results were used for inundation and risk area mapping.

3.1 Digital Elevation Model

Geographic information systems (GIS) provide a standard spatial framework for modeling and mapping. The DSA Team used ESRI ArcGIS software as a platform for geospatial data management and analyses. ArcGIS uses “raster” datasets, where space is defined as an array of discrete cells and arranged in uniform rows and columns. Cells contain values representing characteristics of that location, such as the elevation of the earth surface. Topographic data are often stored in a raster format called a digital elevation model (DEM).

Quantum Spatial (2016) developed DEM datasets for the City of Seattle using topographic surveys collected and compiled by King County and the Puget Sound LiDAR⁵ Consortium. The DEM is based on a 2-foot grid resolution and projected into the State Plane coordinate system, North American Datum of 1983 (NAD83).

Even with rapid computational methods, the city had to be divided into basins to efficiently run the modeling analyses. The Consultant used the DEM to delineate watersheds, or surface basins, where surface water flows and accumulates according to the surface gradient⁶. The available DEM data extend beyond the city limits, which allowed the Consultant to delineate complete watersheds covering all areas of the city and discharging to a receiving water body, such as Elliot Bay, Lake Union, or Lake Washington. Figure 3-3 shows the 15 surface basins delineated for this study.

Once the surface basins were delineated, the Consultant prepared separate DEM grids for each basin, with “no data” values in all cells outside of the basin of interest. The Consultant modified the elevation grids for use with the WCA2D model, as follows:

- **Extrude Buildings.** Buildings are obstructions that can block and divert surface flows. Therefore, the Consultant used building planimetry (SPU geospatial data, 2015) to identify grid cells covered by buildings and then raised each block of “building” cells by approximately 10 feet.
- **Reduce Grid Resolution.** The Consultant assessed the tradeoffs between grid resolution and computational speeds and found that a 4-foot grid resolution offers a reasonable balance between precision and practical run times. Therefore, the DEM for each basin was resampled to 4-foot cells. Figure 3-4 shows an example area with various grid cell sizes.
- **Add Boundary Buffer.** The Consultant extended DEM grids to represent large water bodies at the boundaries (see Section 3.4.2 for more details).

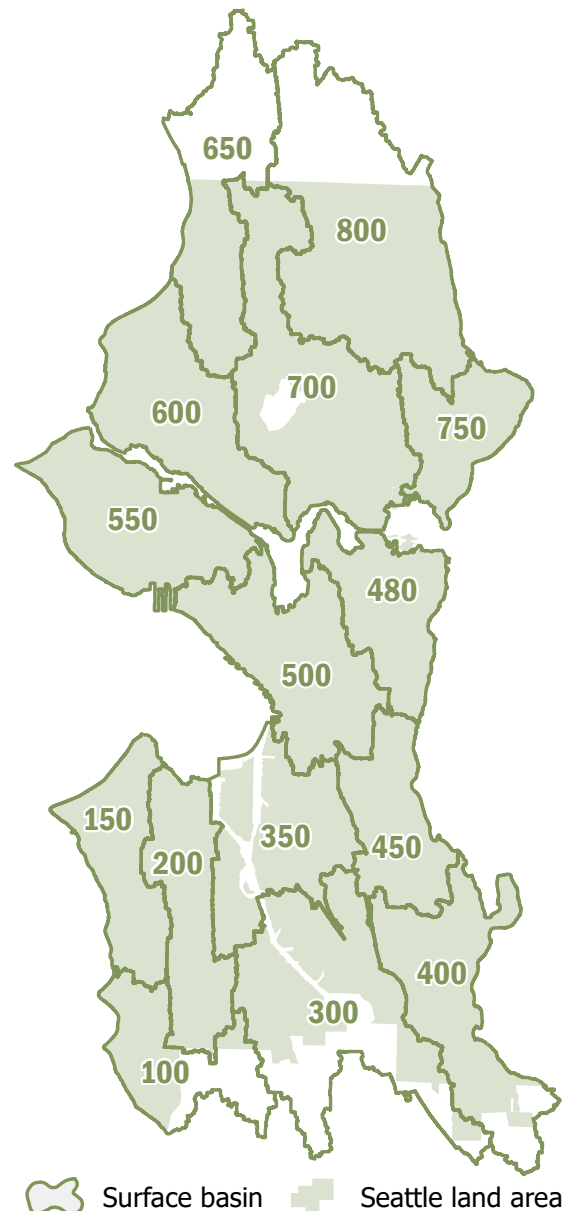
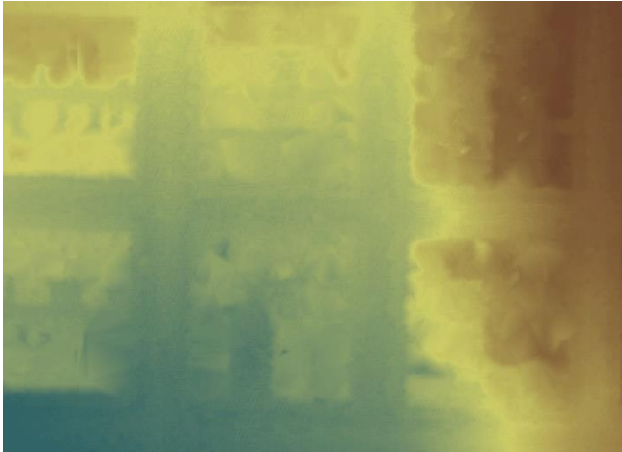


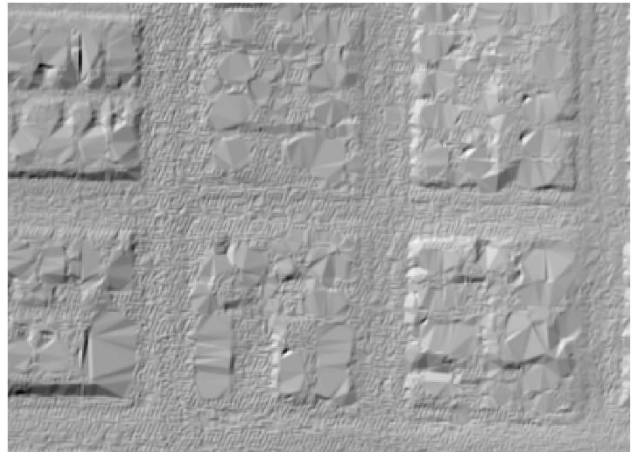
Figure 3-3. Surface Basins for Flood Modeling

⁵ Light Detection and Ranging (LiDAR) is a remote sensing method that uses an airborne scanning laser rangefinder to measure variable distances to the ground surface. Raw LiDAR survey data are processed to develop “bare earth” high-resolution digital surface models.

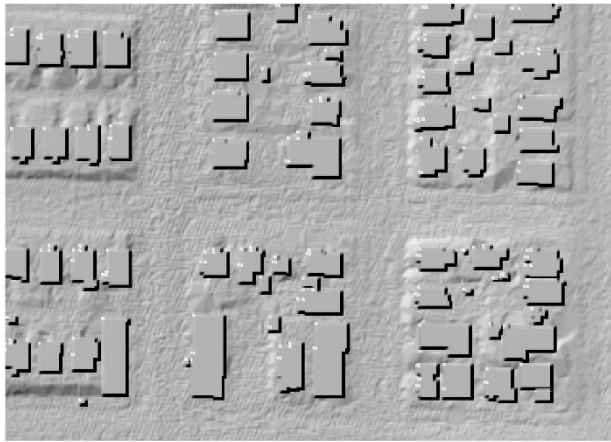
⁶ Surface basins do not align with collection system drainage basins because the latter are influenced by pipe networks.



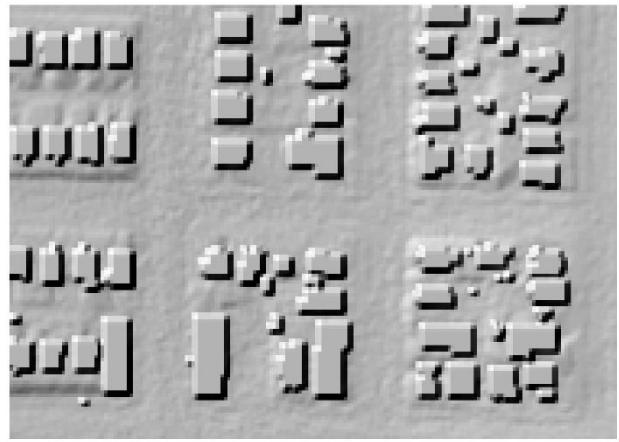
(a) Bare-earth DEM shaded by elevation at 2-foot grid resolution



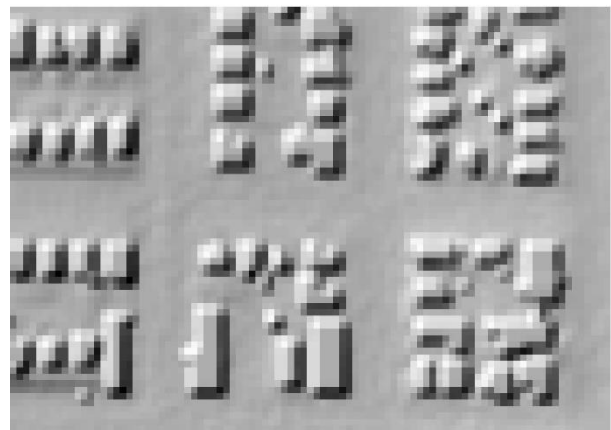
(b) Bare-earth DEM hillshade* at 2-foot grid resolution



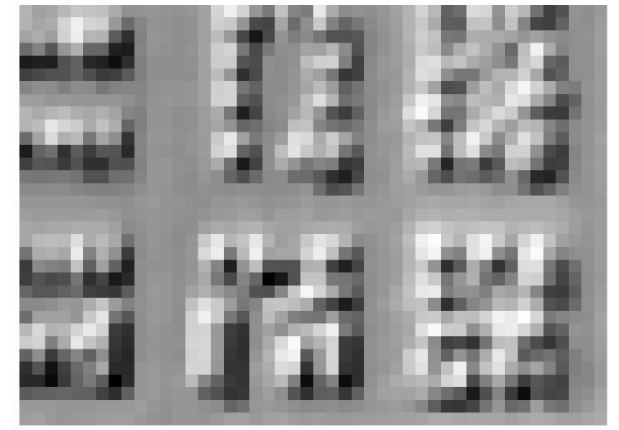
(c) DEM with extruded buildings at 2-foot grid resolution



(d) DEM with extruded buildings at 4-foot grid resolution**



(e) DEM with extruded buildings at 8-foot grid resolution



(f) DEM with extruded buildings at 16-foot grid resolution

Figure 3-4. Example area showing modified DEM grids

*Hillshade: a grayscale representation of a 3-dimensional surface where the shading imitates the relative position of the sun or light source.

**The modified DEM with 4-foot resolution was used for WCA2D modeling; 2, 8, and 16-foot resolutions are shown for comparison.

3.2 Excess Precipitation

When rain falls on a watershed it can be intercepted by vegetation, collect in surface depressions, infiltrate into the ground, or run off the surface (runoff). Runoff flowing over the land surface concentrates along low-lying areas, drainageways, and streams, and eventually discharges to a receiving water body. A rainfall-runoff model generally simulates the response of a watershed to rainfall by removing abstractions, or losses, such as interception, depression storage, and infiltration, and then converting the remaining “excess” precipitation to runoff. This section describes how the Consultant adjusted for losses to estimate the excess precipitation becoming runoff.

Initial abstractions. At the beginning of a rainfall event, interception storage and depression storage capture and retain water before excess precipitation is generated. The amount of rainfall that is intercepted depends on the coverage, density, and types of vegetation in the watershed; however, during large rainfall events in urban catchments, interception is relatively minor compared to infiltration rates, and quickly reduces to zero after rainfall begins. Similarly, small depressions in the urban landscape and low points in undulating terrain are considered relatively minor. Therefore, as a conservative assumption, the Consultant assumed that interception and small-depression storage are full, or effectively zero, at the onset of an extreme storm event. Note that medium and large depressions in the land surface do not need to be accounted for as losses because these features are represented in the DEM; thus, the storage effects are explicitly represented by the 2D hydraulic simulation of surface flows.

Infiltration model. Infiltration rates are highly variable and depend largely on pervious areas and underlying soil conditions. Green and Ampt (1911) developed a physically based infiltration loss function based on porous media characteristics. The Green-Ampt method is widely used for rainfall-runoff modeling because of its simple analytical solution and extensive studies by the United States Department of Agriculture (USDA) using pedotransfer functions that relate empirical data to hydraulic properties. The Green-Ampt equation is presented by Chow et al. (1988) as follows:

$$f(t) = K \left(\frac{\psi \Delta \theta}{F} + 1 \right)$$

where, $f(t)$ = infiltration rate as a function of time, F = cumulative infiltration, K = hydraulic conductivity of the soil, ψ = wetting front suction head, and $\Delta \theta$ = soil water gradient at the wetting front. Bouwer (1966) suggests using an effective hydraulic conductivity that is approximately half of the saturated hydraulic conductivity due to hysteresis observed in wetting and drying soil water retention curves. The soil water gradient is calculated from the effective saturation of the soil, which is the ratio between the available moisture and the maximum available moisture content (Chow et al. 1988):

$$\Delta \theta = \left(1 - \frac{\theta_i - \theta_r}{\eta - \theta_r} \right) \theta_e = \eta - \theta_i$$

where θ_i = initial soil water content, θ_r = residual soil water content, η = porosity, and $\theta_e = (\eta - \theta_r)$ = effective porosity. The initial soil water content depends on the antecedent moisture condition of the soil. For this study, the Consultant assumed the initial soil water content at the onset of an extreme event is approximately equal to the “field capacity” of the soil matrix (θ_{fc}), which is the moisture content retained in the soil after water has drained away by gravity.

The Consultant used Microsoft Excel to develop a Green-Ampt infiltration model and calculate pervious-area infiltration losses for each extreme storm event (impervious areas are assumed to have zero infiltration). Infiltration losses were calculated in 5-minute increments and subtracted from the incremental precipitation values in the hyetographs to obtain a new graph with only excess precipitation (see Figure 3-5).

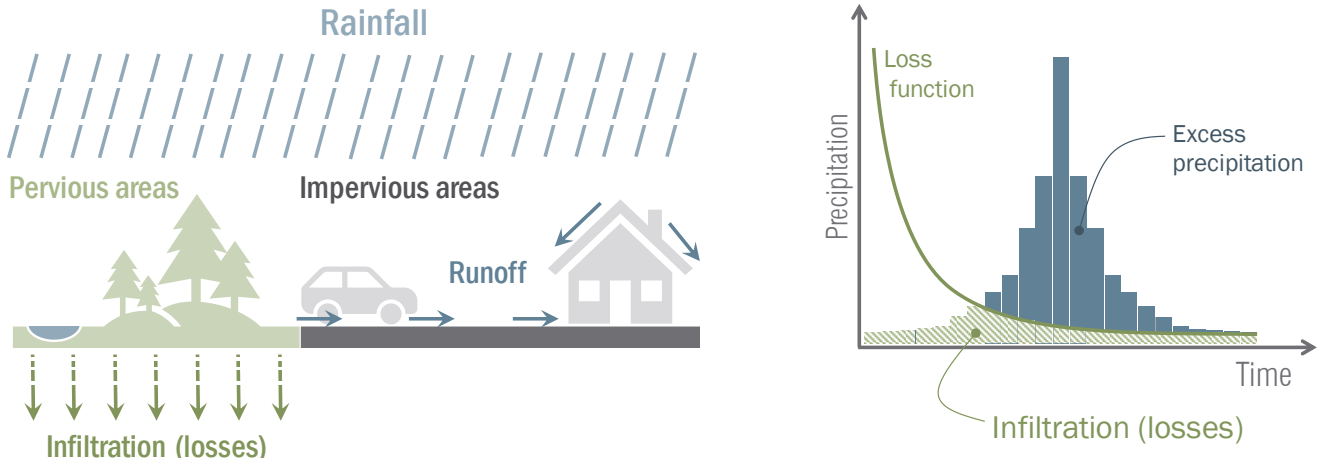


Figure 3-5. Schematic of infiltration losses and excess precipitation calculation

The Consultant converted the excess precipitation time series to rainfall input data for the WCA2D hydraulic model. WCA2D does not allow spatially variable rainfall inputs; thus, rainfall depths are assumed to be uniformly distributed across the basin. Given this limitation, the Consultant developed a basin-average rainfall time series, using area-weighted calculations for infiltration losses. Areal adjustment factors were determined for each basin as follows:

- Infiltration rates were reduced proportionally to account for the area covered by impervious surfaces, which are assumed to have zero infiltration.
- Infiltration loss rates for pervious areas were estimated based on the hydraulic properties of the soils found within the basin and the areas covered by the various soil types (see Appendix A for details).

Figure 3-6 shows the areas and percentages of impervious surfaces for each surface basin.

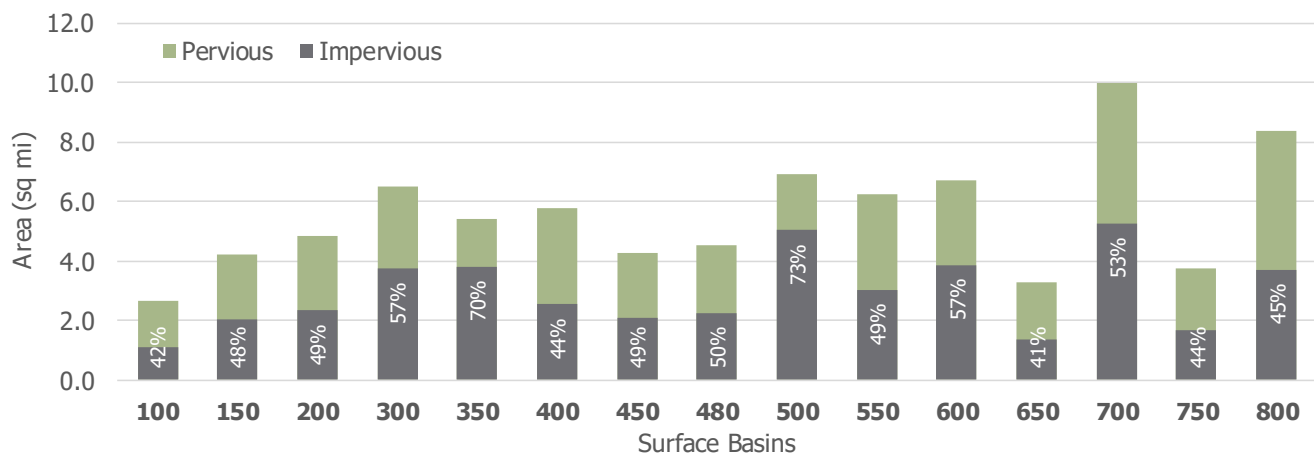


Figure 3-6. Surface basin areas and impervious area percentages

When estimating hydraulic properties for soils, the Consultant made assumptions that resulted in reasonably conservative estimates of hydraulic conductivity to account for the variability and uncertainty of such data.

3.3 Collection System Inflows

As described previously, the Consultant developed simplified and efficient modeling procedures to simulate flooding at city scale. Since the collection system, is likely to be overwhelmed during an extreme event, was not going to be explicitly modeled, the Consultant estimated inflows to the collection system, converted the flow rates to fluxes, and then removed the fluxes from excess precipitation. Figure 3-7 shows a schematic representation of system losses as analogous to infiltration losses.

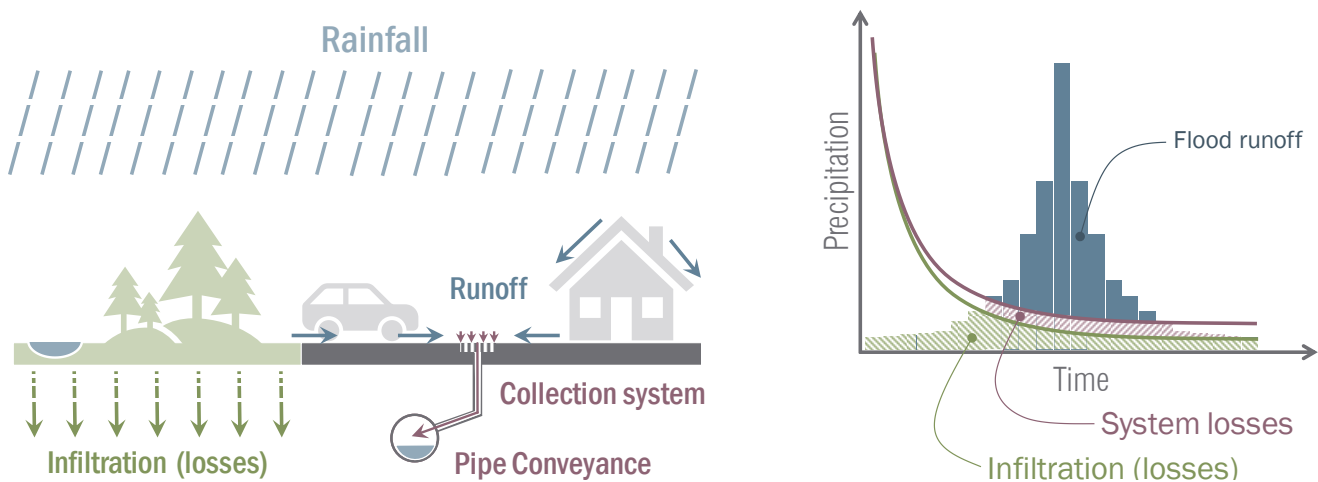


Figure 3-7. Schematic of infiltration losses and system losses

The Consultant estimated inflows to the collection system based on the number of inlets within each basin and a limited rate of inflow per inlet. Brown and Caldwell (2008) performed a rigorous modeling analysis for SPU for the Madison Valley area that included detailed calibration and validation of an extreme event that caused flooding in the basin. Brown and Caldwell found that “restrictions on the ability for surface flows to enter the collection system via storm inlets appear to be a major factor in the flow of water in street gutters to the low spots in the basin.” The study estimated inlet capacities based on the size of the conduit connecting each inlet to the main collection system, ranging from 0.25 cubic feet per second (cfs) for 4-inch conduits to 0.55 cfs for 12-inch conduits.

Brown and Caldwell (2008) goes on to describe how flows into collection systems are highly uncertain, stating that “the ability for storm water inflow to enter the collection system through storm inlets depends on the construction of the inlets, the steepness of the street surface, diameter and slope of the conduit connecting the storm inlet to the main sewers, the occurrence of sediment and debris on the inlet grate and in the basin itself, the air venting capacity of the sewer or drain near the connection, and other factors, including the elevation of the water surface in the collection system.” Inlets to SPU’s piped collection system vary widely in terms of age, condition, size, type, and configuration (see Figure 3-8). Even if the inlets were similar, the effectiveness and efficiency of each inlet can be affected by:

- The shape of the curb, gutter, roadway, or land surface diverting water toward the inlets
- Leaves, sediment, and other debris carried by stormwater runoff that lead to clogging
- The steepness of the roadway or surface where the inlet is installed



Figure 3-8. Examples of different inlets to SPU collection systems

Google Street View, Image Capture April, May, June, July 2019 (Google 2020)

Given the uncertainties associated with inlet capacities and possible conveyance constraints, the Consultant used a conservative approach to approximate flows at the inlets, accounting for multiple factors that could limit the flows into the collection system. The Consultant started by assuming a maximum inflow of 2.0 cfs per inlet based on a review of simple slotted stormwater grates and charts presented in the *Urban Drainage Design Manual* published by the Federal Highway Administration (FHWA 2009). The Consultant then reduced this value by an average efficiency factor of approximately 0.16, resulting in a reduced inlet inflow of 0.32 cfs, which is similar to the capacities estimated by Brown and Caldwell (2008). The Consultant then further reduced the inflows by a clogging factor of 0.5 based on research by Guo and McKenzie (2012), resulting in an average inflow of 0.16 cfs per inlet. Details and supporting calculations are provided in Appendix B.

While inflows to collection systems may be viewed as losses in upland areas, these flows return to the surface when collection systems discharge into open channels and streams. Therefore, in basins with significant discharges to streams, the Consultant used a simple transform function to calculate discharge hydrographs and add return flows to point locations in the WCA2D model. Additional information on the routing method is provided in Appendix C.

3.4 Urban Flooding Simulations

The WCA2D model (Guidolin et al. 2016) is the crux of this analysis. The model uses cellular automata⁷ (CA) to reduce computational overhead and perform exceptionally fast simulations of urban flooding. Researchers have made significant progress in the development of CA techniques for urban flooding applications (Chen et al. 2007; Dottori and Todini 2011; Chen et al. 2012; Ghimire et al. 2013; Jamali et al. 2019). In bench testing and real-world studies, Guidolin et al. (2016) demonstrated that WCA2D can run up to 8 times faster than commonly used hydrodynamic models and produce comparably accurate results.

The Centre for Water Systems at the University of Exeter has been developing CA applications as part of its Cellular Automata Dual-Drainage Simulation (CADDIES 2015) project. Ghimire et al. (2013) developed a CADDIES module that uses a von Neumann neighborhood⁸ to calculate flows in two horizontal dimensions. The model applies a simple method that ranks neighboring cells by water level and calculates flows between cells based on the hydraulic gradients between them (Figure 3-9). The flow rate from one cell to a neighboring cell is limited to a transferrable volume calculated by the Manning's formula and critical flow equations. Building on the work of Ghimire et al. (2013), Guidolin et al. (2016) developed the WCA2D model using similar techniques; however, the methods were modified to use a weight-based approach to calculate the ratios of water transferred to downstream neighbor cells.

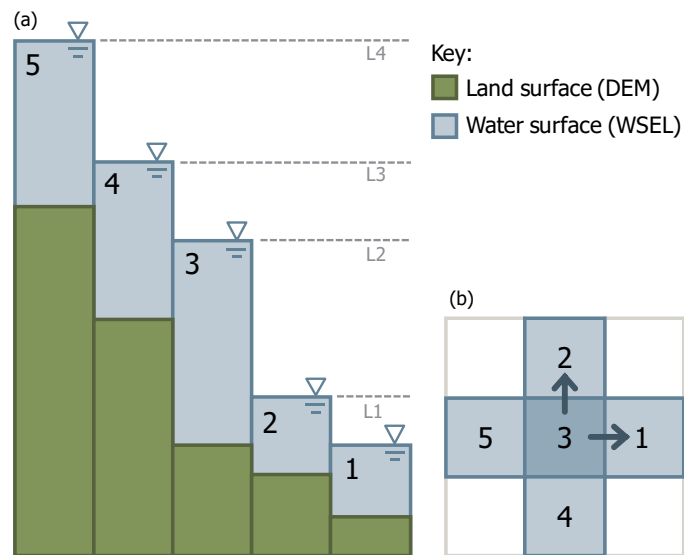


Figure 3-9. CA neighborhood used by CA2D and WCA2D

(a) Cells are ranked by water level differences; L1–L4 indicate layers of free spaces between two cells that are available for water distribution.

(b) Outflow fluxes from a central cell are shown by arrows.

WCA2D achieves rapid simulations by using simplified hydraulic computations. Hydrodynamic flood models typically solve shallow water equations⁹, which can be computationally intensive and often generate significant numerical instabilities. To overcome these challenges, models may reduce or neglect inertial (local acceleration) and advection (convective acceleration) terms where those factors are significantly less

⁷ Cellular automata (CA) are spatially and temporally discrete computational systems composed of a finite set of simple cells, or units. Each cell stores one or more state variables. The cells evolve in parallel at discrete time steps using update functions, or transition rules, based on the states of the adjacent cells within each cell's local neighborhood. CA models display complex emergent behavior, which has been found to be useful for simulating the spatial dynamics of physical systems (Itami 1994).

⁸ A von Neumann neighborhood is a two-dimensional square lattice with a central cell connected to four adjacent cells. This structure works well with gridded geospatial techniques where neighboring cells essentially align with cardinal directions.

⁹ Shallow water equations are partial differential equations for continuity and conservation of momentum solved in two horizontal dimensions (vertical velocity assumed to be zero). In one dimension, they are known as the Saint Venant equations.

than the effects of gravity, friction, and pressure—known as a diffusive wave approximation. WCA2D functions like a diffusive wave model, ignoring inertial terms and momentum conservation.

3.4.1 Model Grid

One of the major advantages of the WCA2D model is the straightforward approach to developing input data and setting up the model. In particular, the square grid used for CA computations is well-suited for geospatial computations, and DEM raster formats are readily compatible with the gridded inputs required by the model. Similarly, location-specific inputs can be referenced to cartesian coordinates (x, y) that are consistent with a projected geospatial coordinate system.

The Consultant used ArcGIS to convert the modified DEM (described in Section 3.1) to a standard ASCII¹⁰ grid format (Figure 3-10). While the grids must be rectangular, values can be flagged as “no data” using a value such as “-9999,” thereby removing those grid cells from the computations. This allows the computational grid to conform to the irregular shape of the delineated surface basin.

The WCA2D model uses metric units for all data inputs and outputs; therefore, the Consultant converted the horizontal and vertical units of the DEM to meters. As part of the conversion process, the Consultant re-projected the geospatial coordinate system to Universal Transverse Mercator (UTM), which is based on metric units.

```
ncols          4888
nrows          8372
xllcorner      548990.97313325
yllcorner      5280786.8092196
cellsize       1.2192024384049
NODATA_value   -9999
-9999 -9999 -9999 -9999 -9999 -9999...
-9999 -9999 -9999 -9999 -9999 -9999...
-9999 -9999 -9999 -9999 -9999 -9999...
-9999 -9999 -9999 -9999 -9999 -9999...
-9999 -9999 -9999 -9999 -9999 -9999...
-9999 -9999 -9999 -9999 -9999 -9999...
...
```

Figure 3-10. Example of an ASCII grid text file

Note: only a portion of the data are shown; the full example file contains values for 8372 columns and 4888 rows.

The Consultant also used ASCII text files to prepare input data for the excess precipitation time series and routed discharge hydrographs. As with the DEM, all values were converted to metric units. Section 3.5 (Running the Application) provides additional information on input data, files, and processes the Consultant used to run the WCA2D model.

3.4.2 Boundary Conditions

The current implementation of the WCA2D provides limited options for setting boundary conditions. One of the advantages of delineating large surface basins is that each basin discharges to a major water body, and thus avoids the need for internal boundaries along streams and drainage networks. Therefore, the Consultant needed to define boundaries for two conditions: upland/headwater cells and downslope receiving water cells.

The WCA2D model allows users to set a universal boundary elevation at all peripheral cells (i.e., cells with real values along the edges of the basin). Investigations by the Consultant found that the universal boundary elevation expands the computational grid by one cell in any open cardinal direction and assigns

¹⁰ American Standard Code for Information Interchange (ASCII) is a widely used character encoding standard that can be read and manipulated by any common text editor.

the boundary elevation to those cells. A very high elevation creates a closed boundary (acting like a wall). A very low elevation creates an open boundary, or free discharge (acting like a moat). The WCA2D model also allows users to set internal boundaries, where a cell or block of cells is assigned a water surface elevation (constant or variable).

Edge cells along the upland portions of surface basins primarily drain inward, so the boundary condition at those cells is inconsequential. In contrast, edge cells along receiving waters drain outward and must account for the elevation of the water body because it strongly influences flooding along shorelines and backwater at the mouths of streams.

Through a series of tests, the Consultant found that setting the universal boundary to the water surface elevation of the receiving water body does not treat the conditions appropriately. The cells added to the periphery are the end of computations, conserving mass and effectively trapping the water at the edge. The Consultant also found challenges with setting internal boundaries along irregular edges, where the model gave erroneous results.

Alternatively, the Consultant modified each DEM by adding a 300-foot buffer of cells along receiving water boundaries, with the elevations of those cells set to an assumed water surface elevation for the corresponding water body (Table 3-1).

Table 3-1. Water Surface Elevations for Water Bodies at Model Boundaries

Water body	Water surface elevation (feet NAVD 88)	Assumed condition
Lake Washington and Ship Canal (above the locks)	18.60	High operating level at locks
Puget Sound, Ship Canal (below locks), and Duwamish River	12.14	Highest recorded water level

The Consultant set universal boundary elevation low enough to create a free discharge around the edges of the basin, including the outer edge of the added receiving water buffer (Figure 3-11). The Consultant used an extremely low universal boundary elevation to circumvent the possibility of the boundary cells “filling up” with water during the simulation.

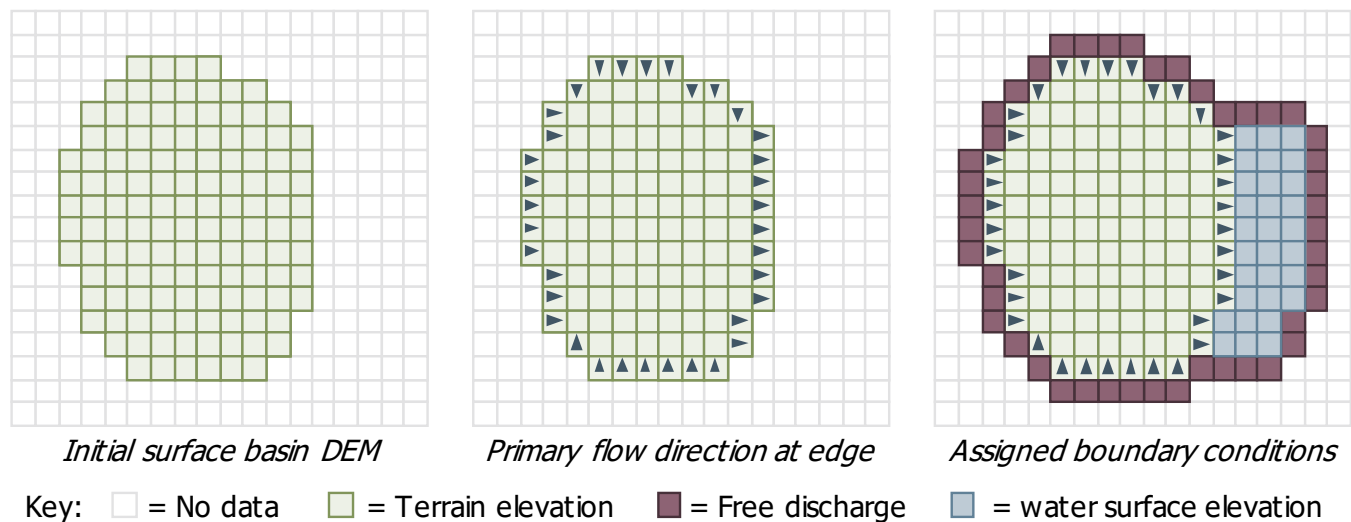


Figure 3-11. Schematic example of the computational grid and boundary conditions

3.4.3 Manning's Roughness

Manning's roughness is a dimensionless coefficient used to measure frictional resistance. Roughness values for overland flow depend on several factors including vegetation, obstructions, and irregularities along the surface. Roughness values for streets and paved areas ($n \approx 0.015$) are much less than roughness values for lawns, parks, or wooded areas ($n > 0.050$). Roughness values also vary depending on the depth of flow.

The application used to run the WCA2D model (see next section) does not allow users to input a spatially distributed Manning's roughness coefficient, but instead uses a single "global roughness" parameter. Given this limitation and considerable uncertainty, the Consultant conducted a sensitivity analysis of the global roughness parameter to determine a reasonable value. The Consultant selected two basins: (1) Basin 350, which has the flattest average surface slope, and (2) Basin 550, which has the steepest average surface slope. The Consultant then ran a series of 10 simulations with global roughness parameters ranging from 0.010 to 0.100 (Figure 3-12).

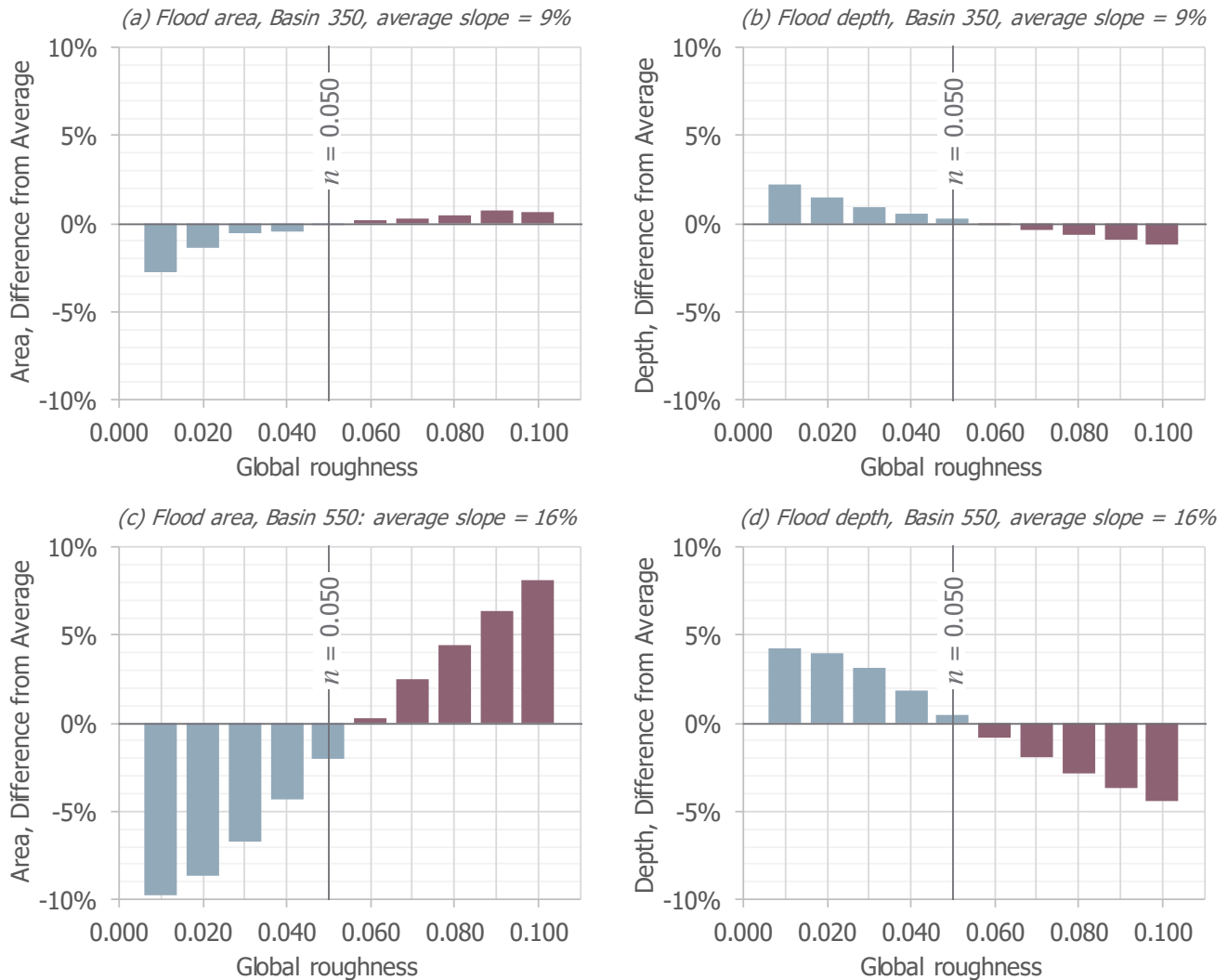


Figure 3-12. Summary plot from sensitivity testing of the global roughness parameter

Comparison of inundated area and average flooding depth; percent difference values based on average results for 10 simulations

The results in Figure 3-12 indicate that flooding inundation increases with increasing Manning's roughness values; however, the variability depends on the slope of the basin. In a basin with relatively flat slopes (approximately 9 percent), the inundated area varied by ± 3 percent when compared with the average result. In a basin with steep slopes (approximately 16 percent), the inundated area varied by ± 10 percent compared with the average.

Conversely, the average depth of flooding decreased with increasing Manning's roughness values due to wider areas of shallow spreading. In a relatively flat basin (approximately 9 percent), the depth varied by about ± 3 percent compared with the average. In a basin with steep slopes (approximately 16 percent), the depth varied by about ± 5 percent compared with the average.

Based on the results of the sensitivity analysis, the Consultant selected a moderate global roughness value of 0.050 for all surface basins. While this global value may be low for wooded areas with dense vegetation, it is considered high for most other areas of the city, especially open streets and paved surfaces.

3.5 Running the Application

The Consultant worked with researchers at the University of Exeter to obtain the code for the WCA2 model, as well as a compiled executable application called CAFlood for running the model. The CAFlood application uses the CADDIES Application Programming Interface (API) to implement the WCA2D model in a structure that facilitates parallel computing and high-performance acceleration techniques (Guidolin et al. 2016). Specifically, the CAFlood application used for this study (Gibson 2019) uses the OpenCL library (Munshi 2011) to run simulations via parallel computing on a graphics processing units (GPU).

Setting up run files. Users run the CAFlood executable at the command prompt by calling the WCA2D model, specifying the setup file, and listing the paths to input and output directories. The setup file provides a list of commands, input filenames, output filenames, instructions, and parameters needed to run a simulation (see Appendix D for an example and detailed discussion of parameters). Figure 3-13 illustrates the links between the setup file and the other input files called by the simulation. Input data development for DEM, precipitation, and discharge files were described in previous sections. Output specification files can produce any number of grids or time series files.

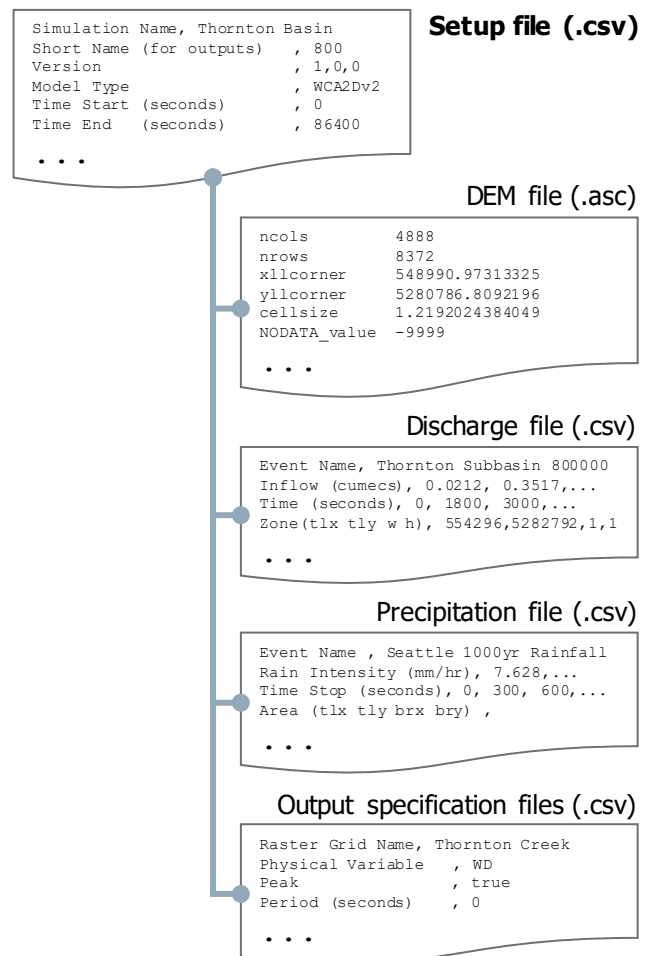


Figure 3-13. Input files used to run CAFlood
.asc = ASCII file, .csv = comma separated variable file

Scaling up and reducing run times. The Consultant began running small test simulations using small grid areas at low resolution and then worked to scale up to full basin simulations. Model simulations were initially run on personal computers (PC) with multicore central processing units (CPU); however, full simulations on standard PCs are impractical due to excessively long run times. To address this, Consultant migrated the simulations to cloud-based virtual machines configured with GPUs¹¹. This shift from serial computing to parallel computing accelerated run times by as much as 90 percent and allowed the Consultant to scale-up to full basin runs at 4-foot resolution while keeping individual run times manageable. Table 3-2 shows model grid sizes for each basin and the final run times.

Basin	DEM grid				Model run time ^a (hr)	
	Columns	Rows	Cells (millions)	File size (MB)	100-yr	1,000-yr
100	4,158	4,002	16.6	118	2.7	2.7
150	2,940	5,918	17.4	123	0.8	1.1
200	2,396	6,846	16.4	120	3.2	3.3
300	6,124	6,958	42.6	297	6.5	5.9
350	3,749	5,529	20.7	150	4.1	3.6
400	4,534	7,488	34.0	232	5.2	5.7
450	2,974	5,216	15.5	112	1.5	1.8
480	3,499	4,942	17.3	124	2.1	2.3
500	5,131	5,530	28.4	200	2.0	3.3
550	5,696	4,315	24.6	175	2.0	2.8
600	4,869	6,322	30.8	214	2.4	3.2
650	2,918	8,432	24.6	178	4.5	4.8
700	4,760	8,274	39.4	280	6.8	7.7
750	3,254	4,150	13.5	98	1.4	1.8
800	4,888	8,372	40.9	300	8.2	9.0

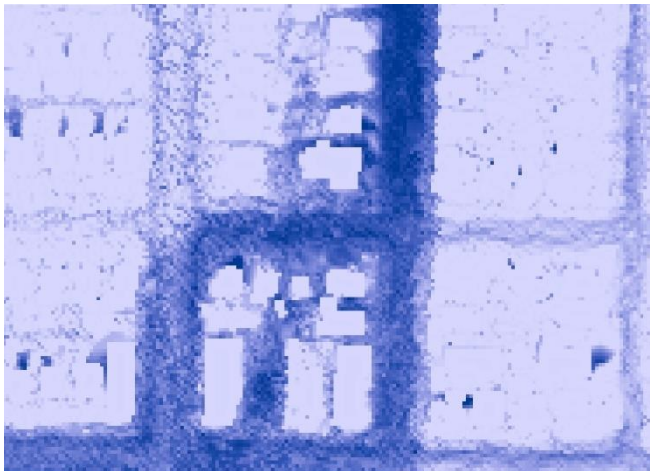
a. Simulated time for each event is 54 hours; 24 hours of rainfall followed by 30 additional hours for flow routing.

Generating output. Three output files were generated for each model run: peak velocity, peak water surface elevation, and a peak water depth. The Consultant converted the peak depth grids from ASCII format to ArcGIS raster format and re-projected the data from UTM coordinates to a State Plane coordinate system with units of feet. The results for each surface basin were merged into a citywide raster—one for each extreme storm event. The Consultant used the citywide peak depth grids to map flooding inundation, delineate the risk area for extreme storms, and perform spatially distributed risk mapping.

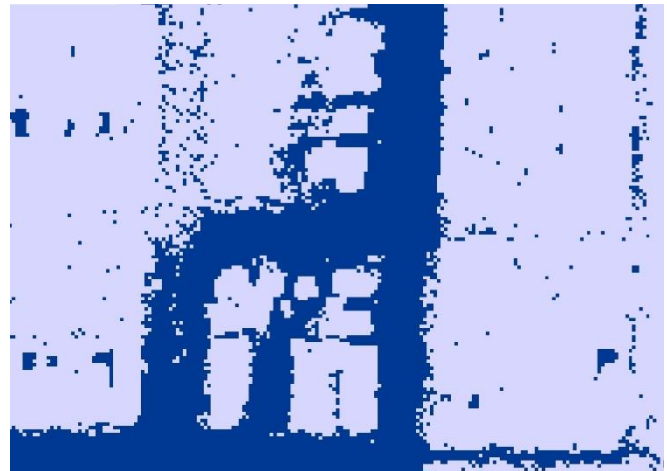
¹¹ The Consultant used virtual machine instances configured with a NVIDIA Tesla V100 GPU to run the CAFlood application, compiled with the OpenCL library.

4. Inundation Mapping

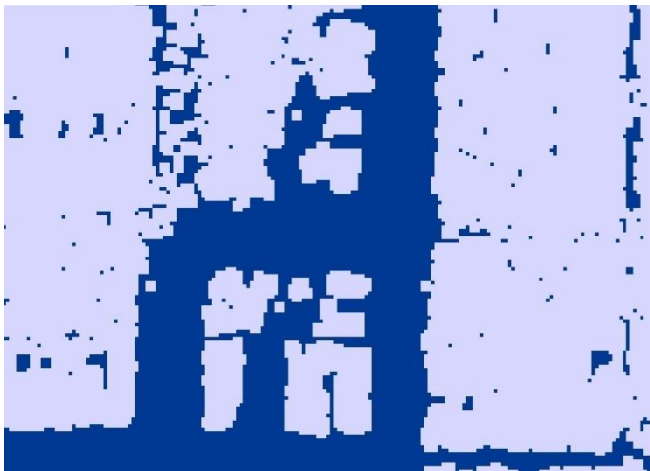
The Consultant prepared citywide peak flooding depth grids for the 100-year and 1,000-year extreme storm events. Nearly every grid cell has a positive depth because rainfall is distributed over the entire model domain. Therefore, a minimum depth threshold of 0.5 feet was used to remove shallow flooding from the inundation area. Consequently, the areas where the peak flooding depth for the 1,000-year event (the larger of the two events) equaled or exceeded 0.5 feet defined the maximum inundation area for this analysis, and thus, the extent of the risk area. However, the Consultant also refined the inundation boundaries as illustrated in Figure 4-1, which results in some small areas with depths less than 0.5 feet.



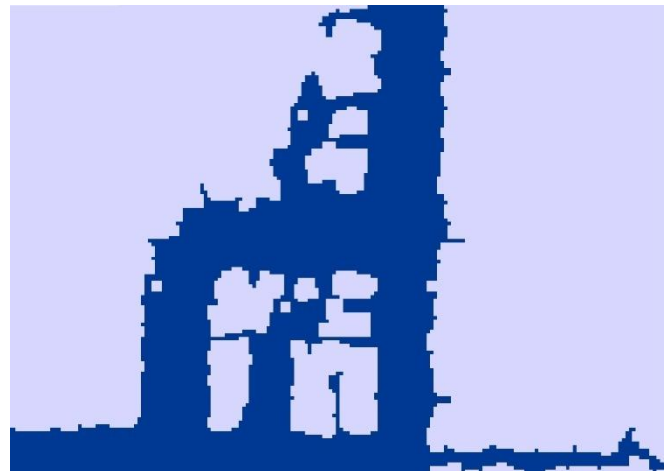
(a) Peak water depth grid with calculated values in units of feet



(b) Dark areas show peak depths greater than or equal to 0.5 feet



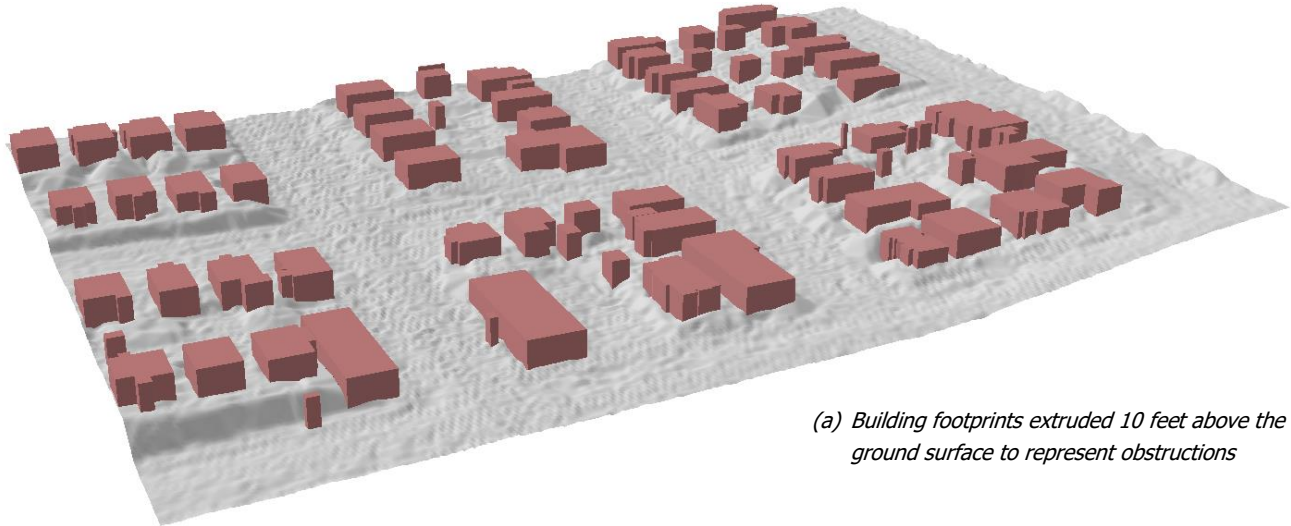
(c) Dark areas show refined inundation area after a GIS "boundary clean" process that fills and aggregates cells along the fringes.



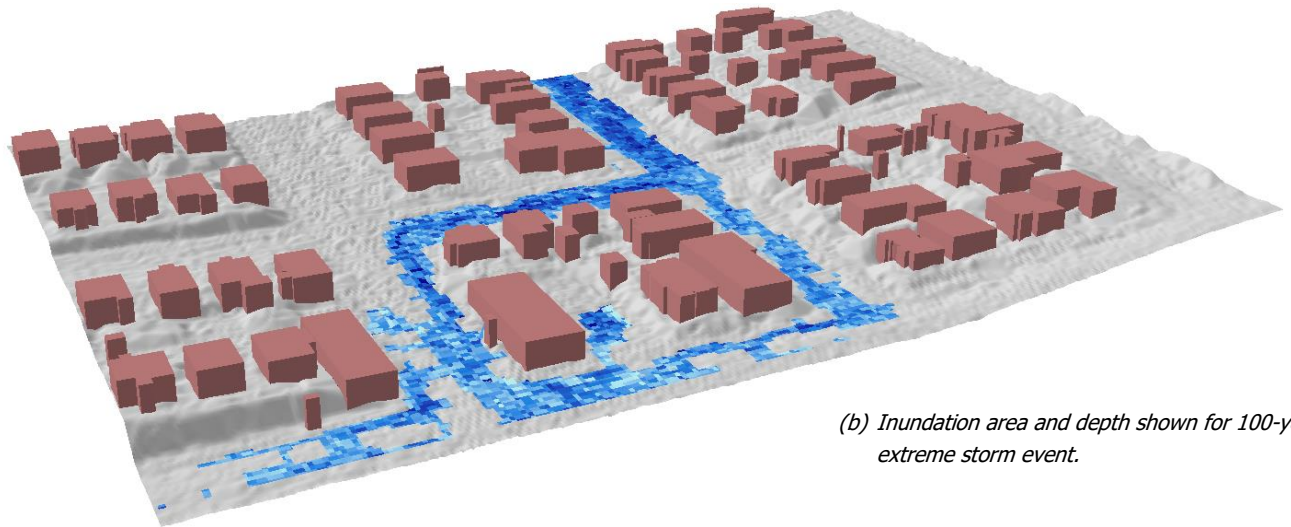
(d) Dark areas show refined inundation area after removing small isolated "ponds" with aggregated areas less than 5,000 square feet.

Figure 4-1. Example of the process used to define the extent of flood inundation for the 1,000-year event

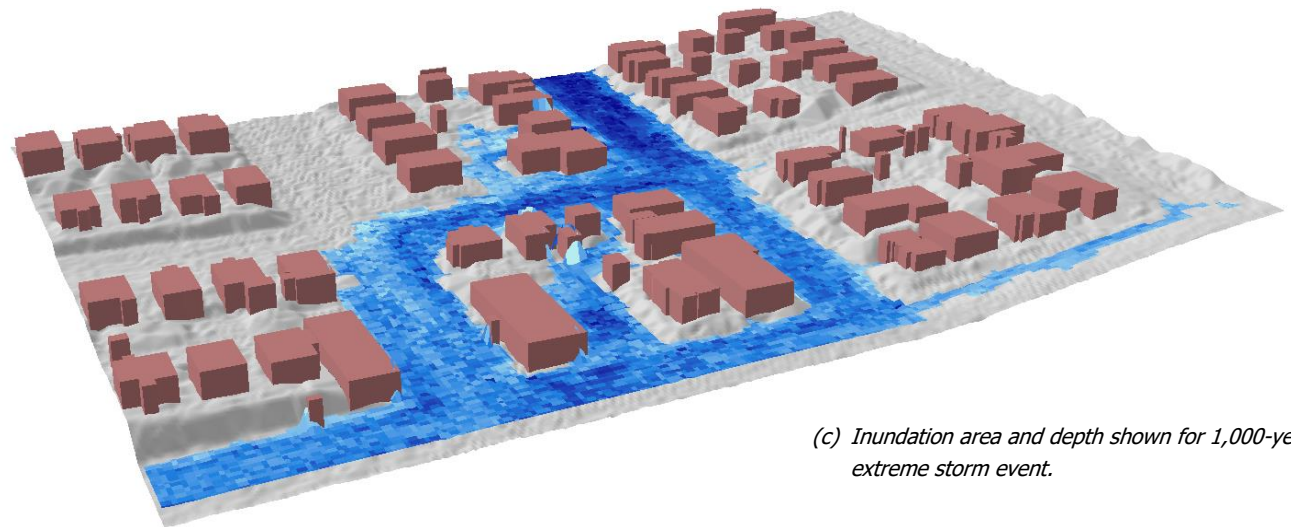
The Consultant generated new flooding depth grids, where calculated peak flooding depths were retained within the refined inundation area (after boundary cleaning and removing ponds). Cells outside of the refined inundation area were changed to null values (no data). Note that the inundation maps (Figure 4-1) show building footprints because they represent obstructions in the model and will not be shown as inundated. Figure 4-2 shows an oblique view for the example area with buildings extruded 10 feet.



(a) Building footprints extruded 10 feet above the ground surface to represent obstructions



(b) Inundation area and depth shown for 100-year extreme storm event.



(c) Inundation area and depth shown for 1,000-year extreme storm event.

Figure 4-2. Inundation areas and depths shown for example area with buildings

Comparison with observed flooding. After the December 2007 storm, SPU collected information on observed and reported flooding locations. The Consultant compared this information with the inundation results for the 100-year simulations and found excellent and consistent agreement. The simulated inundation results confirmed flooding was likely to have occurred along Longfellow Creek, Thornton Creek, near Haller Lake, Licton Springs, Pinehurst, and around Lake City.

Historical waterways. Seattle lies on a narrow strip of land between Puget Sound and Lake Washington. Since white settlers came to the area in 1851, the city has developed over hills and around water bodies, altering the landscape and covering many of the historical waterways. Modeling indicates that if an extreme storm occurs and exceeds the capacity of the drainage infrastructure, waters tend to flow and accumulate along these historical waterways. With this in mind, the DSA Team reviewed the 100-year extreme storm inundation extents in relation to historical streams, waterbodies, tidelands, and wetlands. Figure 4-3 shows an example area where extreme storm flooding roughly coincides with historical waterways. Appendix G shows 100-year inundation areas mapped with historical water features.

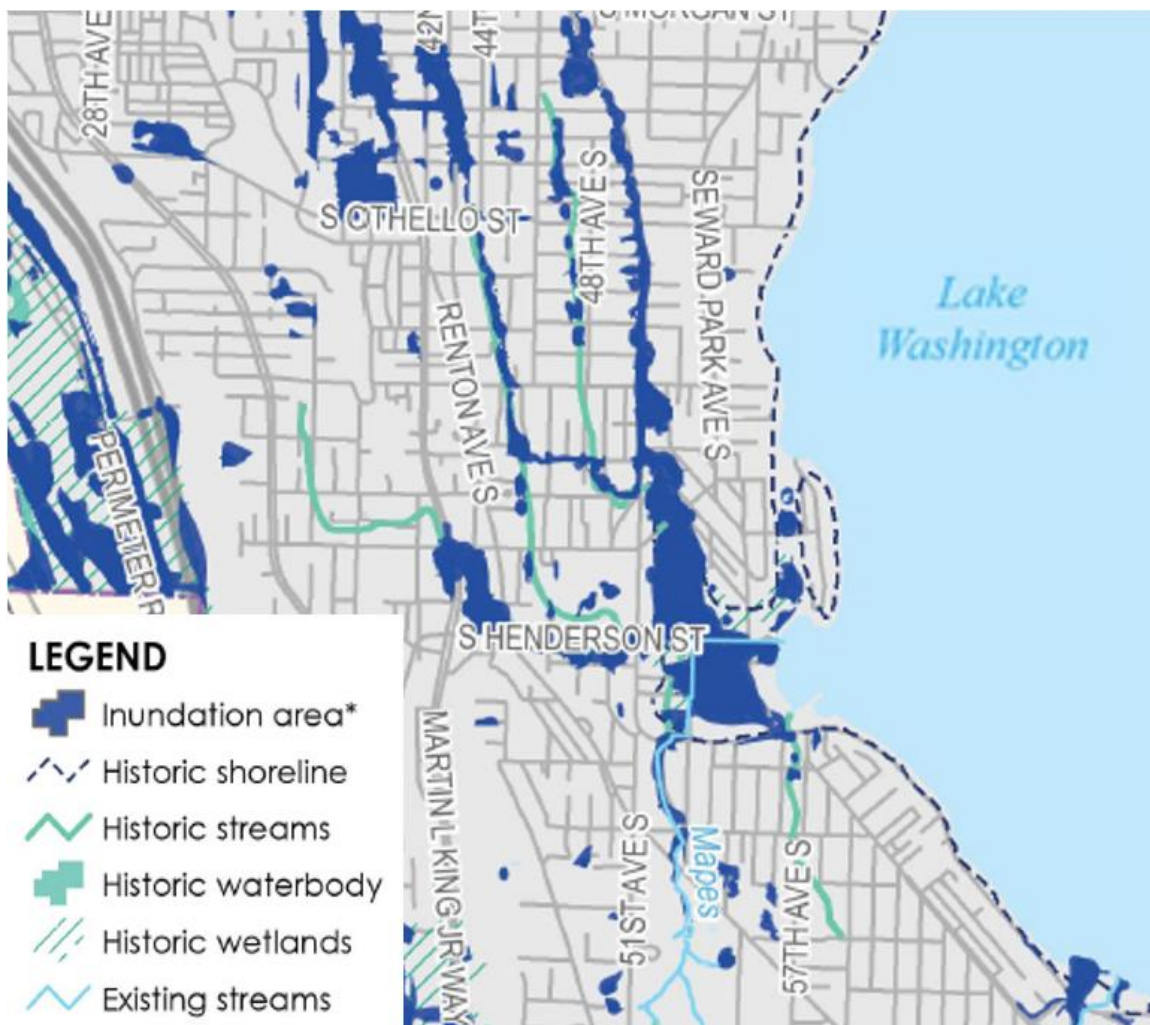


Figure 4-3. Example of simulated 100-year storm inundation compared with historical waterways

*The area of the city shown here is near the outlet for Mapes Creek. Inundation areas for the 100-year extreme storm event roughly align with historical streams, historical wetlands, and areas beyond the historical shoreline for Lake Washington. *Simulated inundation area shown.*

5. Risk Scoring

SPU developed an approach to calculating risk scores based on factors of consequence, likelihood, and equity. Scoring methods and criteria were developed based on methods outlined in SPU's *Risk Assessment Framework* (SPU 2007), staff subject matter expertise, and a review of past prioritization criteria developed and applied by SPU (SPU 2020). The basic equation for calculating risk scores is:

$$\text{Risk Score} = (\text{Consequence Score} \times \text{Likelihood Score}) + \text{Equity Score}$$

where the sum of all consequence scores does not exceed 5; the likelihood score ranges between 1 and 5, and the equity score ranges between 1 and 5. The resultant maximum risk score is 30. The following sections describe the scoring process based on component scores for the consequence, likelihood, and equity. Detailed workflow charts of GIS processes for scoring and risk mapping are provided in Appendix E.

5.1 Consequence Score

The Consultant used the depth and inundation grids described in Section 4 and other consequence data to calculate consequence scores. The consequence score for any single location (i.e., a 4-ft-by-4-ft cell within a spatial grid) was calculated by adding a score associated with the depth of inundation (depth score) with three other component scores related to areas with potentially high consequences of flooding: high-use areas, critical facilities, and major transportation routes.

$$\begin{aligned} \text{Consequence Score} \\ &= \text{Depth Score} + \text{High-Use Area Score} + \text{Critical Facility Score} \\ &\quad + \text{Major Transportation Route Score} \end{aligned}$$

The Consultant calculated depth scores using the relationship shown in Figure 5-1, where a peak flooding depth of 0.5 ft receives a score of 1, a flooding depth of 1.0 ft receives a score of 2, and a flooding depth of 3.0 ft or greater receives a score of 3. Scores for flooding depths between these points were determined by linear interpolation.

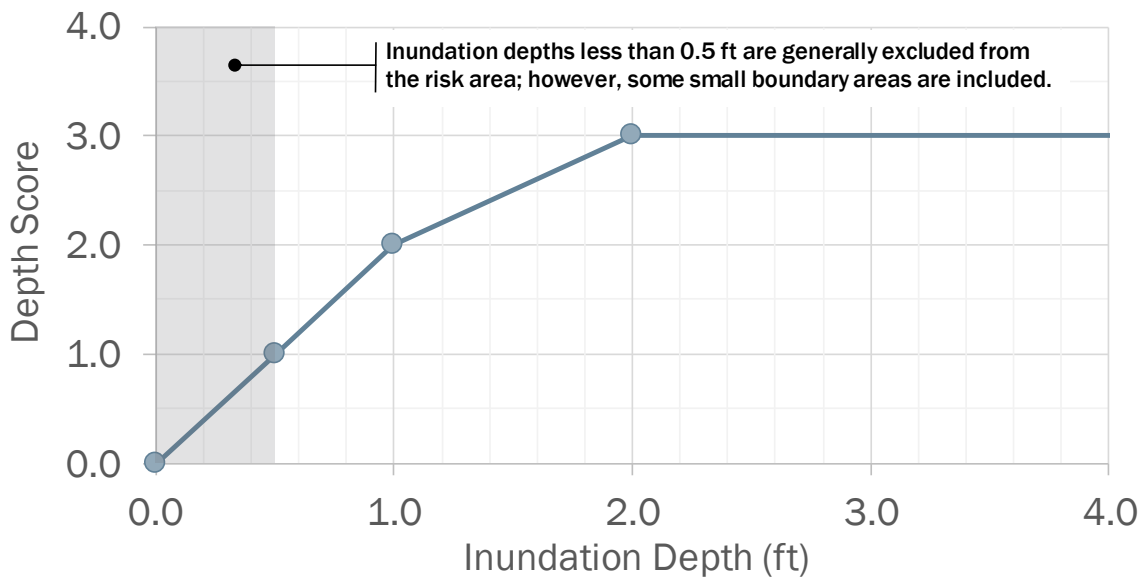


Figure 5-1. Relationship between inundation depth and depth score

Using the same 4-ft grid system as the inundation data, the Consultant developed citywide geospatial grids with scores for each of the three other consequence component datasets:

- **High-use areas.** SPU provided the Consultant team with geospatial data representing areas likely to have a large number of pedestrians traveling through, relative to other areas of the city. These data consist of polygons representing areas with high pedestrian usage and polylines representing Neighborhood Greenways. The Consultant converted the latter to polygons based on the width of the right-of-way (ROW) and then merged with the high pedestrian usage areas to create a single high-use areas dataset. A binary grid was developed by giving grid cells with centroids falling within the mapped high-use areas a value of one (1) and all other cells were given a value of zero (0). Spatially distributed scores were then calculated by multiplying the binary grid by a value of 0.5, assigning high-use areas a consequence score of 0.5.
- **Critical facilities.** SPU provided the Consultant team with geospatial point locations representing critical facilities. The Consultant team downloaded polygons comprising King County's parcel data (King County 2018). Parcel polygon features containing one or more critical facility data points were selected. A binary grid was developed by giving grid cells with centroids falling within the selected parcel areas a value of one (1) and all other cells were given a value of zero (0). Spatially distributed scores were then calculated by multiplying the binary grid by a value of 1.5, assigning critical facilities a consequence score of 1.5.
- **Major transportation route.** SPU provided the Consultant with geospatial polylines representing snow and ice routes for Seattle Department of Transportation, which are indicative of the major arterials within the city. In addition, lines associated with freeways (e.g., Interstate 5, Interstate 90, and State Route 520) were selected from the City's streets geodatabase. All polylines were converted to polygons using the ROW width. A binary grid was developed by giving grid cells with centroids falling within the resulting polygons a value of one (1) and all other cells were given a value of zero (0). Spatially distributed scores were then calculated by multiplying the binary grid by a value of 1.5, assigning major transportation routes a consequence score of 1.5.

Table 5-1 summarizes the component scores used to calculate combined consequence score.

Table 5-1. Summary of Components of Consequence Score	
Component	Score
High-use area	0.5
Critical facility	1.5
Major transportation route	1.5

Parcel data (used to map critical facilities) do not overlap with ROW areas (used to map major transportation routes); therefore, a maximum score between critical facilities and major transportation routes is 1.5. Descriptions of the data provided by SPU are provided in Appendix E. Details regarding the GIS processes used to develop these layers are provided in Appendix E.

The Consultant used the citywide geospatial grids of the component scores described above to perform geospatial analyses (i.e., raster math) to calculate a citywide grid representing the consequence score for each extreme storm event. The consequence score varies from 0 to 5, representing an area (a) with an inundation depth of at least 3 feet, (b) on a parcel with a critical facility or within the ROW of a major transportation route and (c) within a high-use area.

5.2 Frequency Score

The risk associated with an extreme storm event increases with the probability, or likelihood, of occurrence. As described in Section 2, the annual recurrence interval is the reciprocal of the annual exceedance probability; thus, the 100-year event is more likely than the 1,000-year event. Accordingly, the DSA Team assigned a higher frequency score to area inundated by the 100-year event than areas only inundated by the 1,000-year event. Table 5-2 lists the storm events and the selected frequency scores.

Table 5-2. Frequency Scores for Extreme Storm Risk Mapping				
Storm Event				Frequency score
Hyetograph	Average recurrence interval ^a	Annual probability ^a	24-hour rainfall depth (inches)	
December 2007 rainfall	100 years	0.01	5.61	5
Synthetic (from IDF curve)	1,000 years	0.001	8.69	1

a. Based on IDF curves from Tetra Tech (2017) representing existing climate conditions. Observed trends and projected increases in extreme precipitation suggest that the storm events used in this study will become more frequent in the future.

5.3 Equity score

An equity score is included to acknowledge that areas of racial and socioeconomic disparity are at a relative disadvantage to recover from an extreme storm event. The City's Office of Planning and Community Development (OPCD) created a Racial and Social Equity Composite Index and associated geospatial mapping for all City departments to use, which has polygons representing 136 census tracts throughout the city. When developing these data, OPCD assigned an index to tracts based on racial diversity, demographics, health outcomes, and socioeconomic factors provided by the U.S. Census Bureau, American Community Survey, Centers for Disease Control and Prevention, and Washington State public health agencies. The range of indices was divided into five equity categories that reflect relative levels of disadvantage. For the DSA, the tracts with the highest level of disadvantage were assigned a score of 5. The tracts with the lowest level of disadvantage were assigned a score of 1. Table 5-3 provides the equity score for each level of disadvantage.

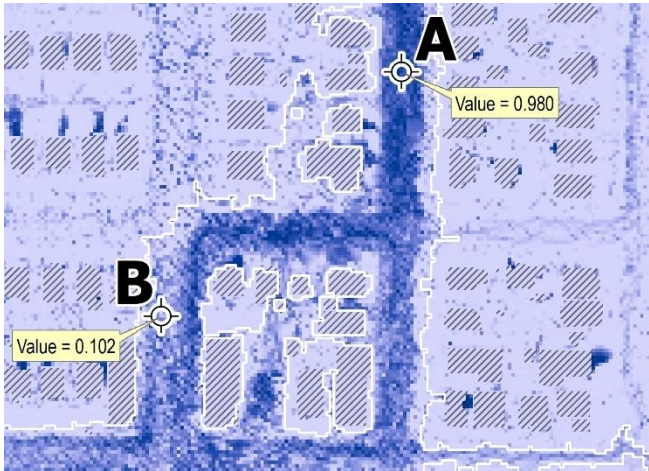
Table 5-3. Equity Scores for the DSA

Level of disadvantage	Equity score
Highest	5
Second highest	4
Middle	3
Second lowest	2
Lowest	1

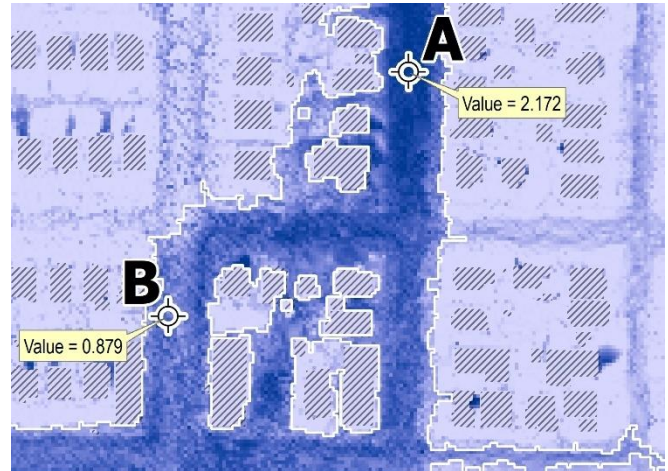
When the risk score method was developed for the wastewater system capacity evaluation completed as part of the Wastewater System Analysis (WWSA), the equity score could have been incorporated into the consequence criteria. SPU, however, decided to separate it out so that it could have greater influence on the risk score. SPU adopted the same risk score method for the DSA.

5.4 Example risk score calculations

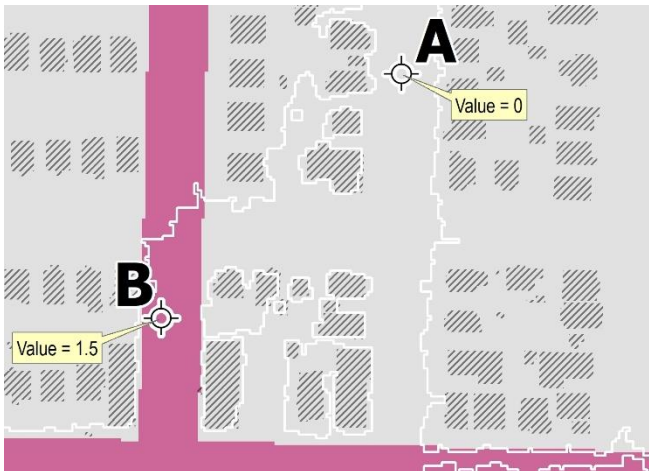
The Consultant used the example area shown previously (Figures 3-4, 4-1, and 4-2) to demonstrate the methods used to perform risk scoring calculations. Figure 5-2 shows two grid cell locations: **A** and **B**. Flooding at location **A** is deeper than at location **B**, resulting in greater depth scores. However, location **B** receives an additional score for being located within a major transportation route. Location **B** also receives a higher equity score than location **A**. The resultant risk scores are similar (10.8 and 10.5 for A and B, respectively); however, each are based on different underlying conditions. Note that risk scores are calculated using both the 100-year and the 1,000-year depth scores multiplied by the respective frequency scores, and the largest resultant value is used in the risk map.



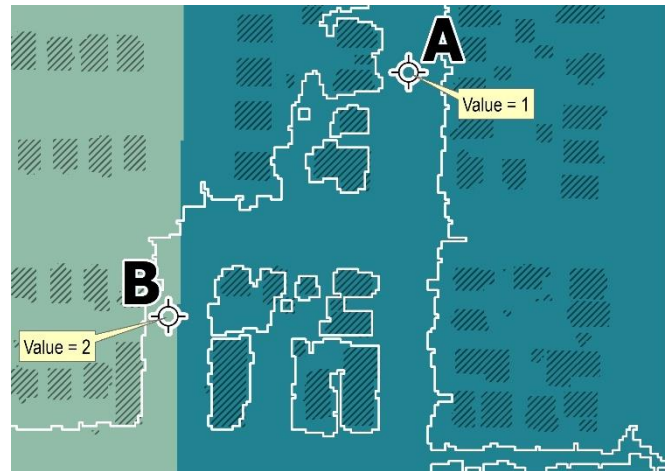
(a) Flooding depths from 100-year event simulation, units of feet



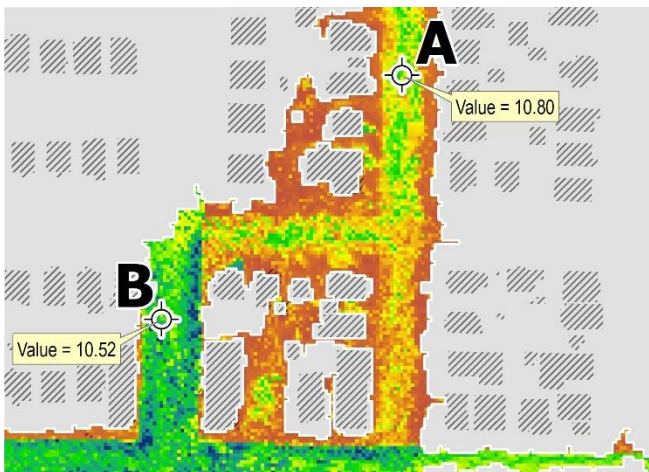
(b) Flooding depths from 1000-year event simulation, units of feet



(c) Location scores with major transportation route shown; no high-use areas or critical facilities within this example area



(d) Equity scores where the dark shaded area is an equity score of 1 and the light shaded area is an equity score of 2



(e) Mapped risk scores for example area

	Location A		Location B	
Parameter	100-year	1000-year	100-year	1000-year
Depth (feet)	0.980	2.172	0.102	0.879
Depth score	1.960	3.000	0.203	1.758
High-use score	0	0	0	0
Location score	0	0	1.5	1.5
Frequency score	5	1	5	1
Equity score	1	1	2	2
Risk score	10.8*	4.0	10.5*	5.3

*Use larger of two values calculated for specified location.

(f) Risk score calculations for example locations A and B

Figure 5-2. Example risk score calculations

6. Results Summary

As described in the previous sections, the DSA Team performed a flooding analysis for two extreme storm events: (1) a 100-year historical event from December 2007, and (2) a 1,000-year synthetic event derived from SPU's most recent IDF curves. Urban flooding simulations produced peak flood depth grids, which the Consultant used to map inundation and compare those areas with historical waterways (Appendix G). The Consultant used the inundation mapping and calculated flooding depths to calculate risk scores and develop a risk map. The total risk area for extreme storms covers 5,235 acres, or approximately 10 percent of the city.

The Consultant tabulated the risk scores and plotted the area-weighted distribution for review. The values and scoring factors presented in Section 5 were the result of an iterative scoring, mapping, plotting, and review process—with the intention of developing a broad, or well-distributed, set of risk scores for planning purposes. Figure 6-1 shows the final distribution of risk scores.

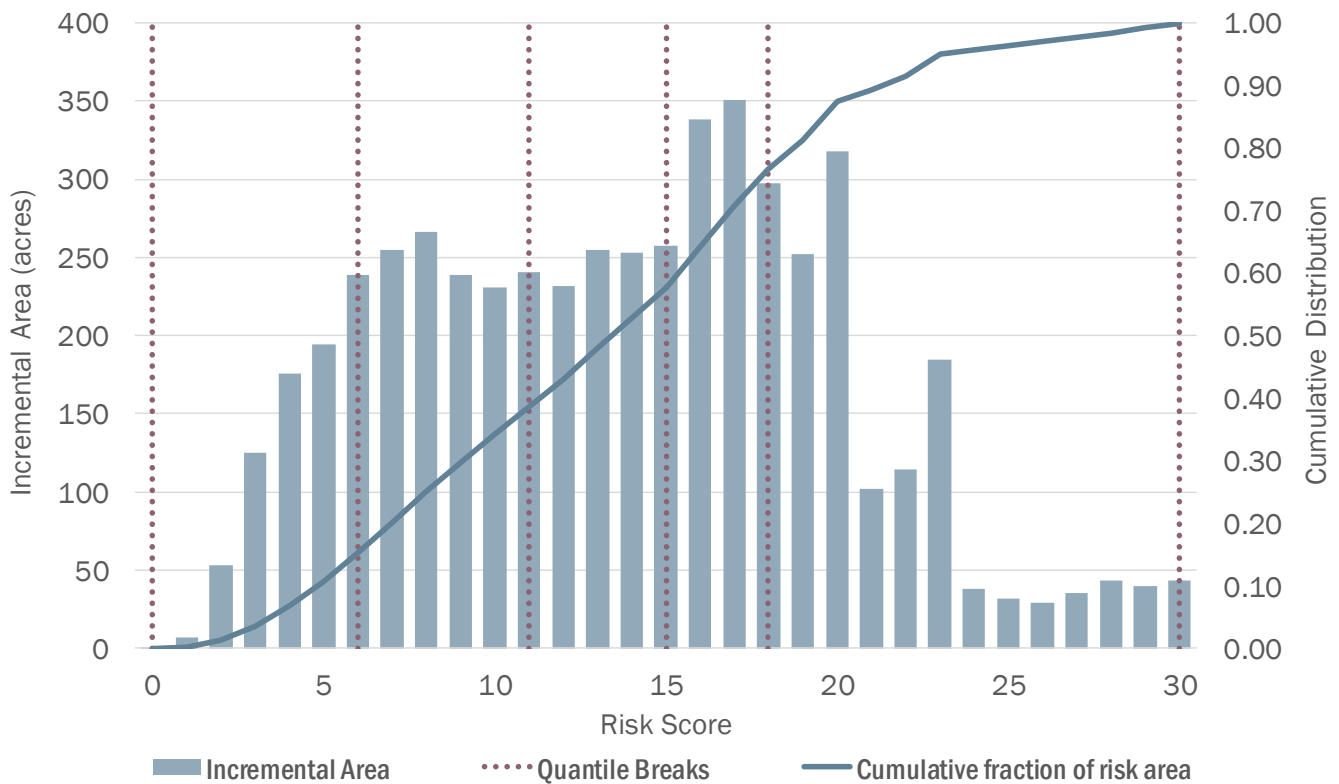


Figure 6-1. Distribution of risk scores within the extreme storms risk area

Once the scoring distribution was established, the Consultant calculated the quantile breaks to map five categories of relative risk: low, medium low, medium, high, and critical. Table 6-1 lists the risk score ranges for each risk category.

Table 6-1. Extreme Storm Risk Categories and Scores	
Relative risk category	Risk score range
Low	1 – 6
Medium low	6 – 11
Medium	11 – 15
High	15 – 18
Critical	18 – 30

The scores in Figure 6-1 and listed in Table 6-1 were used to develop risk maps for the city. Appendix H provides maps of the risk categories based on scoring quantiles from low to critical. The Consultant prepared a GIS-compatible digital map package to accompany this TM. The digital map package contains the following citywide datasets:

- Inundation extent grids for the 100-year and 1,000-year event simulations (floating point format)
- High-use areas, critical areas, major transportation routes (binary raster format)
- Equity categories (integer raster format)
- Risk area with scores (floating point format)
- Risk categories (integer raster format)

7. Limitations

The extreme storm inundation maps and risk scoring data have been developed for informational purposes and to support the development of the ISP for SPU DWW. These data identify areas of the city that may be at higher risk of inundation due to extreme precipitation events. Use and interpretation of these results requires an understanding of the assumptions and limitations associated with the analysis. As planning progresses and focuses more narrowly on specific areas of interest, extreme storm assessments may need to be more advanced and refined. The following limitations have been identified for consideration:

- **Extreme storms are expected to become more frequent and there is substantial uncertainty associated with anticipated changes in precipitation.** The recurrence intervals for the extreme storm events described in this TM (i.e., 100 years and 1,000 years) are based on IDF curves developed using historical data. However, these frequencies are changing and should be viewed within the context of climate change. Tetra Tech (2017) found statistically significant positive trends in extreme precipitation metrics. Likewise, Mauger (2015) and Warner et al. (2015) project significant increases in atmospheric river events and heavy rainfall in the coming decades. Thus, the storm events used in this study are expected to become more frequent in the future. Moreover, estimates regarding future changes in the intensity and frequency of precipitation are highly uncertain.
- **The December 2007 storm does not reflect extreme sub-daily rainfall intensities.** As described in Section 2, rainfall that occurred during this event over durations less than 24 hours—such as 6 hours, 1 hour, or the peak 5-minute intensity—are estimated to have recurrence intervals of less than 100 years. This is important because the critical rainfall intensity or duration that causes flooding depends on time of concentrations for the location of interest. Areas located in the upland portions of a basin, where the contributing drainage area is small, are sensitive to very short and intense rainfall. Areas located in the lower portions of a basin tend to be flooded by longer, extended rainfall durations. Accordingly, 100-year flooding may be underestimated for areas located in upper portions of the basins.
- **Collection systems were not modeled explicitly.** As described in Section 3, the urban flood modeling approach had to conform to practical constraints and considerations that limited the effort and complexity involved in the analysis. One of the key steps in simplifying the analysis was the decision to complete 2D modeling of surface flow without explicitly modeling the collection system. Simple calculations were used to remove system inflows and route those flows to downstream locations; however, conservative assumptions were used to limit those inflows, accounting for numerous uncertainties. This is a conservative approach because more water remains on the surface and could result in a larger simulated extent of flood inundation.
- **Hydrologic processes have been simplified.** Another key step needed to run a simplified flooding modeling process was to perform rainfall-runoff calculations outside the urban flooding model and apply only excess precipitation to the model domain. While losses in the rainfall-runoff calculations accounted for spatial variations in soils (and thus infiltration rates), the resulting excess precipitation was lumped and distributed uniformly over each surface basin. This averaging across a basin could result in both overestimation of runoff in areas with high infiltration rates and underestimation of runoff in areas with low infiltration rates. However, as runoff flows downgradient and accumulates the differences in infiltration rates are likely to counterbalance.

- **Topographic data and geospatial processes used to calculate risk scores are approximate.** Urban flooding simulations and inundation mapping were based on DEM data developed from LiDAR surveys. The accuracy of LiDAR airborne surveys can be limited by thick vegetation, dense clouds, high-reflectance surfaces, or water bodies. In addition, DEMs produced as 2-ft grids were reduced to a 4-ft grid resolution for modeling and geospatial processing. At reduced resolution, DEM grids may not reflect minor structures, small surface features, or microtopographic variations.
- **Runoff is retained behind embankments reflected in the DEM.** Elevated roadways and earthen embankments reflected in the DEM cause runoff to be impounded and accumulate during urban flooding simulations. Culverts and other underground drainage infrastructure that may convey flow under or through these are not represented in the surface flow model. Therefore, the depths and inundation extents behind large embankments may be overestimated.
- **Manning's roughness for the surface flow model is assumed to be uniform.** The CAFlood applications does not accept spatially distributed roughness coefficients as inputs to the WCA2D model. Therefore, the Consultant assumed a global roughness factor of 0.050. This may overpredict flooding along roadways and other paved surfaced. Conversely, this may underpredict flooding along heavily vegetated flow paths.
- **Equity score has less influence, when compared to capacity analyses completed for the WWSA and DSA, on the risk score.** When the risk score method was developed for the WWSA, SPU decided to separate it out from the consequence component of the score, so that it could have greater influence on the risk score. For the extreme storm events risk map, however, it has less influence on the final score when compared to the individual scores of the few consequence score components. For example, for highest frequency events, a critical facility contributes more than the equity score, to the risk score.
- **Factors contributing to impacts and consequences are simplified for relative scoring.** Risk scores are relative and should not be used for risk cost analysis. Flooding risk is often quantified in terms expected annual damage for project planning. In such cases, flooding damage is estimated based on a wide range of event frequencies and a wide range of structural and economic impacts. A detailed risk cost analysis is impractical at a city scale and is generally not necessary for mapping relative risk areas. As mitigation or resiliency strategies are developed, probabilistic estimates of risk and detailed estimates of expected annual damages may be beneficial.

This page intentionally left blank.

References

- Aqualyze, Inc. 2015. *SPU Modeling On-Call Project (C13-031) Work Authorization 1: Drainage Basins Calibration*. Project Report, SPU.
- Bouwer, H. (1966). "Rapid field measurement of air entry value and hydraulic conductivity of soil as significant parameters in flow system analysis." *Water Resources Res.*, 2 (4), pp. 729-738, 10.1029/WR002i004p00729
- Brown and Caldwell (2008). *Madison Valley Regional Hydraulic Model*. Prepared for Seattle Public Utilities.
- CADDIES, 2015. Cellular Automata Dual-drainage Simulation [WWW Document].
<http://emps.exeter.ac.uk/engineering/research/cws/resources/caddiesframework/> (accessed 02/19/2019).
- Chen, A. S., Djordjevic, S., Leandro, J., & Savic, D. (2007). The urban inundation model with bidirectional flow interaction between 2D overland surface and 1D sewer networks. NOVATECH 2007.
- Chen, A. S., Evans, B., Djordjević, S., & Savić, D. A. (2012). Multi-layered coarse grid modelling in 2D urban flood simulations. *Journal of Hydrology*, 470, 1–11. <https://doi.org/10.1016/j.jhydrol.2012.06.022>
- Chow, Ven Te, David R. Maidment, and Larry W. Mays (1988). *Applied Hydrology*. New York: McGraw-Hill.
- Dottori, F., & Todini, E. (2011). Developments of a flood inundation model based on the cellular automata approach: Testing different methods to improve model performance. *Physics and Chemistry of the Earth, Parts A/B/C*, 36(7-8), 266–280. <https://doi.org/10.1016/j.pce.2011.02.004>
- Federal Highway Administration (FHWA) (2009). *Urban Drainage Design Manual September 2009 Hydraulic Engineering Circular 22, Third Edition*
- Ghimire, B., Chen, A. S., Guidolin, M., Keedwell, E. C., Djordjević, S., & Savić, D. A. (2013). Formulation of a fast 2D urban pluvial flood model using a cellular automata approach. *Journal of Hydroinformatics*, 15(3), 676–686. <https://doi.org/10.2166/hydro.2012.245>
- Gibson, M. (2019). *CAFlood Version 120, updated April 2018, OpenCL*. Runs on a Windows 64bit OS and uses double precision floating point values. CADDIES-bin-caflood-opencl-win64-double-120.zip. [accessed February 26, 2019] from URL: <https://emps.exeter.ac.uk/engineering/research/cws/resources/caddies-framework/caddies-download/>.
- Green, W.H. and G. Ampt. 1911. "Studies of Soil Physics, Part I – The Flow of Air and Water Through Soils." *The Journal of Agricultural Science*. 4:1-24.
- Guidolin, M., Chen, A. S., Ghimire, B., Keedwell, E. C., Djordjević, S., & Savić, D. A. (2016). A weighted cellular automata 2D inundation model for rapid flood analysis. *Environmental Modelling & Software*, 84, 378–394. <https://doi.org/10.1016/j.envsoft.2016.07.008>
- Guo, James C.Y. and Ken MacKenzie (2012) *Hydraulic Efficiency of Grate and Curb-Opening Inlets Under Clogging Effect*. Colorado Department of Transportation, Applied Research and Innovation Branch.
- Itami, R. M. (1994). "Simulating spatial dynamics – cellular-automata theory." *Landscape and Urban Planning*. Vol. 30, 27–47.
- Jamali, B., Bach, P. M., Cunningham, L., & Deletic, A. (2019). A Cellular Automata fast flood evaluation (CA-ffé) model. *Water Resources Research*, 55, 4936–4953. <https://doi.org/10.1029/2018WR023679>

King County Assessor (2018). Parcel (tax parcel database). Obtained from the King County GIS FTP Data Portal: <https://www5.kingcounty.gov/gisdataportal/>. [accessed June 14, 2018].

Mauger, G.S., J.H. Casola, H.A. Morgan, R.L. Strauch, B. Jones, B. Curry, T.M. Busch Isaksen, L. Whitely Binder, M.B. Krosby, and A.K. Snover (2015). *State of Knowledge: Climate Change in Puget Sound*. Report prepared for the Puget Sound Partnership and the National Oceanic and Atmospheric Administration. Climate Impacts Group, University of Washington, Seattle. DOI:10.7915/CIG93777D.

Munshi, A. (Ed) 2011. "The OpenCL Specification Version 1.1." *Khronos OpenCL Working Group*.

Quantum Spatial (2016). Digital Elevation Model developed from Light Detection and Ranging (LiDAR) data provided by King County and Puget Sound LiDAR Consortium.

Seattle Public Utilities (SPU). 2007. *Risk Assessment Framework*.

Seattle Public Utilities (SPU). 2020. *GIS data for Risk Mapping and Prioritization for the System Analyses Projects*. Memorandum from Colleen O'Brien to project file, dated July 17, 2020.

Tetra Tech. 2017. "Intensity Duration Frequency Curves and Trends for City of Seattle."

Warner, M., Mass, C., and Salathe, E.P. (2015). "Changes in Winter Atmospheric Rivers along the North American West Coast in CMIP5 Climate Models," *Journal of Hydrometeorology*, DOI:10.1175/JHM-D-14-0080.1.

Appendix A: Green-Ampt Parameters

This section describes the methods and sources used to develop Green-Ampt parameters for infiltration calculations.

This page intentionally left blank.

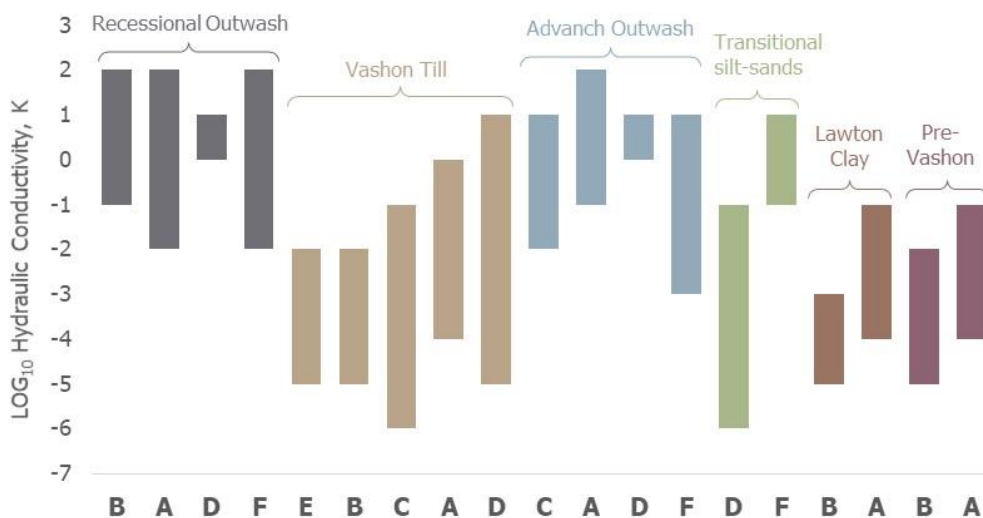
Estimating Green-Ampt Parameters

SPU used the Green-Ampt method for simulating infiltration in SWMM when developing their collection system models (Aqualyze 2015). While the parameters were adjusted during the calibration of the SWMM models, the initial parameters and ranges were based on tables in the SWMM Manual (EPA 2015) that relate standard soil texture classes (USDA 2017) to the hydraulic properties needed for the Green-Ampt method.

The Green-Ampt parameters suggested in the SWMM Manual are based on widely accepted research published by the USDA. Rawls, Brakensiek and Miller (1983) conducted an extensive study of soils across the United States and determined average Green-Ampt parameters for standard USDA soil classes. While soil properties such as hydraulic conductivity tend to vary widely in real-world applications, empirical estimates by Rawls, Brakensiek and Miller (1983) indicate consistent relationships with texture. As the composition of soils becomes finer, moving from sand to clay, wetting front suction head tends to increase while hydraulic conductivity tends to decrease.

The Consultant team obtained geospatial mapping of surficial soils based on the work by Troost et al. (2005) at the University of Washington. A key step in applying published hydraulic properties to basins in the Seattle area is to link the surficial geology and geologic map units defined by Troost et al. (2005) to standard soil classes such as those defined by the USDA (2017). Aqualyze (2015) assigned standard soil texture classes to 12 geologic map units found in drainage area modeled for Seattle. The Consultant revisited those assignments because 6 additional geologic map units were encountered in this study area. In addition, the Consultant wanted to confirm the assigned relationships resulted in reasonably conservative estimates of hydraulic conductivity, given the considerable variability and uncertainty of such data.

The Consultant reviewed the notes on the soil textures found within the different geologic units. The Consultant also reviewed hydraulic conductivity ranges for past studies of geologic units in the Seattle area (Olstead 1969; Laprade and Robinson 1989; Mills and Cordell 1989; Galster and Laprade 1991; Morgan and Jones 1995; Woodward et al. 1995; Savage 2000) (see Figure A-1).



Sources:

- A. Galster and Laprade (1991)
- B. Laprade and Robinson (1989)
- C. Mills and Cordell (1989)
- D. Morgan and Jones (1995)
- E. Olstead (1969)
- F. Woodward et al. (1995)

Figure A-1. Hydraulic conductivity ranges compiled by Savage (2000)

After reviewing previous studies, the Consultant assigned representative soil texture classifications to each of the geologic units found in Seattle (Table A-1).

Table A-1. Geologic Units, Soil Textures, and Representative USDA Soil Classes

Geologic units from Troost et al. (2005)			Soil texture classes (USDA 2017)	
Description	Map unit	Notes on textures	Aqualyze (2015)	This study ^a
Modified land	<i>m</i>	gravel, sand, silt	loam	silt loam
Alluvium	<i>Qal</i>	gravel, sand, silt	silt loam	sandy loam
Beach deposits	<i>Qb</i>	gravel, sand	sand	sand
Landslide deposits (debris)	<i>Qls</i>	gravel, sand, silt	loam	loam
Deposits of Pre-Fraser glaciation age	<i>Qpf</i>	gravel, sand, silt	sandy loam	silt loam
Nonglacial deposits	<i>Qpfn</i>	gravel, sand, silt, clay	--	clay loam
Glacial deposits	<i>Qpog</i>	gravel, sand, silt, till	--	clay loam
Undifferentiated Vashon deposits	<i>Qv</i>	gravel, sand, silt	loam	clay loam
Advance outwash deposits	<i>Qva</i>	gravel, sand, silt	loamy sand	sandy loam
Ice-contact deposits	<i>Qvi</i>	gravel, sand, silt, till	--	clay loam
Lawton clay	<i>Qvlc</i>	Silt, clay	silty clay	silty clay
Recessional outwash deposits	<i>Qvr</i>	gravel, sand, silt	sand	sandy loam
Recessional lacustrine deposits	<i>Qvrl</i>	silt, clay	--	silty clay
Vashon till (hardpan)	<i>Qvt</i>	sand, silt, clay, till	clay loam	clay loam
Wetland deposits	<i>Qw</i>	silt	--	silty clay
Blakely Formation (sandstone)	<i>Tb</i>	weathered rock	sand	sandy loam
Intrusive rock	<i>Ti</i>	weathered rock	--	sandy loam
Tukwila Formation (volcanic flows/sand)	<i>Tpt</i>	weathered rock	loamy sand	sandy loam

a. Soil texture classes assigned based on similar hydraulic properties and conservative estimates for hydraulic conductivity.

As shown in Table A-1, the Consultant assigned six different soil texture classes to the various geologic map units for Seattle. The Consultant revisited the soil texture class assignments Aqualyze (2015) because the Consultant wanted to confirm the assigned relationships resulted in reasonably conservative estimates of hydraulic conductivity, given the considerable variability and uncertainty of such data. The Consultant tabulated a set of hydraulic parameters based on Rawls, Brakensiek and Miller (1983) as cited by the EPA SWMM Manual (EPA 2015). Rawls et al. (1992) provided additional parameters related to porosity and soil water content. Table A-2 lists the Green-Ampt parameters used for this study.

Table A-2. Hydraulic Properties for Soil Types

USDA soil texture class	Geologic map unit (Troost et al. 2005)	Wetting front soil suction Head ^{a,b} ψ (in)	Effective hydraulic conductivity ^{a,b} K (in/hr)	Porosity ^c η --	Field capacity ^c θ_{fc} --	Effective porosity ^c θ_e --	Residual porosity ^c θ_r --
Sand	<i>Qb</i>	1.95	4.64	0.44	0.09	0.42	0.02
Sandy loam	<i>Qal, Qva, Qvr, Tb, Ti, Tpt</i>	4.33	0.43	0.45	0.21	0.41	0.04
Silt loam	<i>M, Qpf</i>	6.57	0.26	0.50	0.33	0.49	0.02
Loam	<i>Qls</i>	3.50	0.13	0.46	0.27	0.43	0.03
Clay loam	<i>Qpfn, Qpog, Qv, Qvi, Qvt</i>	8.22	0.04	0.46	0.32	0.39	0.08
Silty clay	<i>Qvlc, Qvrl, Qw</i>	11.50	0.02	0.48	0.39	0.42	0.06

- a. Rawls, W.J., D.L. Brakensiek, and N. Miller. (1983). "Green-ampt Infiltration Parameters from Soils Data." *Journal of Hydraulic Engineering*. Vol. 109, Issue 1
- b. United States Environmental Protection Agency (2015). *Storm Water Management Model User's Manual Version 5.1*. Reference table 24.2, p 816.
- c. Rawls, W. J., Ahuja, L. R., and Brakensiek, D. L. (1992). "Estimating Soil Hydraulic Properties from Soils Data." *Proceedings of the International Workshop on Indirect Methods for Estimating the Hydraulic Properties of Unsaturated Soils*, van Genuchten, M. Th., Leij, F. J., and Lund, L. J., editors. University of California. Riverside, CA. pp. 329-340.

Appendix A References

- Aqualyze, Inc. 2015. *SPU Modeling On-Call Project (C13-031) Work Authorization 1: Drainage Basins Calibration*. Project Report, SPU.
- Environmental Protection Agency (EPA) (2015). *Storm Water Management Model User's Manual Version 5.1. United States Environmental Protection Agency*. Reference table 24.2, p 816.
- Troost, K.G., D.B. Booth, A.P. Wisher, and S.A. Shimel (2005). *The Geologic Map of Seattle – A Progress Report*. Prepared in cooperation with the City of Seattle and the Pacific Northwest Center for Geologic Mapping Studies at the Department of Earth and Space Sciences, University of Washington. Open File Report 205-1252.
- Galster, R.W., and Laprade, W.T. (1991). "Geology of Seattle, Washington, United States of America." *Bulletin of the Association of Engineering Geologists*, v. 28, no. 3, p.235-302.
- Laprade, W.T., and Robinson (1989). "Foundation and excavation conditions in Washington." *Engineering Geology in Washington*, Richard W Galster, ed., Washington Division of Geology and Earth Resources Bulletin 78, v. I, p. 37-48.
- Mills, D.E., and Cordell, D.A. (1989). "A hydrologic assessment of Cedar Hills Regional Landfill, King County, Washington." *Engineering Geology in Washington*, Richard W Galster, ed., Washington Division of Geology and Earth Resources Bulletin 78, v. I, p. 1063-1070.
- Morgan, D.S., and Jones, J.L. (1995). *Numerical model analysis of the effects of groundwater withdrawals on discharge to streams and springs in small basins typical of the Puget Sound Lowland, Washington*. USGS Water Supply Paper, W 2492, 73 p.
- Olmstead, T.L. (1969). *Geological aspects and engineering properties of glacial till in the Puget Sound Lowland, Washington*. Proceedings of the 7th Annual Engineering Geology and Soils Engineering Symposium: University of Idaho, Moscow, Idaho, p. 223-233.
- Woodward, D.G., Packard, F.A., Dion, N.P., and Sumioka, S.S. (1995). *Occurrence and quality of groundwater in southwestern King County, Washington*. USGS Water Resources Investigations Report 92-4098, 69 p.
- Rawls, W.J., D.L. Brakensiek, and N. Miller (1983). "Green-Ampt Infiltration Parameters from Soils Data." *Journal of Hydraulic Engineering*. Vol. 109, Issue 1
- Rawls, W. J., Ahuja, L. R., and Brakensiek, D. L. (1992). "Estimating Soil Hydraulic Properties from Soils Data." Proceedings of the International Workshop on Indirect Methods for Estimating the Hydraulic Properties of Unsaturated Soils, van Genuchten, M. Th., Leij, F. J., and Lund, L. J., editors. University of California. Riverside, CA. pp. 329-340."
- Savage, N.Z., M.M. Morrissey, and R.L Baum (2000). *Geotechnical Properties for Landslide-Prone Seattle Area Glacial Deposits*. U.S. Geological Survey, Open-file Report 00-228.
- United States Department of Agriculture (USDA). (2017) *Soil Survey Manual*. C. Ditzler, K. Scheffe, and H.C. Monger (eds.). Soil Science Division Staff. USDA Handbook 18. Government Printing Office, Washington, D.C.

Appendix B: Inlet Efficiency Calculations

This section describes the methods and sources used calculate inlet efficiency for use in estimated system inflows.

This page intentionally left blank.

Estimating Inlet Efficiency

Given the uncertainties associated with inlet capacities and possible conveyance constraints, the Consultant used a conservative approach to approximate flows at the inlets, accounting for multiple factors that could limit the flows into the collection system. The Consultant started by assuming a maximum inflow of 2.0 cfs per inlet based on a review of simple slotted stormwater grates and charts presented in the *Urban Drainage Design Manual* published by the Federal Highway Administration (FHWA 2009). The Consultant then reduced this value by an average efficiency factor and a clogging factor to obtain a highly limited inlet capacity.

FHWA (2009) presents a method for calculating inlet efficiency (E) based on the ratio between the frontal flow approaching the inlet grate (Q_w) and the total flow in the channel or roadway (Q) as described by the following equation:

$$E = R_f \left(\frac{Q_w}{Q} \right) + R_s \left(1 - \left(\frac{Q_w}{Q} \right) \right)$$

where R_f and R_s are coefficients for frontal flow and side flow, respectively. These coefficients are calculated as follows:

$$R_f = 1 - K_{uf}(V - V_o)$$

$$R_s = \left(1 + \frac{K_{us}V^{1.8}}{S_x L^{2.3}} \right)^{-1}$$

where $K_{uf} = 0.09$, V = velocity of flow in the gutter, and V_o = velocity at which splash-over first occurs, $K_{us} = 0.15$, S_x = cross slope of the roadway, and L = length of the inlet grate.

Figure B-1 is a schematic of a gutter flow example based on a 10-foot roadway section with a 6-inch curb height. The grate is assumed to have a minimum width of 1 foot and a minimum length of 2 feet. The splash-over velocity (V_o) is estimated using empirical coefficients developed from laboratory tests:

$$V_o = \alpha + \beta L_e - \gamma L_e^2 + \eta L_e^3$$

where V_o = splash-over velocity, L_e = effective length of grate inlet, and α , β , γ , η = empirical constants (UDFCD 2016). The following pages illustrate MathCAD calculations of inlet efficiency.

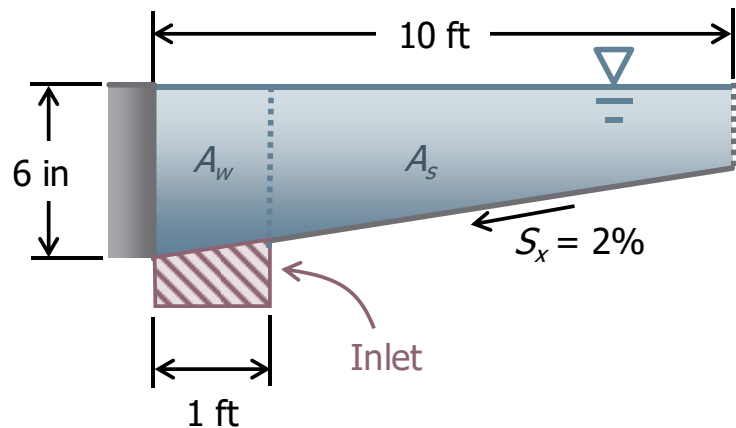


Figure B-1. Schematic of roadway section and inlet

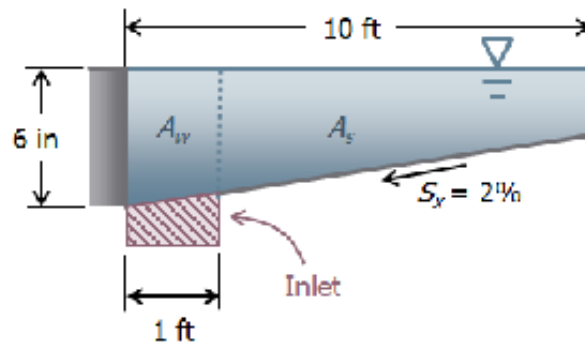
Calculate Gutter Flow

$$S_x := 0.02 \quad \text{cross slope}$$

$$W_r := 10 \quad \text{roadway width}$$

$$W_g := 1 \quad \text{minimum grate width}$$

$$H_g := 0.5 \quad \text{height of gutter}$$



$$E_o := 1 - \left(1 - \frac{W_g}{W_r} \right)^{2.67} \quad \text{frontal flow ratio}$$

$$A := W_r \cdot H_g - \frac{S_x \cdot W_r^2}{2} = 4$$

$$\theta := \text{atan} \left(\frac{S_x \cdot W}{W} \right) = 0.02$$

$$P := \frac{10}{\cos(\theta)} = 10.002$$

$$R := \frac{A}{P}$$

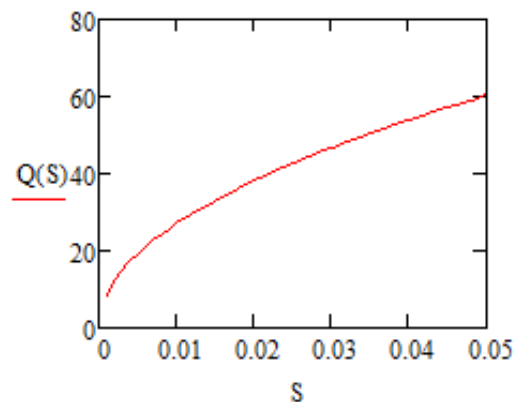
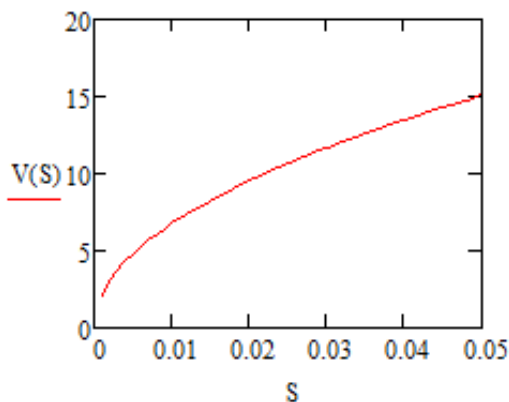
+

$$S := 0.001, 0.002 \dots 0.05 \quad \text{allow roadway slope to vary}$$

$$n := 0.012 \quad \text{use low Manning's roughness for conservative velocity calculation}$$

$$V(S) := \left(\frac{1.49}{n} \right) \cdot R^{\frac{2}{3}} \cdot S^{\frac{1}{2}} \quad \text{calculate velocity by Manning's equation}$$

$$Q(S) := V(S) \cdot A \quad \text{calculate discharge for uniform flow}$$



Calculate splash-over velocity

Assume simple reticuline grate (conservative)

(UDFCD 2008)

$$\alpha := 0.28$$

$$\beta := 2.28$$

$$\gamma := 0.18$$

$$\eta := 0.01$$

$$L_e := 2$$

Type of Grate	α	β	γ	η
Bar P-1-7/8	2.22	4.03	0.65	0.06
Bar P-1-1/8	1.76	3.12	0.45	0.03
Vane Grate	0.30	4.85	1.31	0.15
45° Bar	0.99	2.64	0.36	0.03
Bar P-1-7/8-4	0.74	2.44	0.27	0.02
30° Bar	0.51	2.34	0.20	0.01
Reticuline	0.28	2.28	0.18	0.01

$$V_o := \alpha + \beta \cdot L_e + \gamma \cdot L_e^2 + \eta \cdot L_e^3 = 5.64$$

calculate splash-over velocity (UCFCD 2016)

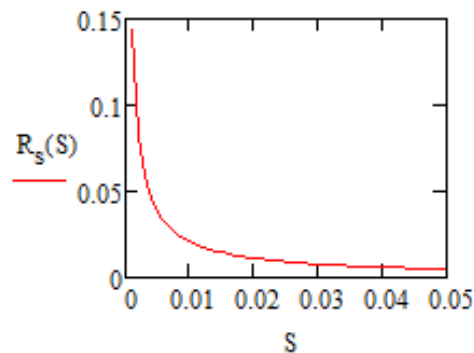
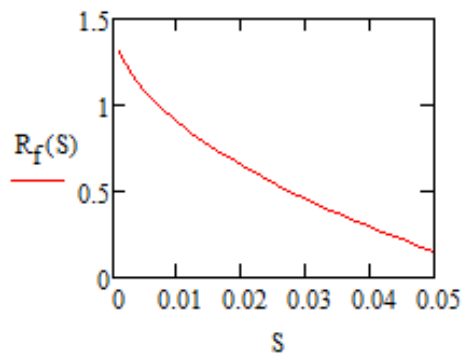
$$L := L_e \quad \text{assume length of 2 feet}$$

$$K_{u1} := 0.09$$

$$K_{us} := 0.15$$

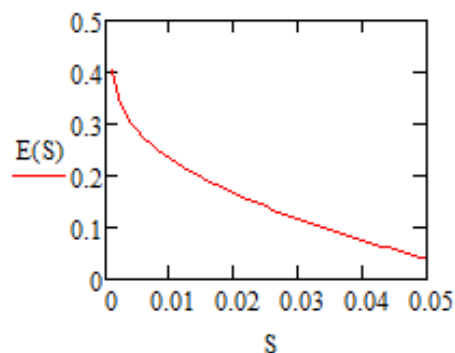
$$R_f(S) := 1 - K_{u1} \cdot (V(S) - V_o)$$

$$R_s(S) := \left(1 + \frac{K_{us} \cdot V(S)^{1.8}}{S_x \cdot L^{2.3}} \right)^{-1}$$



$$E(S) := E_o R_f(S) + 0.75(1 - E_o) R_s(S)$$

Calculate inlet grate efficiency (FHWA 2009)



For a relatively steep roadway:

$$E := E_o R_f(0.021) + 0.75(1 - E_o) R_s(0.021) = 0.16$$

Inlet efficiency used to calculate inflow rate.

Appendix B References

Federal Highway Administration (FHWA) (2009). Urban Drainage Design Manual September 2009 Hydraulic Engineering Circular 22, Third Edition

Urban Drainage and Flood Control District (UDFCD) (2008). *Urban Storm Drainage Criteria Manual*. Denver, CO.

Urban Drainage and Flood Control District (UDFCD) (2016). *Urban Storm Drainage Criteria Manual*. Denver, CO.

Appendix C: Routing System Inflows

This section describes methods and sources used to route system inflows and calculate discharge hydrographs for returning those flows to streams.

SPU Drainage System Analysis

Flooding Topic Area | Extreme Storms Analysis

This page intentionally left blank.

Method for Routing System Inflows to Streams

To calculate discharge hydrographs to streams, the Consultant needed a transform function to convert distributed inflows to discharges at downstream outfalls. Stubchaer (1975) proposed a computationally simple approach known as the Santa Barbara Unit Hydrograph (SBUH) method. Instead of using a derived unit hydrograph to transform excess precipitation to runoff, the SBUH method calculates a discharge hydrograph directly by routing the instantaneous hydrograph¹² through a hypothetical linear reservoir that causes a time delay equal to the time of concentration.

The Consultant divided each basin into roughly evenly spaced subbasins, with discharge points located along major streams and tributaries. As described previously, the collection system inflows or “losses” were assumed to be uniformly distributed over the basin. Similarly, the inflows to the system were calculated in units of depth per time increment. The incremental depths for each time step were multiplied by the contributing drainage area for the subbasin and then divided by the time step to obtain the instantaneous hydrograph as follows:

$$M_j = \frac{D_j A_{sb}}{\Delta t}$$

Where, M_j = instantaneous system flow rate for time increment j , D_j = depth of inflows to the collection system for time increment j , A_{sb} = contributing drainage area for the subbasin, and Δt = time step. The instantaneous system flow rates were then routed to obtain discharge rates using the following equations:

$$Q_j = Q_{j-1} + \kappa(M_{j-1} + M_j - 2Q_{j-1})$$

$$\kappa = \frac{\Delta t}{2T_c + \Delta t}$$

Where, Q_j = discharge for time increment j , Q_{j-1} = discharge for previous time increment $j-1$, M_j = instantaneous hydrograph for time increment j , M_{j-1} = instantaneous hydrograph for previous time increment $j-1$, Δt = time increment, κ = routing constant, T_c = time of concentration, sum of all travel times.

Flow was added back to creek channels in surface basins 100, 200, 300, 350, 400, 650, 700, 800—where there is piped drainage system discharging to the creek. Some basins have no formal drainage systems discharging to creeks (e.g., Fauntleroy Creek), for such basins, flow was not added back to the creek.

¹² The instantaneous unit hydrograph is defined as a unit hydrograph produced by one unit-depth of effective rainfall occurring over an infinitesimal duration, thus representing the runoff response of a basin to an instantaneous impulse.

Appendix C References

Stubchaer, J.M. (1975), "The Santa Barbara Urban Hydrology Method." Proceedings, *National Symposium on Urban Hydrology and Sediment Control*, University of Kentucky, Lexington, Kentucky. July 28–31, 1975.

Appendix D: CAFlood Setup File

This sections describes the input setup file used to run the CAFlood application, which simulates surface flow using the WCA2D model.

This page intentionally left blank.

CAFlood Setup File

The CAFlood application uses the CADDIES Application Programming Interface (API) to implement the WCA2D model (Guidolin et al. 2015). The CAFlood application used for this study (Gibson 2019) was compiled using the OpenCL library (Munshi 2011) to run simulations on a graphics processing units (GPU). Users run the CAFlood executable at the command prompt by calling the WCA2D model, specifying the setup file, and listing the paths to input and output directories. The setup file provides a list of commands, input filenames, output filenames, instructions, and parameters needed to run a simulation. Setup files use a comma separated variable (CSV) format and can be developed using a simple text editor. Figure D-1 shows an example setup file for Basin 100.

```

1 Simulation Name , 100_0100
2 Short Name (for outputs) , 100_0100
3 Version , 1,0,0
4 Model Type , WCA2Dv2
5 Time Start (seconds) , 0
6 Time End (seconds) , 194400
7 Max DT (seconds) , 60
8 Min DT (seconds) , 0.01
9 Update DT (seconds) , 60
10 Alpha (Fraction DT 0.0-1.0) , 0.1
11 Max Iterations , 10000000
12 Roughness Global , 0.05
13 Ignore WD (meter) , 0.01
14 Tolerance (meter) , 0.001
15 Slope Tolerance (%) , 1.0
16 Boundary Ele , -99999999
17 Elevation ASCII , dem_bldg04m_utm_100_buf.asc
18 Rain Event CSV , 100_Rain0100yr.csv
19 Water Level Event CSV ,
20 Inflow Event CSV , 0100YR-100-SeolaBeach01.csv
21 Time Plot CSV ,
22 Raster Grid CSV , VELraster.csv, WDraster.csv, WLraster.csv
23 Output Console , true
24 Output Period (s) , 300
25 Output Computation Time , true
26 Check Volumes , true
27 Remove Proc Data , true
28 Remove Pre-Proc Data , true
29 Raster VEL Vector Field , true
30 Raster WD Tolerance (meter) , 0.01
31 Update Peak Every DT , false
32 Expand Domain , false
33 Ignore Upstream , true
34 Upstream Reduction (meter) , 0.5

```

Figure D-1. Example setup file used to run CAFlood

The Consultant referred to the CAFlood User Guide (Guidolin et al. 2015) and performed sensitivity testing to develop input parameters in the setup file. The following is a row-by-row discussion of the input parameters used by the Consultant to run the CAFlood application.

- Row 1: The **Simulation Name** parameter is a descriptor for the model run. The Consultant used numerical codes with three digits for the basin number and four digits for the event. In the example, **100_0100** represents the simulation for Basin 100 using a 100-year storm.
- Row 2: The **Short Name** parameter is simply an abbreviated name for the model run used as a prefix for the data output files. The Consultant used the same text string for both the simulation name and short name.
- Row 3: The **Version** parameter is used to indicate the version of the simulation to be executed and was left as the default value of **1,0,0**.
- Row 4: The **Model Type** parameter indicates the flood model called to perform the simulations. The CAFlood application is designed to run multiple models. The command **WCA2Dv2** calls the current version of the WCA2D model described by Guidolin et al. (2015).
- Row 5: The **Time Start** parameter is the beginning time of the simulation in seconds, equal to the initial time step of the event. For this analysis, the Consultant used a start time of **0** seconds.
- Row 6: The **Time End** parameter is the ending time of the simulation in seconds. Both storm events span 24 hours; however, the Consultant added 30 hours to allow adequate time for runoff to flow through the basin. Accordingly, the Consultant used an end time of $54 \times 60 \times 60 = 194,400$ seconds.
- Row 7: The WCA2D model uses adaptive time step to perform the hydraulic computations. The **Max DT** parameter sets the upper limit for the computational time step (Δt) in seconds. The Consultant used the default value of **60** seconds, as recommended in the CAFlood User Manual.
- Row 8: The adaptive time step may become very small when the flow velocity is high, which can affect model performance and run time. The **Min DT** parameter sets the lower limit for the computational time step (Δt) in seconds. The Consultant used the default value of **0.01** seconds, as recommended in the CAFlood User Manual.
- Row 9: The **Update DT** parameter sets the interval at which the computational time step (Δt) is adjusted according to the velocity. The Consultant used the default value of **60** seconds, as recommended in the CAFlood User Manual.
- Row 10: The **Alpha** parameter is a coefficient used to adjust the computational time step (Δt) defined as a fraction between 0 and 1. The Consultant used a value of **0.1**, which was used in the example files that accompany the CAFlood application.
- Row 11: The **Max Iterations** parameter limits the number of iterations in case the computational time step becomes extremely small. The Consultant set this value to **10,000,000** for all simulations.
- Row 12: The **Roughness Global** parameter represents the Manning's roughness coefficient applied to all the cells of the domain. As discussed in Section 3.4.3, the Consultant used a value of **0.05** for all simulations.
- Row 13: The **Ignore WD** parameter is used to speed up the simulation by ignoring flow dynamics for cells with very shallow water, skipping the computations for those cells and speeding up the simulation. The Consultant set this parameter to **0.01** meters for all simulations.

- Row 14: The **Tolerance** parameter is used to speed up the simulation by assuming no flow where the water level difference between neighboring cells is less than the specified value. The Consultant set this parameter to 0.001 meters for all simulations.
- Row 15: The **Slope Tolerance** parameter is used to ignore all the cells where the hydraulic gradient is less than the specified tolerance. The CAFlood User Manual recommends a value that is roughly one order of magnitude smaller than the average slope of the basin. The Consultant used a value of 1.0 percent for all simulations.
- Row 16: The **Boundary Ele** parameter sets a boundary condition around the outside perimeter of the model grid as described in Section 3.4.2. A low elevation effectively creates a free discharge boundary condition, while a high elevation creates a closed boundary condition and water accumulates at the edges. The Consultant set this parameter to a value of -99999999 for all simulations.
- Row 17: The **Elevation ASCII** parameter calls the DEM, or terrain input file, which must be prepared using a standard ASCII DEM grid format. For the example in Figure D-1, the filename is **dem_bldg04m_utm_100_buf.asc**, which indicates the data are based on a DEM (**dem**) that is modified for buildings as obstructions (**bldg**), 4-foot resolution (**1.2192 meters**), projected to UTM coordinates (**utm**), Basin 100 (**100**), with a buffer added at the boundary (**buf**).
- Row 18: The **Rain Event CSV** parameter calls the rainfall event applied to the model domain. The rainfall event is defined as a variable time series (hyetograph) in units of millimeters per hour (mm/hr). This input is prepared as a separate CSV for each event. For the example in Figure D-1, the filename is **100_Rain0100yr.csv**, which indicates the data are based on a 100-year storm (**0100**).
- Row 19: The **Water Level Event CSV** parameter calls a water level event applied to the model domain. The water level event is a stage graph, or variable time series, used to define known water surface elevations in unit of meters. This input is prepared as a separate CSV for each event. As discussed in Section 3.4.2, no internal or external boundary conditions were defined using this command, indicated in the setup file as a blank set (,).
- Row 20: The **Inflow Event CSV** parameter calls inflow event, which can be applied to a specific location or area in the model domain. The inflow event is a discharge hydrograph, or variable time series, used to define flow rates in units of cubic meters per second (m^3/s). This input is prepared as a separate CSV for each event. This input differs from the rain event because the values used within the simulation are calculated by interpolation. For the example in Figure D-1, there is one inflow point with the filename **0100YR-100-SeolaBeach01.csv**, which indicates it is based on the 100-year storm (**0100**) for Basin 100 (**100**), discharging to Seola Beach (**SeolaBeach**).
- Row 21: The **Time Plot CSV** parameter calls an input file that specifies points in the model domain where the time varying values of a specific given physical variable (e.g., water depth, water surface elevation, velocity) will be output and saved as separate files. For the example in Figure D-1, no time series output is generated, which is indicated in the setup file as a blank set (,).
- Row 22: The **Raster Grid CSV** parameter calls an input file that specifies the time interval(s) where all the values in the domain are saved for a specific physical variable (e.g., water depth, water surface elevation, velocity). It is also possible to save the maximum, or “peak” values and the final values at the end of the simulation. Output data are generated as an ASCII grid file. For the example in Figure D-1,

output grids are generated for peak velocity (**VELraster.csv**), peak water depth (**WDraster.csv**), and peak water surface elevation (**WLRaster.csv**).

- Row 23: The **Output Console** parameter determines whether the progress of the simulation will be displayed on the console once every specified period in seconds. For the example in Figure D-1, the parameter is flagged as **true** and simulation progress is displayed on the console.
- Row 24: If the **Output Console** parameter is true, then the **Output Period** parameter specifies how frequently the simulation progress is updated on the console in seconds. For the example in Figure D-1, the simulation progress is output every 300 seconds.
- Row 25: The **Output Computation Time** parameter determines whether the computation time will be displayed on the console once every specified period in seconds. For the example in Figure D-1, the parameter is flagged as **true** and computation time is displayed on the console.
- Row 26: The **Check Volumes** parameter used to check that the mass conservation is respected or at least preserved within a certain error. For the example in Figure D-1, this parameter is flagged as **true** to check mass conservation.
- Row 27: The **Remove Proc Data** parameter removes all the temporary data files generated during simulation processing. For the example in Figure D-1, this parameter is flagged as **true** to remove temporary files.
- Row 28: The **Remove Pre-Proc Data** parameter removes all the temporary data files generated during the pre-processing for the simulation. For the example in Figure D-1, this parameter is flagged as **true** to remove temporary files.
- Row 29: The **Raster VEL Vector Field** parameter controls the output of velocity data such as the speed and angle of the velocity vectors for each cell. When this command is not activated (false) and a velocity output grid is specified, two additional output ASCII grid files are generated that show the speed and the angle of the velocity for each cell. If this command is activated (true), only a single output CSV file is generated where each line contains the velocity information of one cell. For the example in Figure D-1, this parameter is flagged as **true** to limit the velocity output.
- Row 30: The **Raster WD Tolerance** parameter sets a threshold for wet and dry cells before saving the output. The CAFlood User Manual recommends that users consider the value of this parameter within the context of the vertical accuracy of DEM, the grid resolution, and the quality of the precipitation data. For the example in Figure D-1, all cells with less than 0.01 meters of water depth will be treated as dry and therefore no water depth will be exported for those cells.
- Row 31: The **Update Peak Every DT** parameter activates a step where peak values of a physical variable are saved at every time step. If this parameter is false, the maximum values are saved only every **update DT** (usually 60 seconds). According to the CAFlood User Manual, when activated, this parameter has an insignificant impact on the accuracy but a large impact on the run time of the simulation. For the example in Figure D-1, this parameter is **false** to avoid saving at every time step.
- Row 32: The **Expand Domain** parameter is used to limit the domain used in the computations. If this parameter is false, the computational domain is the full domain and every cell with an elevation is processed. For the example in Figure D-1, this parameter is **false** to use the full domain.
- Row 33: The **Ignore Upstream** parameter When this command is activated the model identifies the elevation height where the water is still, i.e. no outflow is generated during an update step. Once a new

height is identified all cells with elevation above the height are not considered for computation any more. This can save some run-time depending on the terrain and on the type of events modeled. At the worst case scenario, it might add around 1% of extra run-time. true

- Row 34: The **Upstream Reduction** parameter it is used by the **Ignore Upstream** command to identify the amount of meter to reduce the possible elevation height at each update step. 0.5

The instruction lines can be entered in the setup file in any order. If the model does not recognize an instruction line in the setup file, it will stop the computation and return an error. An example of command line execution of the CAFlood program is as follows:

```
caflood /WCA2D C:\CAFLOOD\100\IN 100_0100.csv C:\CAFLOOD\100\OUT
```

Appendix D References

Guidolin, M., A.S. Chen, N. Pasquale (2015). *CADDIES caflowd application, User Guide*. Application Version 110

Gibson, M. (2019). *CAflowd Version 120, updated April 2018, OpenCL*. Runs on a Windows 64bit OS and uses double precision floating point values. CADDIES-bin-caflowd-opencl-win64-double-120.zip. [accessed February 26, 2019] from URL: <https://emps.exeter.ac.uk/engineering/research/cws/resources/caddies-framework/caddies-download/>.

Munshi, A. (Ed) 2011. "The OpenCL Specification Version 1.1." *Khronos OpenCL Working Group*.

Appendix E: GIS Data and Processes

SPU Memorandum: "GIS data for Risk Mapping and Prioritization for the System Analyses Projects," by Colleen O'Brien, dated July 17, 2020

Figure E-1. ArcGIS model builder for 1,000-year inundation area boundary

Figure E-2. ArcGIS model builder for developing high-use area raster

Figure E-3. ArcGIS model builder for developing critical facility area raster

Figure E-4. ArcGIS model builder of street buffers for major transportation routes

Figure E-5. ArcGIS model builder for developing street equity raster

Figure E-6. ArcGIS model builder calculating risk score

Figure E-7. ArcGIS model builder for clipping risk area and calculating histograms

Geoprocessing Coordinate System

NAD_1983_HARN_StatePlane_Washington_North_FIPS_4601_Feet

WKID: 2926 Authority: EPSG

Projection: Lambert_Conformal_Conic

False_Easting: 1640416.666666667

False_Northing: 0.0

Central_Meridian: -120.83333333333333

Standard_Parallel_1: 47.5

Standard_Parallel_2: 48.73333333333333

Latitude_Of_Origin: 47.0

Linear Unit: Foot_US (0.3048006096012192)

Geographic Coordinate System: GCS_North_American_1983_HARN

Angular Unit: Degree (0.0174532925199433)

Prime Meridian: Greenwich (0.0)

Datum: D_North_American_1983_HARN

Spheroid: GRS_1980

Semimajor Axis: 6378137.0

Semiminor Axis: 6356752.314140356

Inverse Flattening: 298.257222101

SPU Drainage System Analysis

Flooding Topic Area | Extreme Storms Analysis

This page intentionally left blank.



Date: 7/17/20

To: Project File

From: Colleen O'Brien

Re: GIS data for Risk Mapping and Prioritization for the System Analyses Projects

This memorandum describes the GIS data used in developing risk scores for the Wastewater System Analysis (WWSA) and Drainage System Analysis (DSA), particularly the DSA Sea Level Rise risk map.

For each data set it includes:

- For the source data, summarized in Table 1:
 - Description
 - Source and date
 - Storage location
 - What data set it became part of or was used to create (process data) for an analysis or map
- For processed data, summarized in Table 2:
 - Description, including how it was modified from the source data
 - Storage location (includes network drive location and may include a SharePoint location)
 - Date of the file
 - Which analysis it was used in

Table 1. GIS Source Data used in Risk Mapping and Prioritization for the System Analyses Projects

Name	Description	Source	Date	Storage Location	Name of Analysis Data Set Used In
City of Seattle	Polygons of city limits, land, and water bodies. Does not extend far enough east to include Mercer Island or Bellevue landforms. This feature class reflects the visual interface between land and water based upon our 1993 ortho photos. It essentially follows the 8 foot contour line, except where the ortho offered further clarification. That 8 foot contour line matches closest to what NAVD88 shows as "mean high water" (see official definition below) at 7.97 feet. MEAN HIGH WATER (MHW): "A tidal datum. The average of all the high water heights observed over the National Tidal Datum Epoch. For stations with shorter series, simultaneous observational comparisons are made with a control tide station in order to derive the equivalent datum of the National Tidal Datum Epoch."	City	3/18/20 (downloaded from Seattle Tools)	<i>Seattle Tools</i> , Streets (CARTO.SHORE)	land area
Colleges and universities (Figure 1)	Boundaries of colleges and universities in the city of Seattle.	City	Sept 2018	<i>Seattle Tools</i> , Colleges and Universities (CARTO.COLLEGE)	high use area
Critical facilities (Figure 2)	Provide services and functions essential to a community, especially during and after a disaster.	OEM	10/8/2018 (received from OEM)	<i>X:\Separated Systems\Business_Areas\Planning\DSA\analysis\CriticalFacilities Critical Facilities (OEM).txt</i>	critical facilities
High frequency bus stops (Figure 1)	On-street location where transit vehicles stop inline to pick-up and discharge passengers.	KC Metro	Sept 2018	<i>Seattle Tools</i> , King County Metro Bus Stop, Active & In Service (KCGIS.TransitStop_point)	high use area
Hospital campuses (Figure 1)	Boundaries of licensed acute care hospitals and associated buildings.	City	Sept 2018	<i>Seattle Tools</i> , Hospitals (CARTO.HOSPITAL)	high use area
King County parcels	Tax parcels polygons in King County.	KC	1/14/2018 (downloaded from website)	https://gis-kingcounty.opendata.arcgis.com/datasets/8058a0c540434dadb3ea0ade6565143_439	properties and critical facilities
Link light rail stops (Figure 1)	Contains the entire set of existing Central Link, University Link, and Airport Link light rail station points located in the City of Seattle from Northgate Mall to SeaTac Airport.	ST	Sept 2018	<i>Seattle Tools</i> , Sound Transit Link Light Rail Stations (CARTO.LinkStations)	high use area
Neighborhood Greenways (Figure 1)	Safer, calmer residential streets that can include: <ul style="list-style-type: none"> • easier crossings of busy streets with crosswalks, flashing beacons, or crossing signals • speed humps to calm traffic • stop signs for side streets crossing the greenway • signs and pavement markings to help people find their way • 20 mph speed limit signs 	SDOT	Sept 2018	<i>P:\PrjMgmt\C316073 2018 Wastewater System Analysis\02-Plan Inputs\G-GIS\To Aqualyze Prioritization-Layers.mpk</i>	high use area
Public and private schools (Figure 1)	Parcels that contain kindergarten through 12th grade public and private schools approved through the Washington State Board of Education.	City	Sept 2018	<i>Seattle Tools</i> , Public School and Private School (CARTO.PRIV_SCH and CARTO.PUB_SCH)	high use area

Name	Description	Source	Date	Storage Location	Name of Analysis Data Set Used In
Racial and Social Equity Composite Index (Figure 3)	<p>Census tract-based data that consists of a composite of the following sub-indices:</p> <ul style="list-style-type: none"> • Race, English Language Learners, and Origin Index ranks census tracts by an index of three measures weighted as follows: (shares of population who are) <ul style="list-style-type: none"> - persons of color (weight: 1.0) - English language learners (weight: 0.5) - foreign born (weight: 0.5) • Socioeconomic Disadvantage Index ranks census tracts by an index of two equally weighted measures: (shares of population with) <ul style="list-style-type: none"> - income below 200 percent of poverty level - educational attainment less than a bachelor's degree • Health Disadvantage Index ranks census tracts by an index of seven equally weighted measures: <ul style="list-style-type: none"> - no leisure-time physical activity - diagnosed diabetes - obesity - mental health not good - asthma - low life expectancy at birth - disability 	OPCD	2018 (DSA) 2017 (WWSA)	<p><u>DSA</u> DWW GIS Library (DSA) on SharePoint Racial and Social Equity Composite Index – 2018.zip (RaceSECCI_2018.shp)</p> <p><i>X:\Separated Systems\Business_Areas\Planning\DSA\data\Impacts RaceSECCI_2018.shp</i></p> <p><u>WWSA</u> <i>P:\PrjMgmt\C316073 2018 Wastewater System Analysis\02-Plan Inputs\G-GIS\To Aqualyze Prioritization-Layers.mpk</i></p>	Racial and Social Equity Composite Index
Residential and Hub Urban Villages (Figure 1)	Areas in the city with residential development as well as a broad mix of uses with lower densities than urban centers. (See the Comprehensive Plan 20-year Growth Strategy, http://www.seattle.gov/Documents/Departments/OPCD/OngoingInitiatives/SeattlesComprehensivePlan/CouncilAdopted2016_CitywidePlanning.pdf)	OPCD	Sept 2018	Seattle Tools, Urban Centers, Villages, Manufacturing Industrial Centers (CITYPLAN.URBAN_VILLAGE_CENTER_MIC)	high use area
Snow and ice routes (Figure 4)	City of Seattle streets covered under SDOT's Winter Storm Response Plan, showing snow and ice removal routes.	SDOT	9/21/18 (downloaded from Seattle Tools)	<p>DWW GIS Library (DSA) on SharePoint SDOT_snowice.zip (SDOT_snowice.shp)</p> <p><i>X:\Separated Systems\Business_Areas\Planning\DSA\data\Impacts SDOT_snowice.shp</i></p>	major transportation routes and street type
Streets	The City's Street Network Database showing driveable public streets within the Seattle city limits.	SDOT	1/24/2020 (downloaded from Seattle Tools)	Seattle Tools, Streets (SDOT.STREETS)	streets

Name	Description	Source	Date	Storage Location	Name of Analysis Data Set Used In
Urban center (Figure 1)	Densest developed areas in the city with the widest range of land uses. (See the Comprehensive Plan 20-year Growth Strategy, http://www.seattle.gov/Documents/Departments/OPCD/OngoingInitiatives/SeattlesComprehensivePlan/CouncilAdopted2016_CitywidePlanning.pdf)	OPCD	Sept 2018	<i>Seattle Tools</i> , Urban Centers, Villages, Manufacturing Industrial Centers (CITYPLAN.URBAN_VILLAGE_CENTER_MIC)	high use area

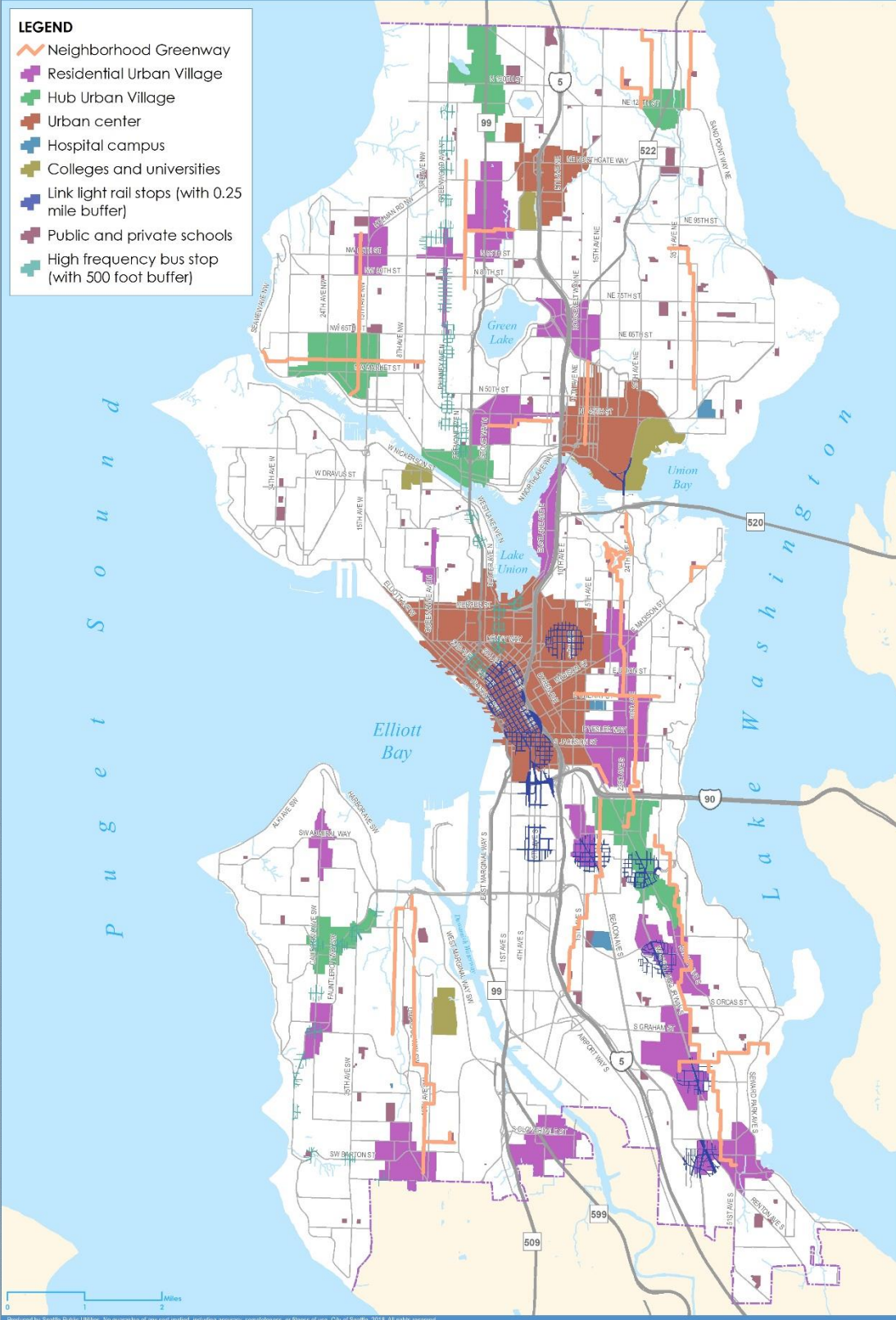
OPCD = Office of Community Planning and Development
City = City of Seattle
ST = Sound Transit
KC = King County
SDOT = Seattle Department of Transportation
OEM = Office of Emergency Management
[DWW GIS Library \(DSA\) on SharePoint = https://seattlegov.sharepoint.com/:f:/r/sites/spu-D1/Planning/DWW%20GIS%20Library/DSA/Data/SPU?csf=1&web=1&e=UBk4k2](https://seattlegov.sharepoint.com/:f:/r/sites/spu-D1/Planning/DWW%20GIS%20Library/DSA/Data/SPU?csf=1&web=1&e=UBk4k2)



Figure 1. High Use Areas

LEGEND

- Neighborhood Greenway
- Residential Urban Village
- Hub Urban Village
- Urban center
- Hospital campus
- Colleges and universities
- Link light rail stops (with 0.25 mile buffer)
- Public and private schools
- High frequency bus stop (with 500 foot buffer)



Author: Filled Map Document Properties Date: 7/17/2020 File Path: X:\Separated Systems\Business Areas\Planning\DS\AreaData\Map - High Use.mxd

Produced by Seattle Public Utilities. No guarantee of any sort implied, including accuracy, completeness, or fitness for use. City of Seattle, 2018. All rights reserved.

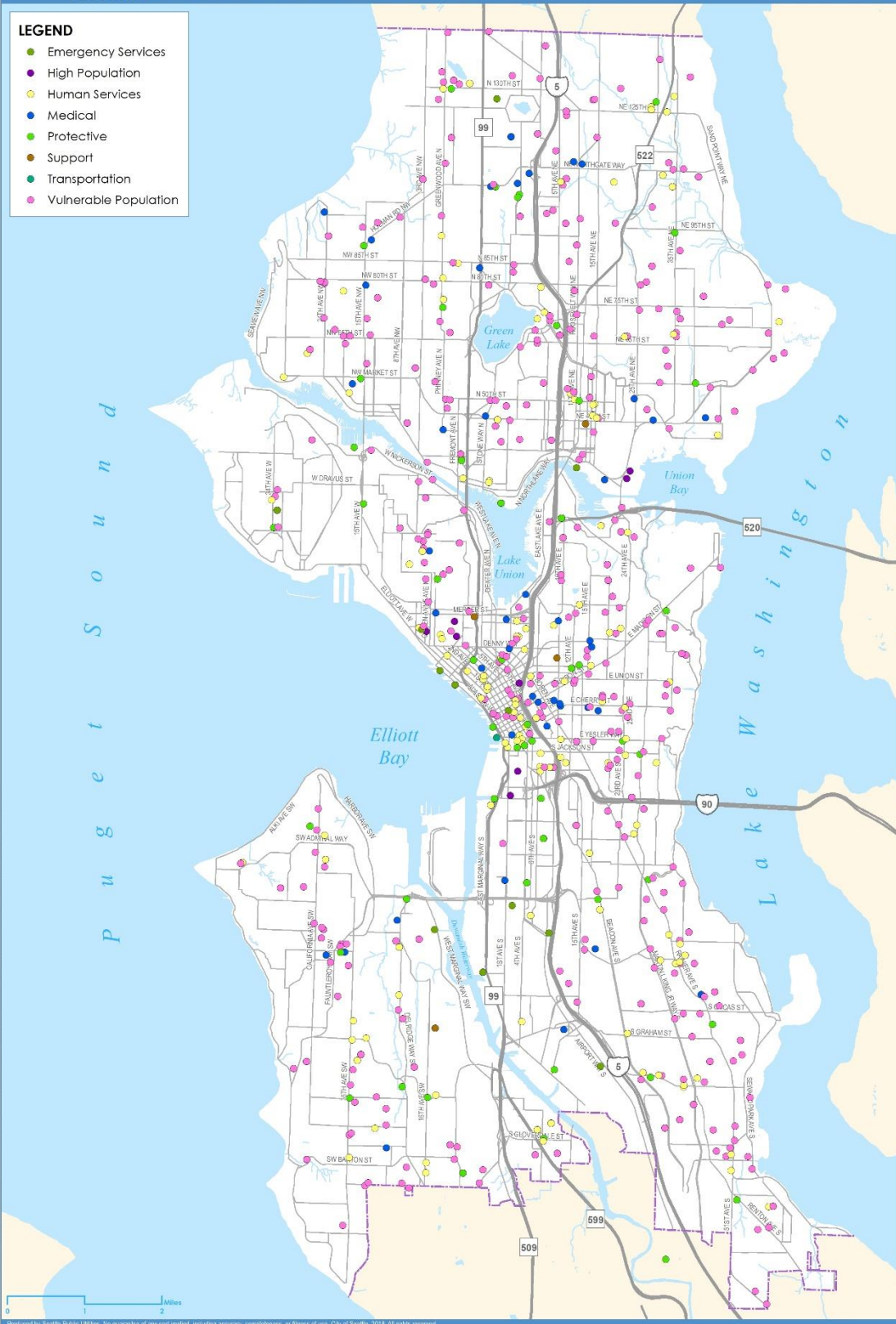


Figure 2. Critical Facilities

LEGEND

- Emergency Services
- High Population
- Human Services
- Medical
- Protective
- Support
- Transportation
- Vulnerable Population

Author: Filled Map Document Properties Date: 7/17/2020 File Path: X:\Seasat\Systems\Business Areas\Planning\DS\MapData\Map_CriticalFacilities.mxd



Produced by Seattle Public Utilities. No guarantee of any sort implied, including accuracy, completeness, or fitness of use. City of Seattle, 2018. All rights reserved.



Figure 3. Racial and Social Equity Composite Index - 2018

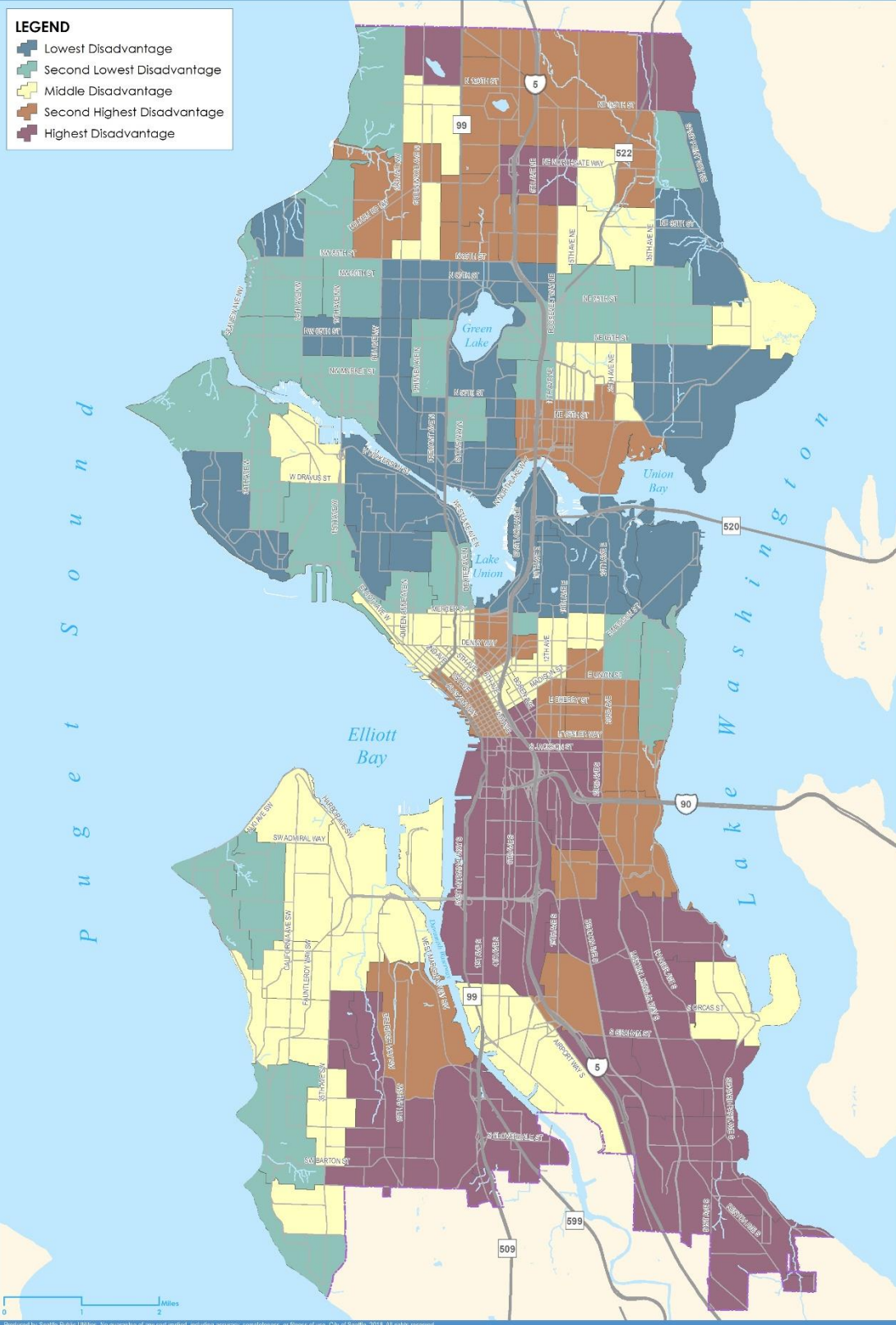

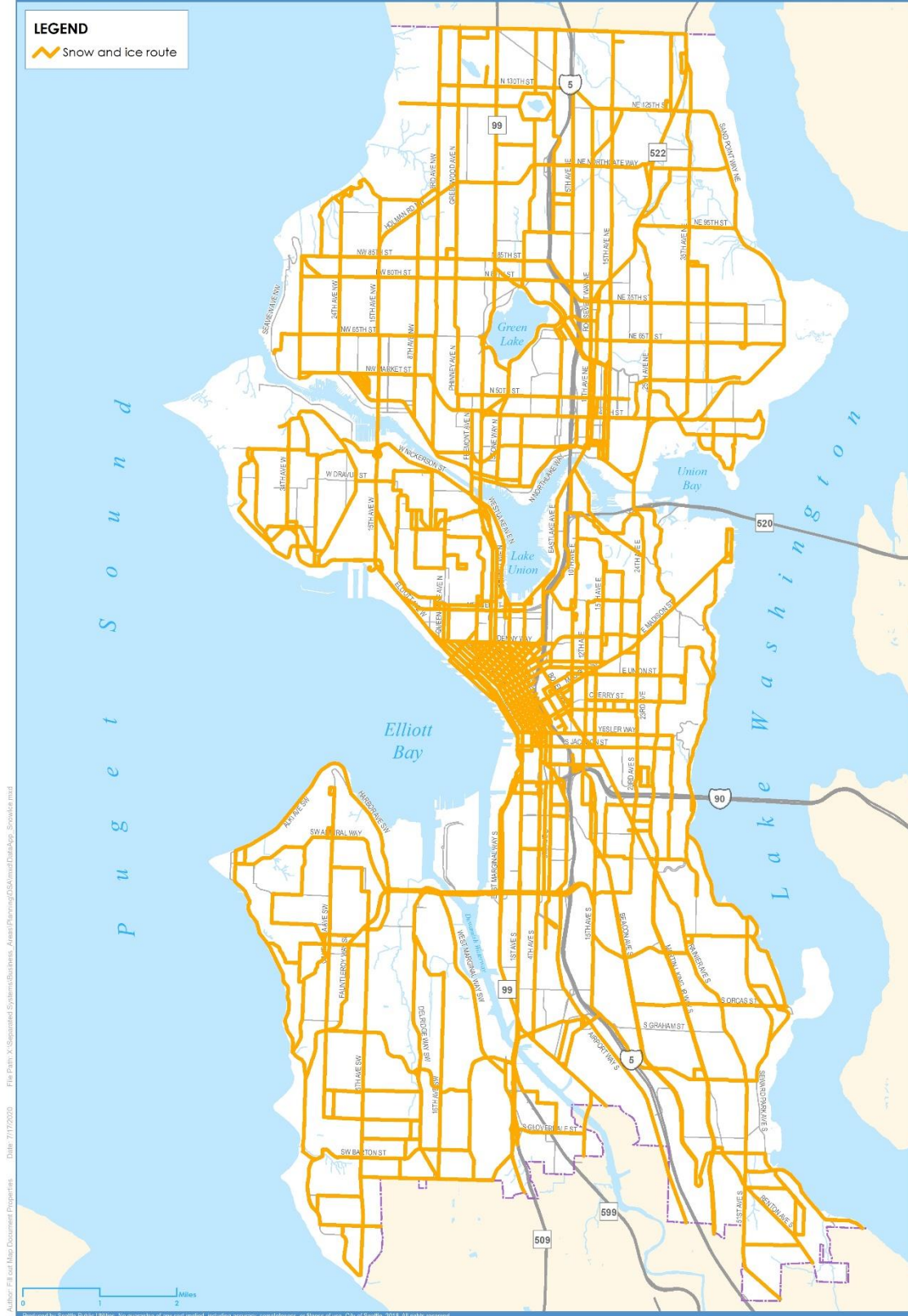




Figure 4. Snow and Ice Routes

LEGEND

 Snow and Ice route



Author: Filled Map Document Properties Date: 7/17/2020 File Path: X:\Seasat Systems\Business Areas\Planning\DS\MapData\Map_SnowIce.mxd

Produced by Seattle Public Utilities. No guarantee of any sort implied, including accuracy, completeness, or fitness for use. City of Seattle, 2018. All rights reserved.

Table 2. Processed Data used in the Systems Analyses Projects

Name	Description	Storage Location(s)	File Name	Data Type	File Date	Analysis in Which the Data were Used				
						Wastewater system capacity risk areas	Drainage system capacity risk areas	Sea level rise risk map	Creek flooding risk map	Extreme storm event risk map
critical facilities	<p>Point data of the following types of critical facilities:</p> <ul style="list-style-type: none">• emergency serviced• high population• human services• medical• protective• support• vulnerable populations <p>The raw data were mapped by lat/long. Sites that mapped outside a parcel, were moved to the parcel based on the address and mapping review.</p> <p>The list was paired down to reflect facilities related to human health and safety for people at that location. See additional information below, after the tables. Exact duplicates were removed. List consists of 746 facilities on 612 unique parcels.</p>	DWW GIS Library on SharePoint <i>Project files</i>	CriticalFac_rev.zip/.shp	point	12/21/18	✓				
critical facilities	King County parcel data developed from the critical facilities point data. Consists of parcels with at least one critical facility point within it.	<i>Project files</i>	CriticalFacility_parcel.shp	polygon	5/5/20		✓			
critical facilities	Raster data developed from critical facilities polygon data. A binary grid (4 foot by 4 foot) was developed by giving grid cells falling within the parcel polygons a value of 1 and all other cells were given a value of 0.	<i>Project files \rasterdata.gdb</i>	CritFacility	raster	7/17/20			✓	✓	✓
high use area	<p>An area likely to have a large number of pedestrians traveling in or through it relative to other areas of the city. It consists of the following land uses and right-of-way (ROW) buffers:</p> <ul style="list-style-type: none">• Residential and Hub Urban Villages, including a 50-foot ROW buffer• Urban Center, including a 50-foot ROW buffer• Hospital campuses, including a 50-foot ROW buffer• Colleges and universities, including a 50-foot ROW buffer• Public and private schools, including a 50-foot ROW buffer• Link light rail stops, including a quarter mile ROW buffer• High frequency bus stops, including a 50-foot ROW buffer• Neighborhood greenways <p>After each polygon data were buffered, they were merged into one data set.</p>	DWW GIS Library on SharePoint	Pedestrian_Areas_for_Prioritization.mpk	polygon and polyline	1/7/19	✓ If at least 50% of a risk area included a high use area, the risk score was increased.				
high use area	Neighborhood greenways were buffered by the ½ of right-of-way width with the attribute “ROWWIDTH”, equating to an area equal to the right-of-way width centered on the street polyline. The resulting polygon data were merged with the polygon data set of the other high use areas.	<i>Project files</i>	HighUseAreas.shp	polygon	7/15/20		✓			

Name	Description	Storage Location(s)	File Name	Data Type	File Date	Analysis in Which the Data were Used				
						Wastewater system capacity risk areas	Drainage system capacity risk areas	Sea level rise risk map	Creek flooding risk map	Extreme storm event risk map
high use area	Raster data developed from high use area polygon data. A binary grid (4 foot by 4 foot) was developed by giving grid cells falling within the high use area polygons a value of 1 and all other cells were given a value of 0.	<i>Project files \rasterdata.gdb</i>	HighUse	raster	7/17/20			✓	✓	✓
land area	Land within the city, and, except for Green Lake, no inland water bodies.	DWW GIS Library (DSA) on SharePoint <i>Project files</i>	CityofSeattle_DSA.zip/shp	polygon	3/25/20			✓	✓	✓
major transportation routes	From the streets data (Streets_DSA.shp), (1) Snow and ice routes were identified through a spatial join, and (2) interstates/freeways were identified based on attribute "OWNER" = "WSDOT". Identified features were merged into one dataset. Right-of-way widths (attribute "ROWWIDTH") of 60 feet were added to interstates/freeways. The polyline data were buffered by the ½ of right-of-way width equating to an area equal to the right-of-way width centered on the street polyline. A binary grid (4 foot by 4 foot) was developed by giving grid cells falling within the major transportation route polygons a value of 1 and all other cells were given a value of 0. (The dataset available has a grid cell value of 1.5 for major transportation routes.)	<i>Project files \rasterdata.gdb</i>	MajorTrans	raster	7/17/20			✓	✓	✓
Racial and Social Equity Composite Index	Polygon data were dissolved on the composite index. A binary grid (4 foot by 4 foot) was developed by giving grid cells falling within each disadvantage category the following value: <ul style="list-style-type: none"> • highest = 5 • second highest = 4 • middle = 3 • second lowest = 2 • lowest = 1 	<i>Project files \rasterdata.gdb</i>	Equity	raster	7/17/20			✓	✓	✓
street type	Streets_DSA polyline data were buffered by the ½ of right-of-way width (attribute "ROWWIDTH") equating to an area equal to the right-of-way width centered on the street polyline. Snow and ice routes were identified through a spatial join. Major transportations are the routes with attribute "Type" = "SnowIceRoute". Non-arterial streets have the attribute "Type" = "Non-arterial".	<i>Project files</i>	StreetType_DSA.shp	polygon	5/5/20		✓			
streets	Street with right-of-way widths added to attribute "ROWWIDTH", where missing, when near a risk area. ROWWIDTHs added were based on aerial photo review.	DWW GIS Library on SharePoint <i>Project files</i>	Streets_DSA.zip/.shp	polyline	1/24/20		✓ (intermediate data set)			

[DWW GIS Library on SharePoint](https://seattlegov.sharepoint.com/sites/spu-D1/Planning/DWW%20GIS%20Library/Forms/AllItems.aspx) = <https://seattlegov.sharepoint.com/sites/spu-D1/Planning/DWW%20GIS%20Library/Forms/AllItems.aspx>

[DWW GIS Library \(DSA\) on SharePoint](https://seattlegov.sharepoint.com/:f:/r/sites/spu-D1/Planning/DWW%20GIS%20Library/DSA/Data/SPU?csf=1&web=1&e=UBk4k2) = <https://seattlegov.sharepoint.com/:f:/r/sites/spu-D1/Planning/DWW%20GIS%20Library/DSA/Data/SPU?csf=1&web=1&e=UBk4k2>

Project files = X:\Separated Systems\Business_Areas\Planning\DSA\data\Impacts

Table 3. Critical Facilities Included in Analyses

Category	Primary Use	Count
Emergency Services	Emergency Cache	4
Emergency Services	Fire - Support	1
Emergency Services	Government Function	2
Emergency Services	Medical	1
Emergency Services	Parking Garage	1
Emergency Services	Police Station	3
High Population	Conference Center	2
High Population	Landmark	1
High Population	Stadium	6
Human Services	Community Center	31
Human Services	Customer Service	4
Human Services	Family Center	7
Human Services	Food Bank	30
Human Services	Food Distribution Center	1
Human Services	Library	26
Human Services	Meal Program	17
Human Services	Non-Profit	10
Human Services	Shelter	22
Human Services	Support	4
Human Services	Teen Center	1
Medical	Blood Center	5
Medical	Dialysis Center	7
Medical	Hospital	12
Medical	Medical	1
Medical	Public Health	2
Medical	Urgent Care Clinic	17
Protective	Coast Guard Station	1
Protective	Fire - Support	1
Protective	Fire Headquarters	1
Protective	Fire Station	34
Protective	Joint: Fire Station / EOC	1
Protective	Joint: Fire Station / Senior Center	1
Protective	Joint: Police and Courts	1
Protective	Offices	1
Protective	Parking Garage	2
Protective	Police - Support	6
Protective	Police Harbor Patrol	2
Protective	Police Station	6

Category	Primary Use	Count
Support	Backup EOC	5
Transportation	Ferry Terminal	1
Vulnerable Population	Child Care Center	252
Vulnerable Population	Nursing Home	25
Vulnerable Population	School	90
Vulnerable Population	School - 6-12	2
Vulnerable Population	School - 6-8	10
Vulnerable Population	School - 9-12	13
Vulnerable Population	School - Gym	1
Vulnerable Population	School - K-5	59
Vulnerable Population	School - K-8	11
Vulnerable Population	School - Service School	2

ArcGIS Model Builder Flow Charts

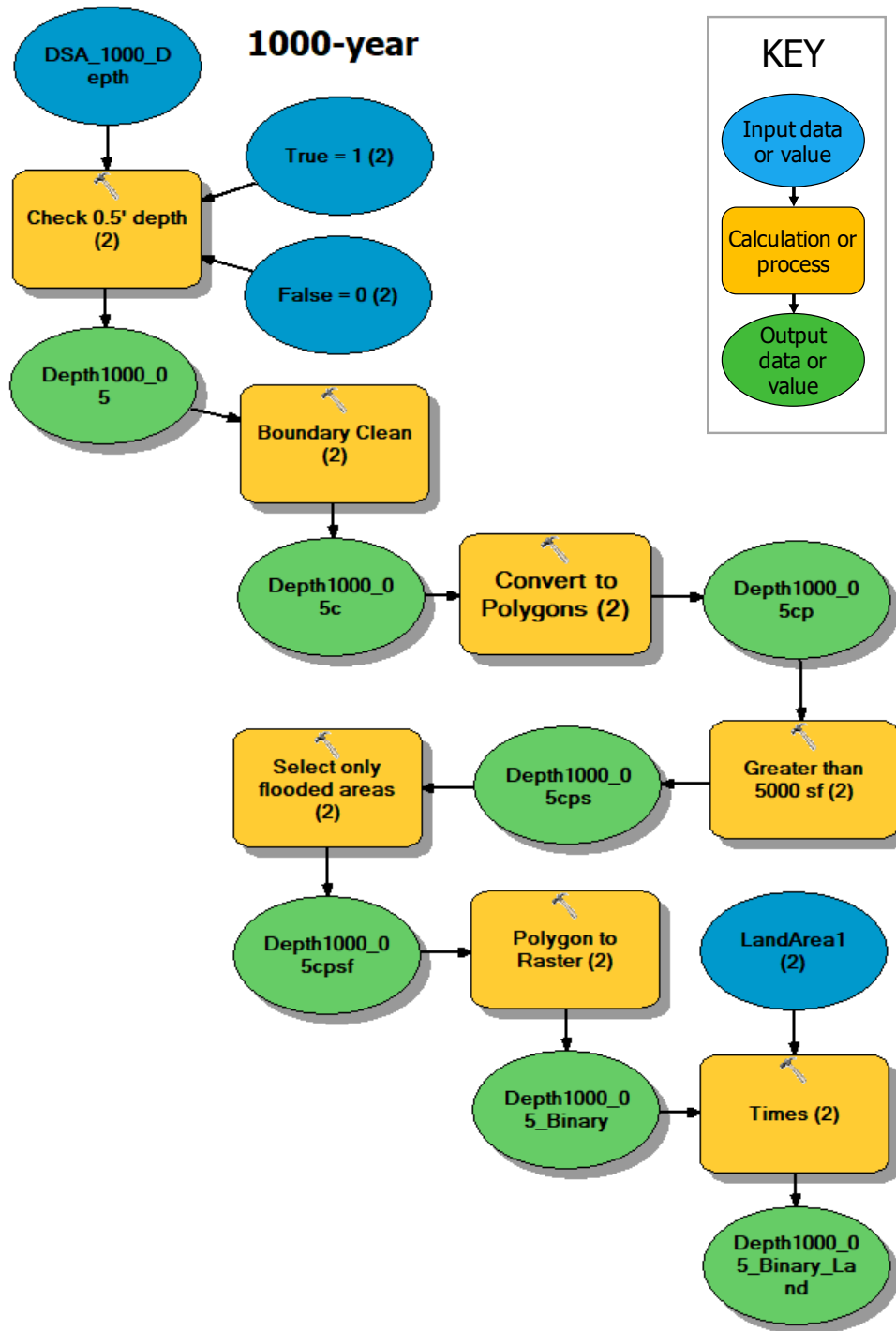


Figure B-1. ArcGIS model builder for 1,000-year inundation area boundary

Create Critical Facility polygon Layer

To start:

1. Right click on the input data labels (dark blue) and download the data
2. Unzip the parcel layer and save the two layers into the InputData.gdb dataset
3. Change the Workspace in the Model Environment to set the outputs to OutputData.gdb
4. Run the model and review the outputs

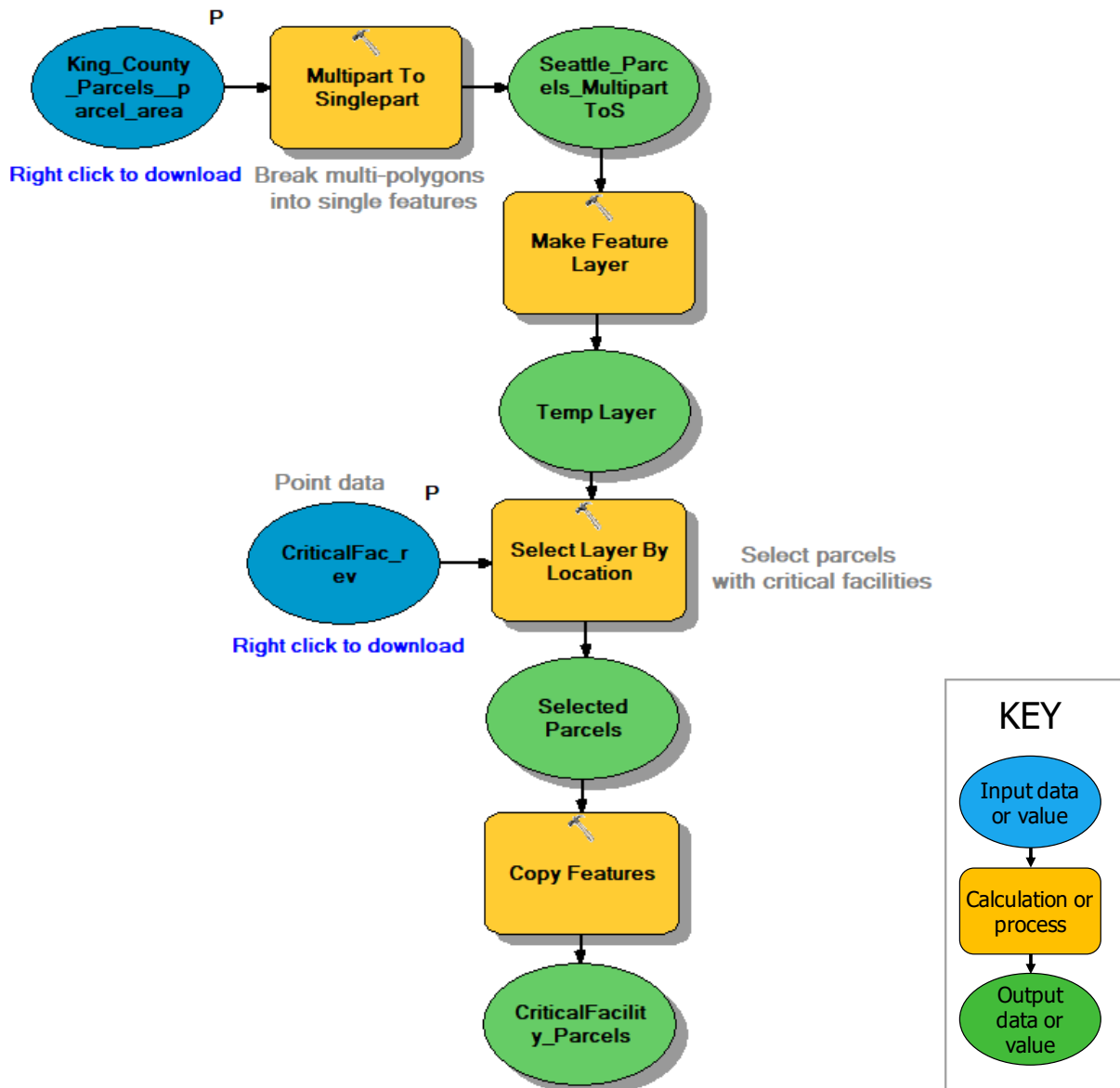


Figure E-3. ArcGIS model builder for developing critical facility area raster

Create Buffered Streets Layer

1. Right click on the input data labels (dark blue) and download the Street_DSA.zip
2. Save the layers to the InputData.gdb
3. change the WorkSpace in the Model Environment for the outputs to OutputData.gdb
4. Run the tool and review the outputs

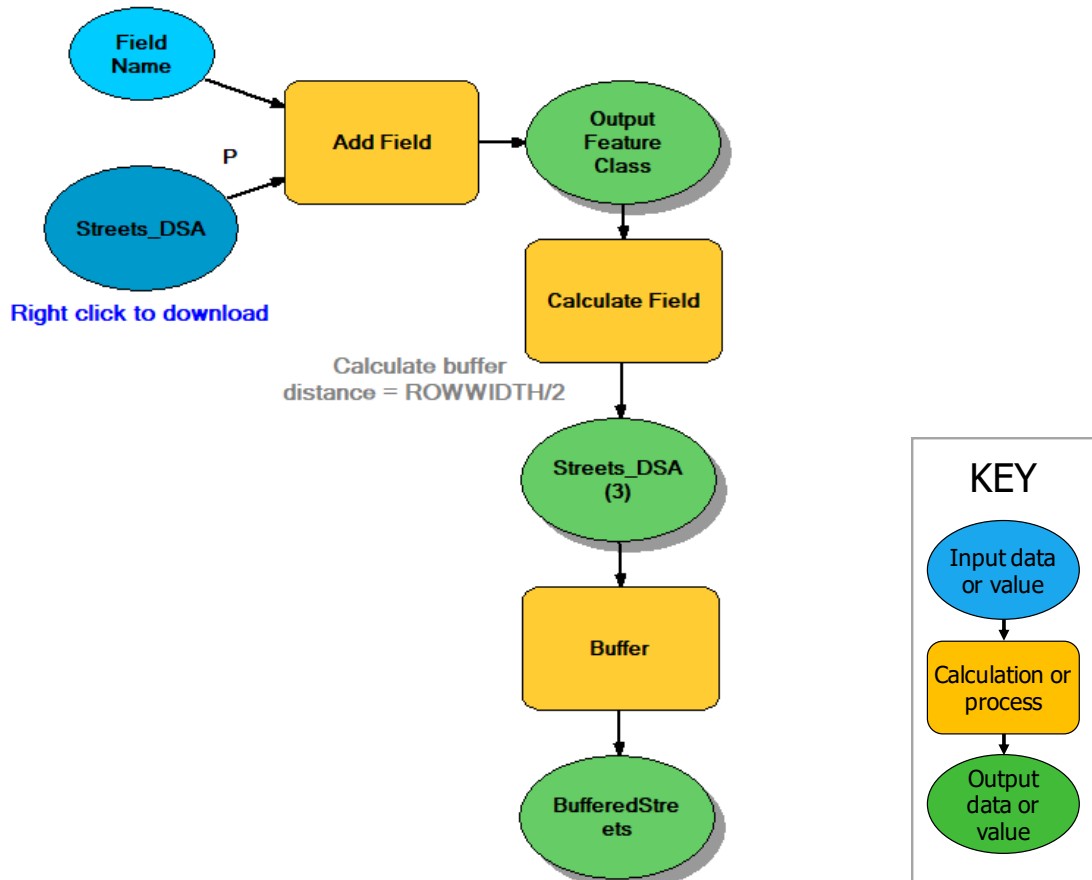


Figure E-4. ArcGIS model builder of street buffers for major transportation routes raster

Create Equity Layer:

To start:

1. Right click on the input data labels (dark blue) and download Racial and Social Equity Composite Index - 2018.zip
2. Unzip the shapefile and add to the InputData.gdb database
3. If necessary, change the WorkSpace in the Model Environment to set the outputs to OutputData.gdb
4. Run the tool and review the outputs

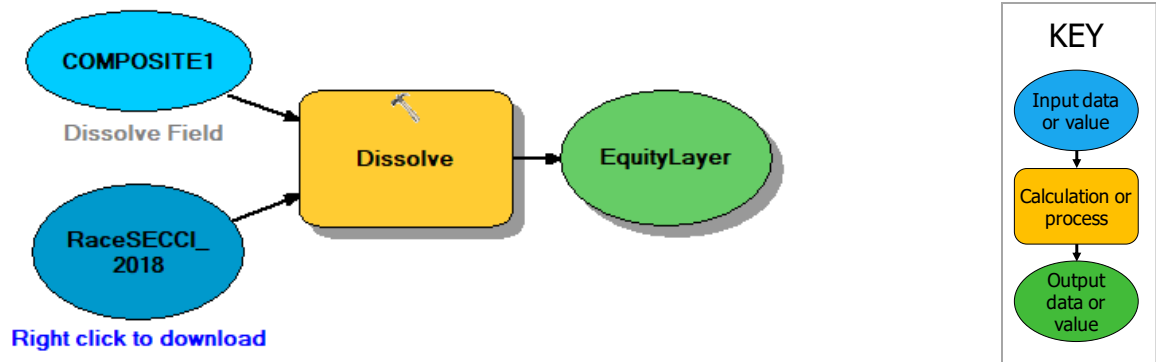


Figure E-5. ArcGIS model builder for developing equity raster

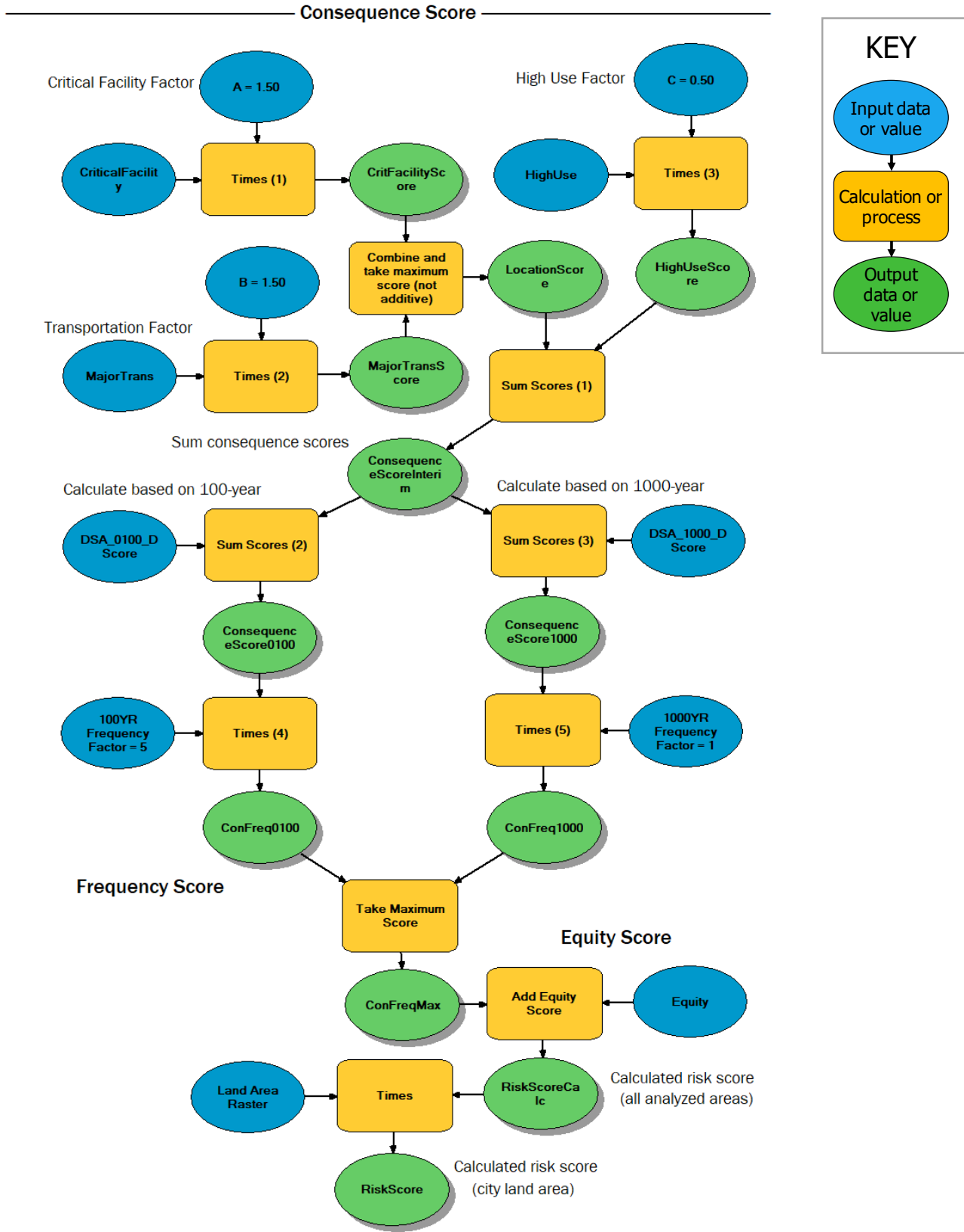


Figure E-6. ArcGIS model builder calculating risk score

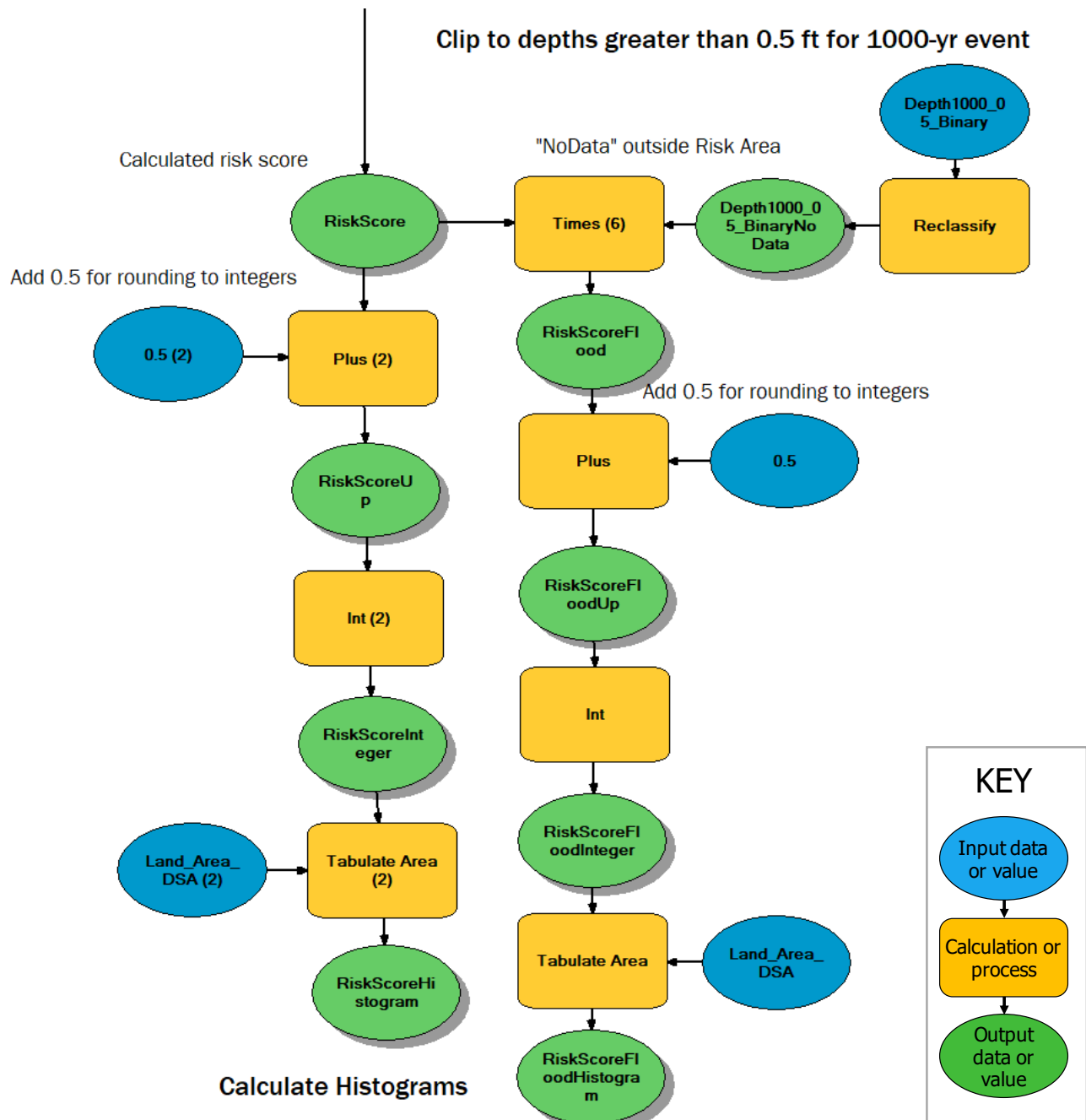


Figure E-7. ArcGIS model builder for clipping risk area and calculating histograms

Appendix F: Maps of Simulated Inundation with Historical Watershed Conditions

Figure F-1. Simulated 100-year Storm Inundation with Historical Watershed Conditions (southwest quadrant)

Figure F-2. Simulated 100-year Storm Inundation with Historical Watershed Conditions (southeast quadrant)

Figure F-3. Simulated 100-year Storm Inundation with Historical Watershed Conditions (northwest quadrant)

Figure F-4. Simulated 100-year Storm Inundation with Historical Watershed Conditions (northeast quadrant)

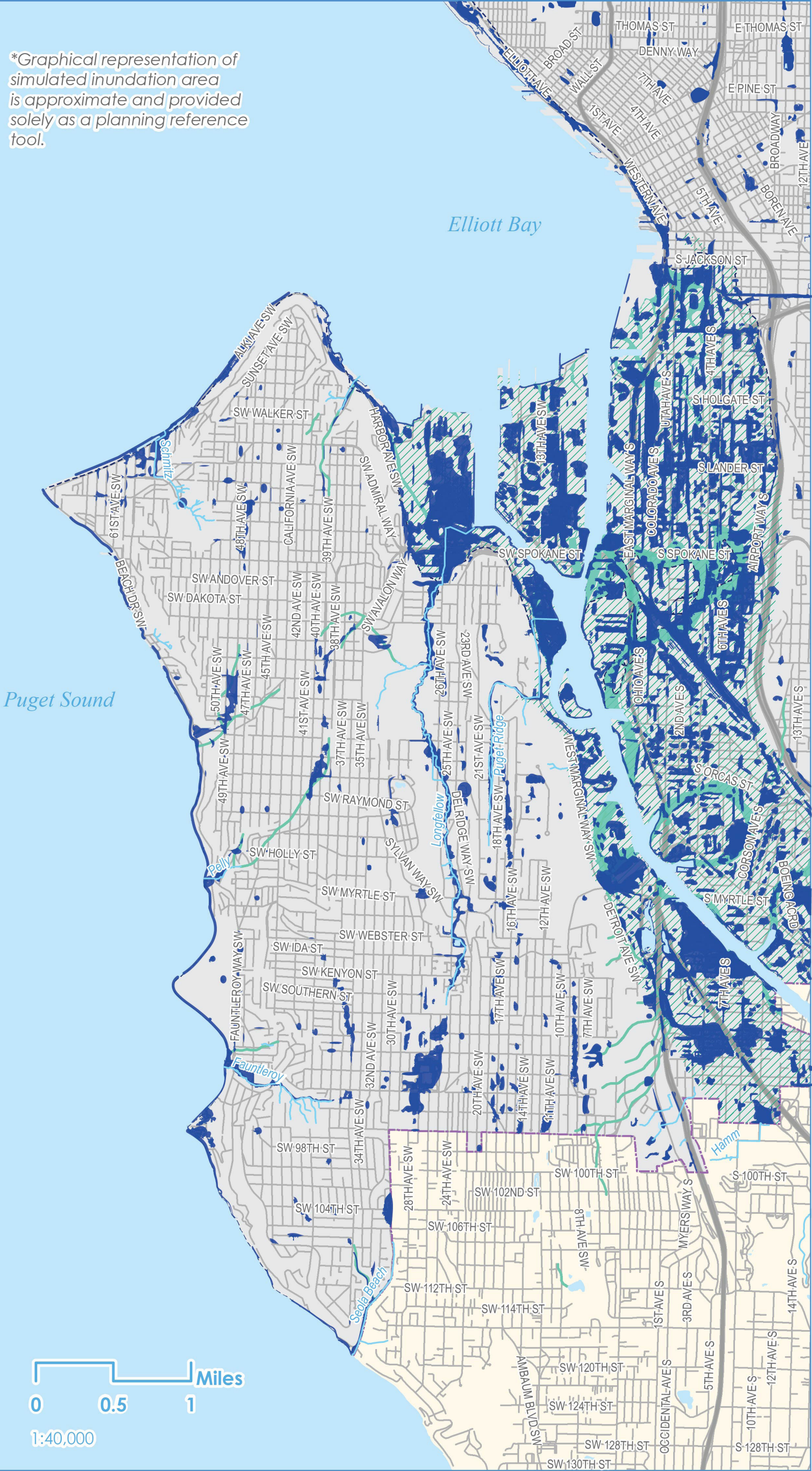
This page intentionally left blank.



LEGEND

- Inundation area*
- Historic shoreline
- Historic streams
- Historic waterbody
- Historic wetlands
- City limits
- Existing streams

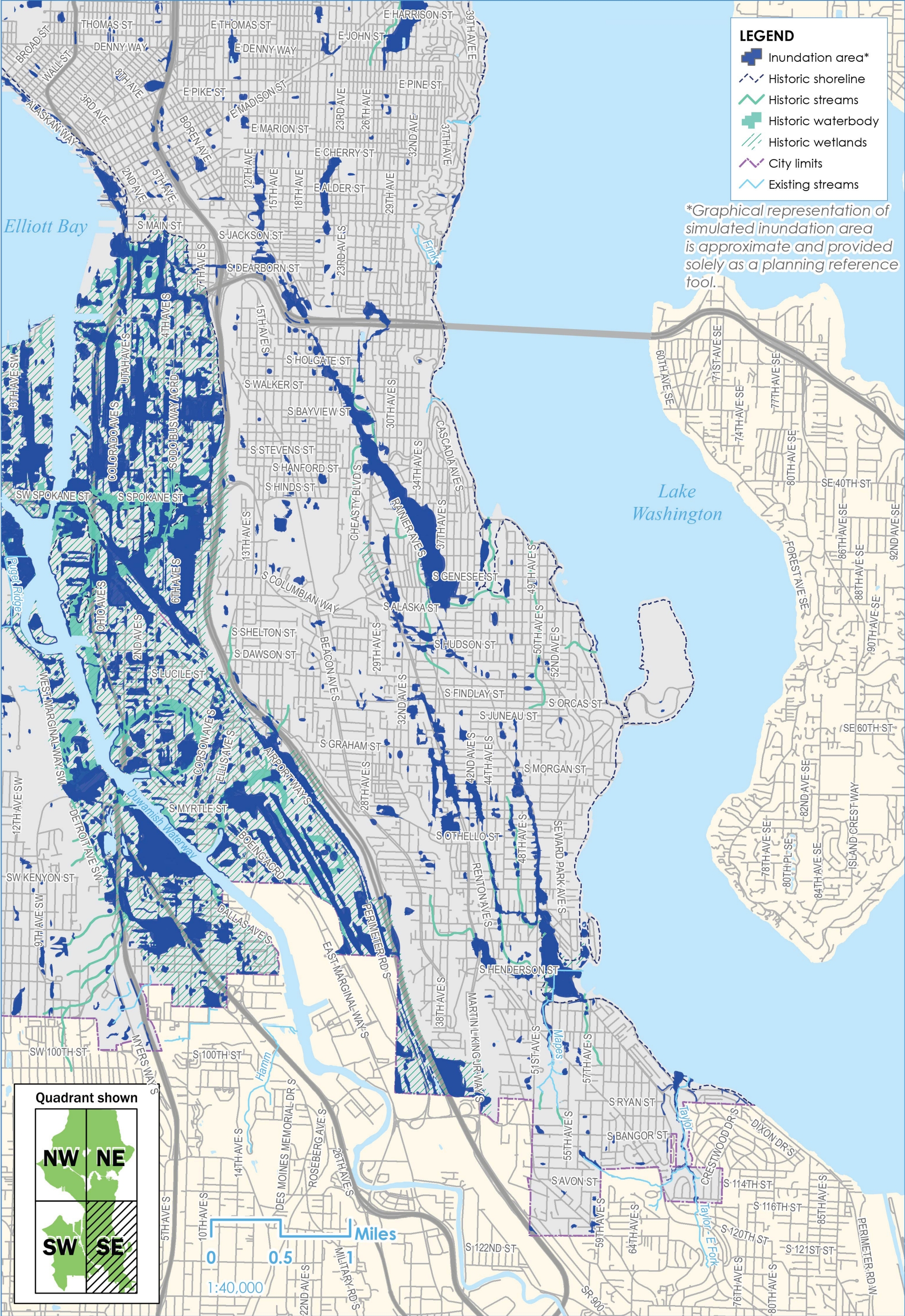
*Graphical representation of simulated inundation area is approximate and provided solely as a planning reference tool.



Quadrant shown

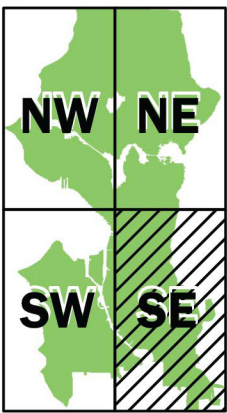


Figure F-2. Simulated 100-year Storm Inundation with Historical Watershed Conditions



*Graphical representation of simulated inundation area is approximate and provided solely as a planning reference tool.

Quadrant shown



Miles

0 0.5 1
1:40,000



LEGEND

Inundation area*

Historic shoreline

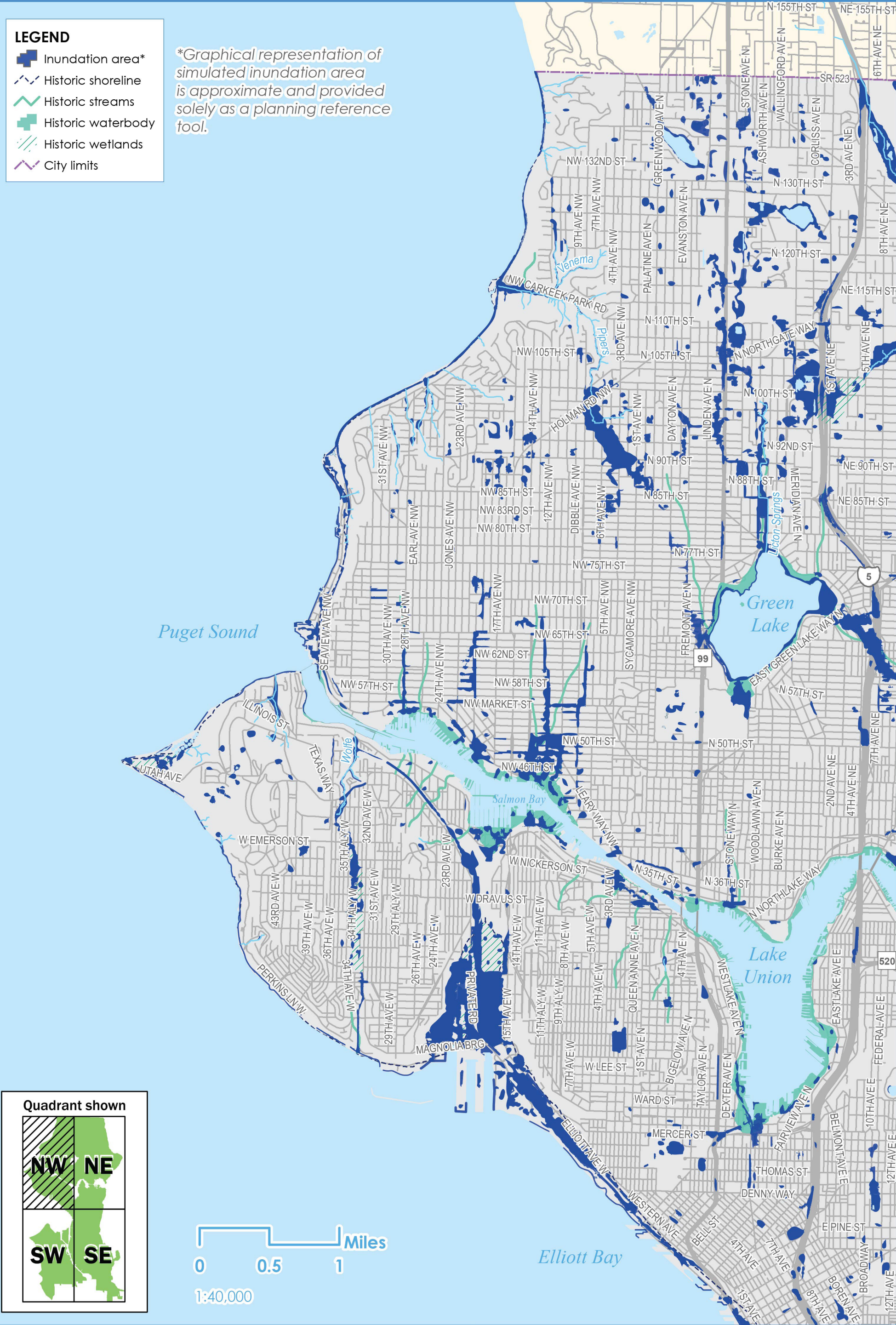
Historic streams

Historic waterbody

Historic wetlands

City limits

*Graphical representation of simulated inundation area is approximate and provided solely as a planning reference tool.



File Path: X:\Separated Systems\Business_Areas\Planning\DSA\mxd\DSA_T2_ExtStorms_historical_nw.mxd

Date: 8/27/2020

Author: Fill out Map Document Properties

Quadrant shown

NW

NE

SW

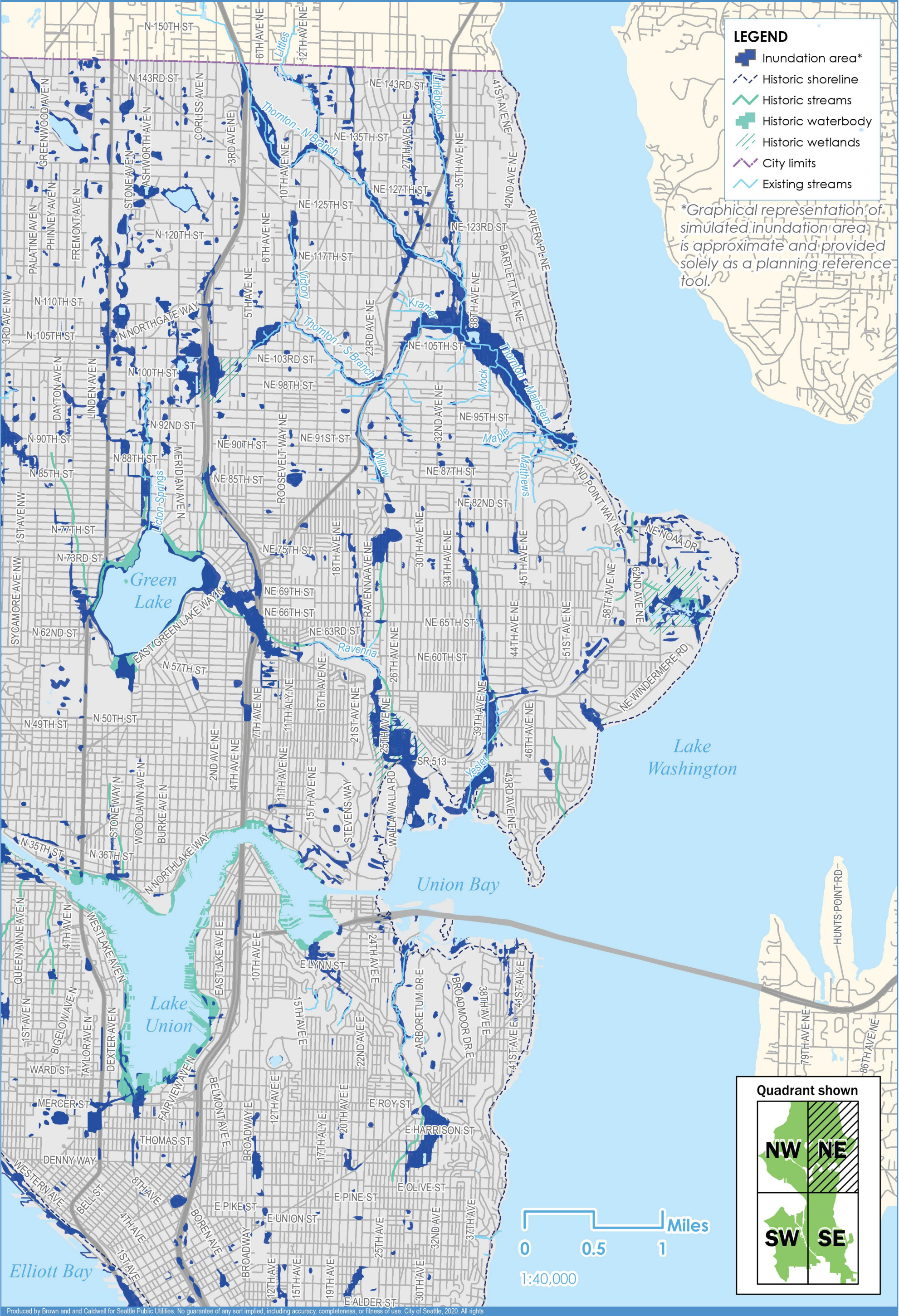
SE

Produced by Brown and Caldwell for Seattle Public Utilities. No guarantee of any sort implied, including accuracy, completeness, or fitness of use. City of Seattle, 2020. All rights reserved.

LIMITATIONS: This document was prepared solely for Seattle Public Utilities in accordance with professional standards at the time the services were performed and in accordance with the contract between Seattle Public Utilities and Brown and Caldwell dated May 9, 2018. This document is governed by the specific scope of work authorized by Client Name; it is not intended to be relied upon by any other party except for regulatory authorities contemplated by the scope of work. We have relied on information or instructions provided by Seattle Public Utilities and other parties and, unless otherwise expressly indicated, have made no independent investigation as to the validity, completeness, or accuracy of such information.



Figure F-4. Simulated 100-year Storm Inundation
with Historical Watershed Conditions



Author: Fill out Map Document Properties Date: 8/27/2020 File Path: X:\Separated Systems\Business Areas\Planning\DSA\mxd\DSA_T2_ExtStorms_historical_ne.mxd

Produced by Brown and Caldwell for Seattle Public Utilities. No guarantee of any sort implied, including accuracy, completeness, or fitness of use. City of Seattle, 2020. All rights reserved.

LIMITATIONS: This document was prepared solely for Seattle Public Utilities in accordance with professional standards at the time the services were performed and in accordance with the contract between Seattle Public Utilities and Brown and Caldwell dated May 9, 2018. This document is governed by the specific scope of work authorized by Client Name; it is not intended to be relied upon by any other party except for regulatory authorities contemplated by the scope of work. We have relied on information or instructions provided by Seattle Public Utilities and other parties and, unless otherwise expressly indicated, have made no independent investigation as to the validity, completeness, or accuracy of such information.

Appendix G: Extreme Storm Risk Maps

Figure G-1. Extreme Storms Risk Area (southwest quadrant)

Figure G-2. Extreme Storms Risk Area (southeast quadrant)

Figure G-3. Extreme Storms Risk Area (northwest quadrant)

Figure G-4. Extreme Storms Risk Area (northeast quadrant)

SPU Drainage System Analysis

Flooding Topic Area | Extreme Storms Analysis

This page intentionally left blank.

Figure G-1. Extreme Storms Risk Area



LEGEND

City limits

Existing streams

Building

Relative Risk Category

low

medium low

medium

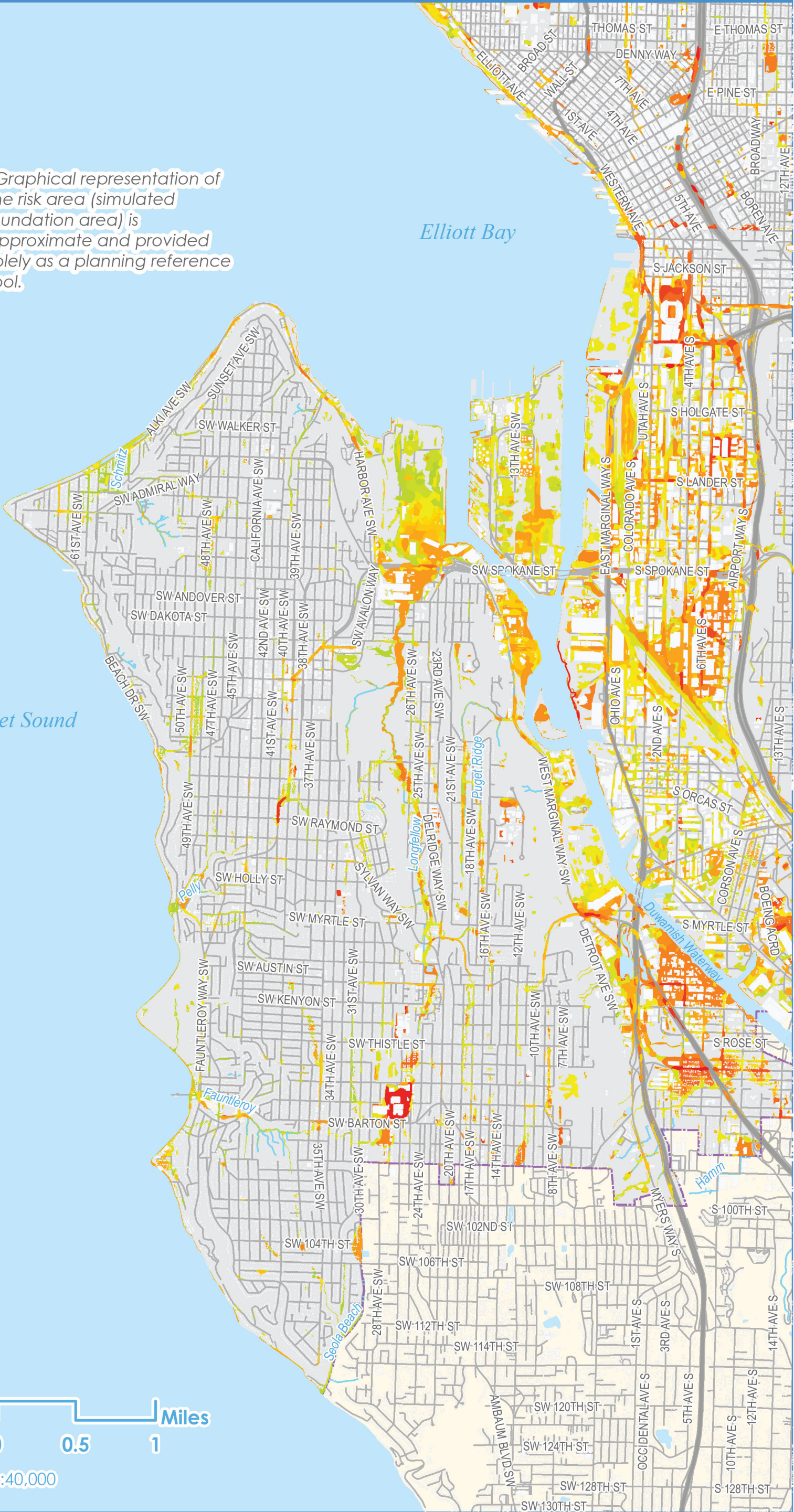
high

critical

*Graphical representation of the risk area (simulated inundation area) is approximate and provided solely as a planning reference tool.

Puget Sound

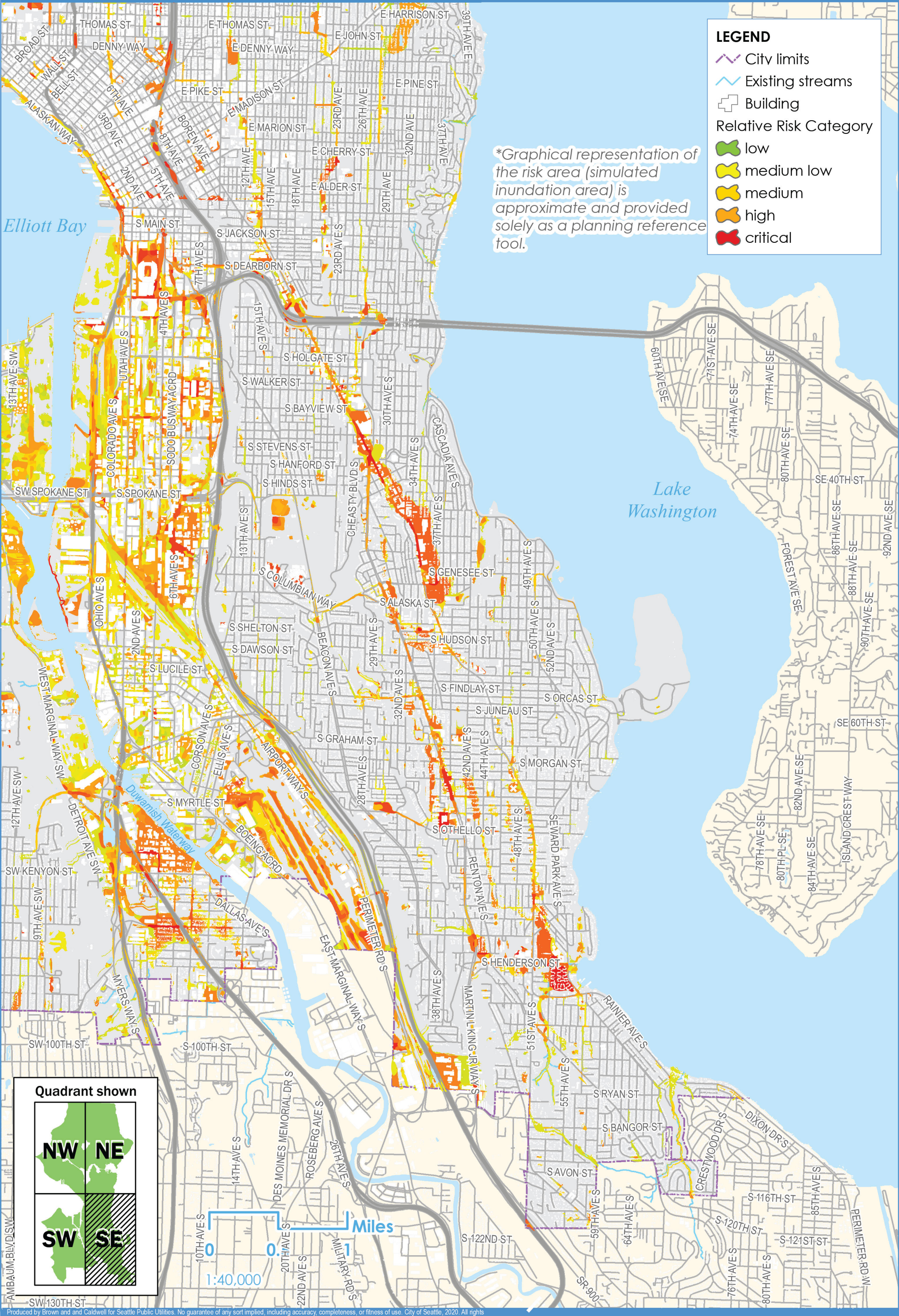
Elliott Bay



Quadrant shown



Figure G-2. Extreme Storms Risk Area



LIMITATIONS: This document was prepared solely for Seattle Public Utilities in accordance with professional standards at the time the services were performed and in accordance with the contract between Seattle Public Utilities and Brown and Caldwell dated May 9, 2018. This document is governed by the specific scope of work authorized by Client Name; it is not intended to be relied upon by any other party except for regulatory authorities contemplated by the scope of work. We have relied on information or instructions provided by Seattle Public Utilities and other parties and, unless otherwise expressly indicated, have made no independent investigation as to the validity, completeness, or accuracy of such information.

Figure G-3. Extreme Storms Risk Area

LEGEND

City limits

Existing streams

Building

Relative Risk Category

low

medium low

medium

high

critical

*Graphical representation of the risk area (simulated inundation area) is approximate and provided solely as a planning reference tool.

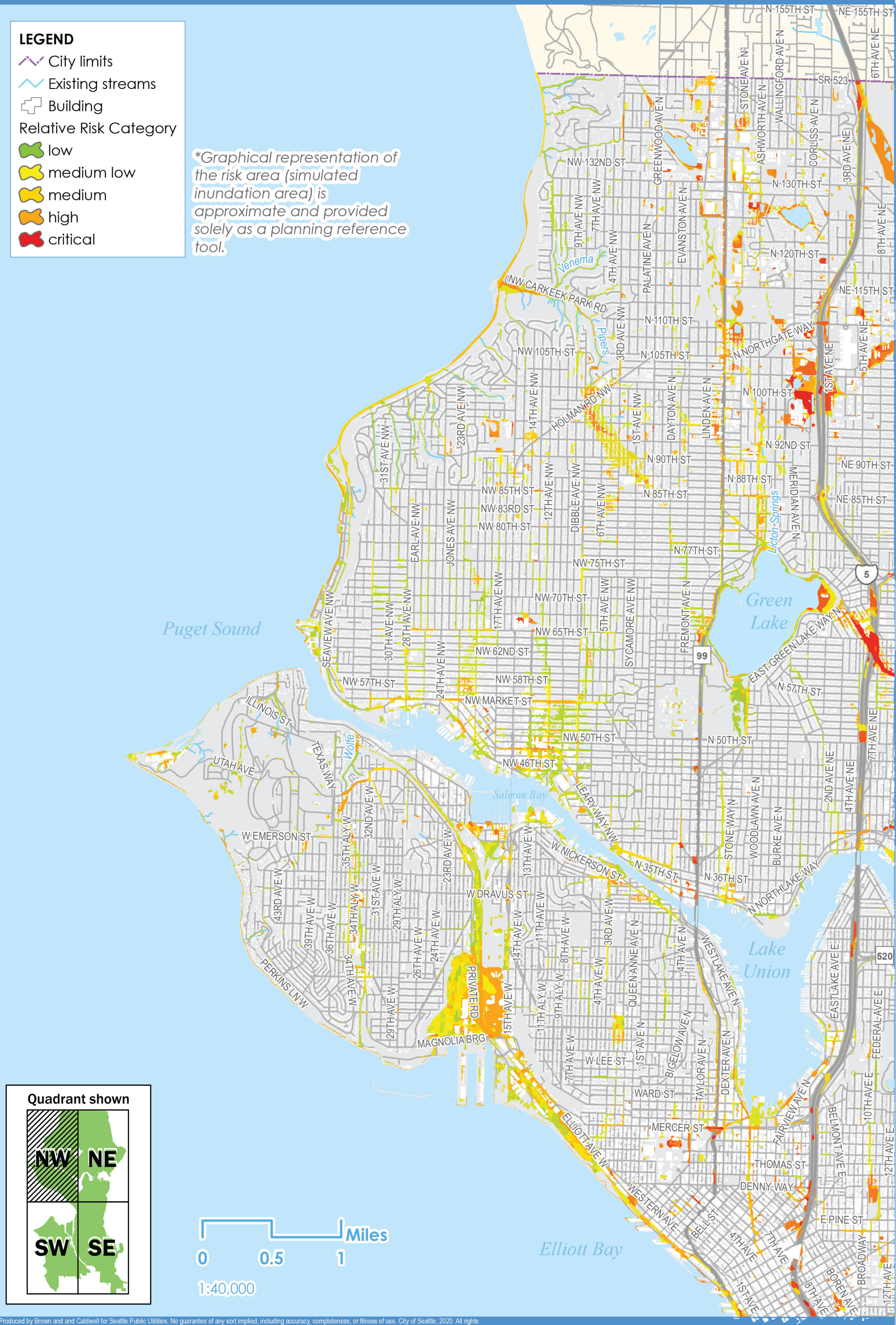
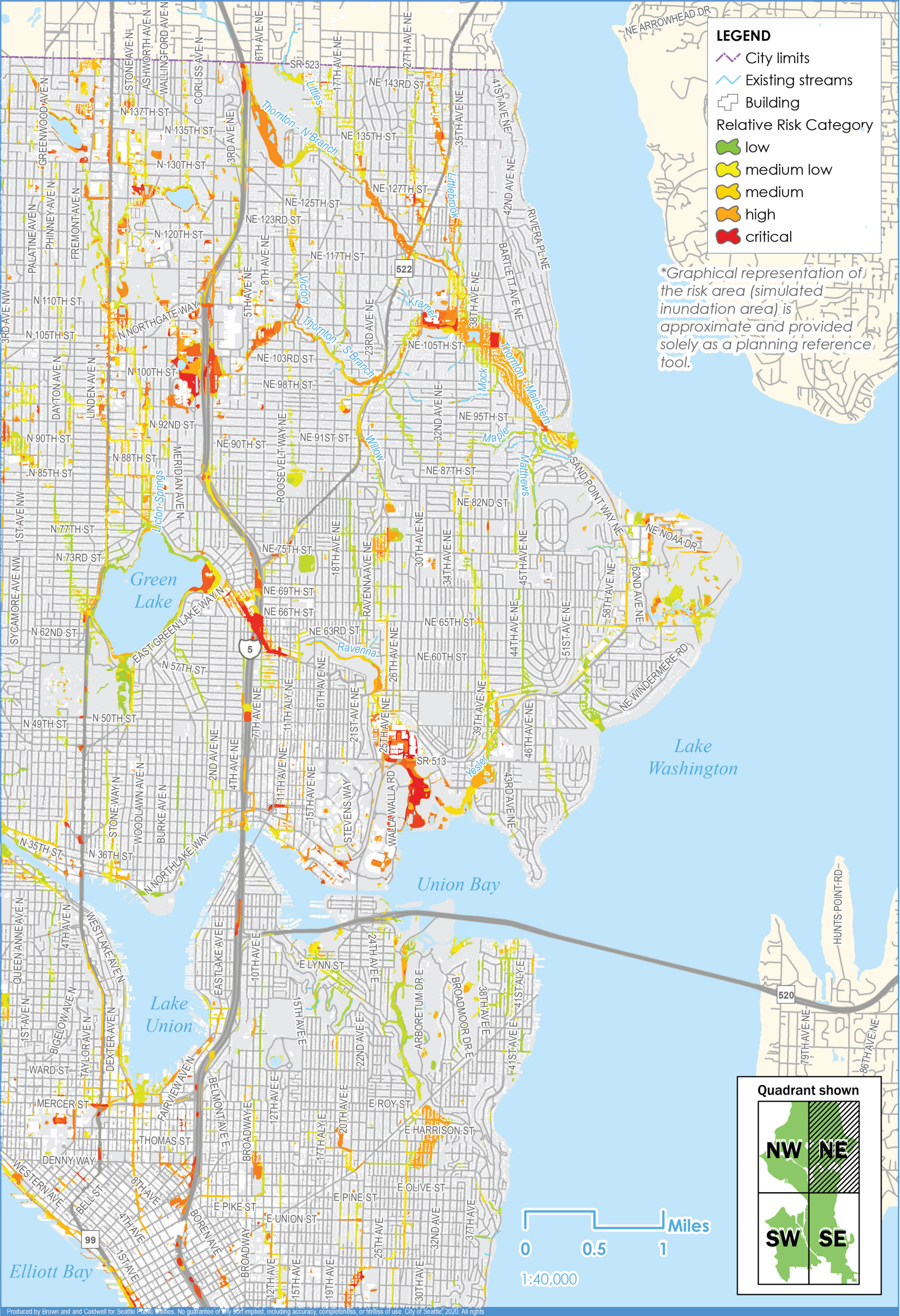




Figure G-4. Extreme Storms Risk Area



LIMITATIONS: This document was prepared solely for Seattle Public Utilities in accordance with professional standards at the time the services were performed and in accordance with the contract between Seattle Public Utilities and Brown and Caldwell dated May 9, 2018. This document is governed by the specific scope of work authorized by Client Name; it is not intended to be relied upon by any other party except for regulatory authorities contemplated by the scope of work. We have relied on information or instructions provided by Seattle Public Utilities and other parties and, unless otherwise expressly indicated, have made no independent investigation as to the validity, completeness, or accuracy of such information.